

**COMBINING IRREVERSIBLE ELECTROPORATION (IRE)  
WITH TLR3/9 AGONISTS AND PD-1 BLOCKADE FOR POTENT  
ANTI-TUMOR IMMUNITY**

A Thesis Submitted to the College of  
Graduates and Postdoctoral Studies  
In Partial Fulfillment of the Requirements  
For the Degree of Master of Science  
In the Department of Vaccinology and Immunotherapeutics  
In school of Public Health  
University of Saskatchewan  
Saskatoon

By

Fatma Babikr

© Copyright Fatma Babikr, Dec 6, 2021. All rights reserved

Unless otherwise noted, copyright of the material in this thesis belongs to the author.

## **PERMISSION TO USE**

In presenting this thesis in partial fulfillment of the requirements for a Master of Science degree from the University of Saskatchewan, I agree that Libraries of this University may make it freely available for inspection. I further agree that permission for copying of the thesis in any manner, in whole or in part, for scholarly purposes may be granted by the supervisor of my thesis work or, in his absence, by the Head of the School of Public Health or the Dean of the College of Graduate Studies and Research. It is understood that any copying or publication or use of this thesis or parts thereof for financial gain shall not be allowed without my written permission. It is also understood that due recognition shall be given to me and to the University of Saskatchewan in any scholarly use which may be made of any material in my thesis.

Requests for permission to copy or to make other use of material in this thesis in whole or part should be addressed to:

Dean of the College of Graduate and Postdoctoral Studies  
University of Saskatchewan  
116 Thorvaldson Building, 110 Science Place  
Saskatoon, Saskatchewan S7N 5C9, Canada

OR

School of Public Health  
University of Saskatchewan  
104 Clinic Place  
Saskatoon, Saskatchewan S7N 2Z4, Canada

## ACKNOWLEDGEMENTS

I would like to express the deepest appreciation and gratitude to my supervisor, Dr. Jim Xiang, for his continuous support throughout my undergraduate and graduate studies. Without his valuable guidance, encouragement and immense knowledge this thesis would not have been completed. I would also like to thank my advisory committee members, Dr. Suresh Tikoo and Dr. Qiang Liu, for their enthusiastic encouragement and valuable feedback in this research. I would like to extend my appreciation to Lisa Rendall Breast Cancer Graduate Student Scholarship of Saskatchewan Cancer Agency.

A special thanks to our post-doctoral fellow, Dr. Aizhang Xu, for all his support and help in learning laboratory techniques and data analysis. In addition, I would like to thank my lab members Dr. Anjuman Ara and Dr. Zhaojia Wu for all their help and support in my research and our cluster manager Mark Boyd for all his help.

Most significantly, I would not have been able to successfully complete my graduate studies without the love and support of my family, especially my mother, Amna Hamid.

## ABSTRACT

Cancer is a leading cause of death worldwide, taking nearly 10 million lives each year. CD8<sup>+</sup> T cytotoxic lymphocytes (CTLs) play a critical role in human immunity against cancer. Irreversible electroporation (IRE) is a new cancer ablation technology that utilizes electric current to induce tumor cell apoptosis. Compared to other thermal ablative techniques, IRE is safer to use around sensitive structures such as blood vessels or nerves. Although IRE has been successful as a cancer ablation therapy, patients often die due to the recurrence of residual tumors. Therefore, it is critical to improve tumor ablation technology to achieve better therapeutic outcomes for cancer patients. Toll-like receptors (TLRs) are conserved pattern recognition receptors (PRRs) that recognize microbial compounds and stimulate innate and adaptive immune responses. TLR3 agonist Poly I:C (pIC) and TLR9 agonist CpG are known to stimulate strong CD4<sup>+</sup> Th1 and CD8<sup>+</sup> CTL responses and have been used in combination with other treatments to improve cancer immunotherapy. Programmed death 1 (PD-1) receptors are expressed on activated CTLs, and the interaction between PD-1 and its ligand (PDL-1) on activated CTLs leads to CTL exhaustion and inhibition of CTL-mediated anti-tumor immunity. PD-1 blockade by monoclonal antibodies against PD-1 or PDL-1 blocks their interaction, relieves T cell inhibition and enhances T cell responses. In this study, we developed a mouse model bearing large primary (300 mm<sup>3</sup>) and medium distant (100 mm<sup>3</sup>) EG7 lymphomas engineered to express ovalbumin (OVA) as a nominal tumor antigen. We established experimental protocols including IRE alone and IRE combined with TLR3/9 agonists (poly I:C/CpG) (IRE+pIC/CpG) or PD-1 blockade (IRE+PD-1 blockade) or both (IRE+Combo) to investigate the therapeutic effects on primary and distant EG7 tumors and conversional effects on an immunotolerant tumor microenvironment (TME). A dominant immunosuppressive TME is created by tumor cells to promote tumor progression and inhibit effective anti-tumor immune responses. We demonstrate that IRE alone stimulates very weak OVA-specific CD8<sup>+</sup> T cell responses and does not inhibit primary tumor growth. IRE+pIC/CpG synergistically stimulates more efficient OVA-specific CD8<sup>+</sup> T cell responses and inhibition of primary tumor growth than IRE+PD-1 blockade. IRE+pIC/CpG plays a major role in the modulation of immune cell profiles (ICP), but a minor role in the down-regulation of PDL-1 expression in the TME, and *vice versa* for IRE+PD-1 blockade. IRE+Combo cooperatively induces potent OVA-specific CD8<sup>+</sup> T cell immunity and rescues exhausted intratumoral CD8<sup>+</sup> T cell, leading to eradication of not only primary but also untreated concomitant distant tumors and lung metastases. IRE+Combo

efficiently modulates ICPs, as evidenced by a reduction of immunotolerant type-2 macrophages (M2), myeloid-derived suppressor cells (MDSCs), plasmacytoid dendritic cells (pDCs) and CD4<sup>+</sup>Foxp3<sup>+</sup> regulatory T (Treg) cells and an increase of immunogenic M1, CD169<sup>+</sup> macrophages, type-1 conventional dendritic cells (cDC1) and CD8<sup>+</sup> T cells, leading to conversion of immunotolerance in not only primary but also untreated distant TMEs. IRE+Combo also shows effective therapeutic results in two breast cancer models. Targeting immunotolerant subsets in the TME represent a future direction towards improved immunotherapy and IRE-ablated cancer therapy. Therefore, our IRE+Combo protocol capable of eradicating both primary and distant tumors as well as lung metastases *via* converting immunotolerant TME may become a promising strategy for cancer IRE-ablation therapy.

## TABLE OF CONTENTS

<b>PERMISSION TO USE.....</b>	<b>I</b>
<b>ACKNOWLEDGEMENTS.....</b>	<b>II</b>
<b>ABSTRACT.....</b>	<b>III</b>
<b>TABLE OF CONTENTS.....</b>	<b>V</b>
<b>LIST OF FIGURES .....</b>	<b>VIII</b>
<b>LIST OF ABBREVIATIONS .....</b>	<b>X</b>
CHAPTER 1 LITERATURE REVIEW.....	1
1.1 Overview of the immune system.....	1
1.1.1 Innate immunity.....	1
1.1.1.1 Innate defence components.....	1
1.1.1.2 Mechanism of innate immune response.....	2
1.1.2 Adaptive immunity.....	3
1.1.2.1 Adaptive immunity components.....	3
1.1.2.2 CD4 <sup>+</sup> T cells.....	3
1.1.2.3 CD8 <sup>+</sup> T cells .....	4
1.1.2.4 Regulatory CD4 <sup>+</sup> T cells.....	4
1.1.2.5 Mechanism of immune response produced by CD4 and CD8 T cells.....	4
1.1.3 Link between innate and adaptive immunity.....	5
1.1.4 Anti-tumor immunity.....	5
1.2 Toll-like receptors.....	6
1.2.1 Role of TLRs in our immune defence.....	6
1.2.2 CpG as TLR9 agonist.....	6
1.2.3 Poly IC as TLR3 agonist.....	7
1.3 PD-1 blockade.....	8
1.3.1 PD-1/PDL-1 interaction.....	8
1.3.2 PD-1 blockade using anti-PDL-1 Ab .....	8
1.4 Tumor microenvironment.....	10
1.4.1 Overview of immunotolerant TME.....	10
1.4.2 Immunotolerant cells in TME.....	10

1.4.3 Immunogenic cells in TME.....	11
1.4.4 Contribution of tumor cells to immunotolerant TME.....	12
1.5 Tumor ablation.....	13
1.5.1 Types of tumor ablation therapy .....	13
1.5.1.1 IRE ablation .....	13
1.6 Current IRE combinational therapy for cancer.....	14
References.....	16
CHAPTER 2 HYPOTHESIS AND OBJECTIVES.....	23
CHAPTER 3 DISTINCT ROLE BUT COOPERATIVE EFFECT OF TLR3/9 AGONISTS AND PD-1 BLOCKADE IN CONVERTING IMMUNOTOLERANT MICROENVIRONMENT OF IRREVERSIBLE ELECTROPORATION-ABLATED TUMORS.....	24
3.1 Abstract.....	25
3.2 Introduction.....	26
3.3 Materials and Methods.....	29
3.3.1 Reagents, cell lines and animals.....	29
3.3.2 IRE ablation combined with TLR3/9 agonists and PD-1 blockade.....	29
3.3.3 CD8 <sup>+</sup> T cell depletion study.....	31
3.3.4 Analysis of OVA-specific CD8 <sup>+</sup> T cell responses.....	31
3.3.5 Flow cytometric analysis of tumor-infiltrating immune cell profiling.....	32
3.3.6 CD8 <sup>+</sup> T cell proliferation and cytotoxicity assays.....	33
3.3.7 Tumor-draining lymph node cell analysis.....	34
3.3.8 Cytokine ELISA analyses.....	35
3.3.9 Immunohistochemistry.....	35
3.3.10 Statistical analysis.....	35
3.4 Results.....	36
3.4.1 TME immunotolerance increases with tumor stage.....	36
3.4.2 IRE ablation induces massive tumor cell apoptosis and weak OVA-specific CD8 <sup>+</sup> T cell responses, but does not induce any significant inhibition of tumor growth in large tumors.....	39
3.4.3 Combo treatment alone only induces very weak OVA-specific CD8 <sup>+</sup> T cell responses.....	41
3.4.4 PD-1 blockade enhances OVA specific CD8 <sup>+</sup> T cell responses and antitumor immunity in IRE-treated tumors.....	43

3.4.5 TLR3/9 agonists synergistically stimulate potent OVA-specific CD8 <sup>+</sup> T cell responses and strong antitumor immunity in IRE-treated tumors.....	44
3.4.6 TLR3/9 agonists play a major role in modulating immune cell profiles and a minor role in reducing PDL-1 expression in TME and <i>vice versa</i> for PD-1 blockade in IRE-treated tumors.....	44
3.4.7 IRE+Combo cooperatively stimulates potent OVA-specific CD8 <sup>+</sup> T cell responses leading to complete eradication of primary tumors.....	46
3.4.8 IRE+Combo potently modulates immune cell profiling and significantly downregulates PDL-1 expression in TME in IRE-treated tumors.....	49
3.4.9 IRE+Combo edits tolerant immune and tumor cells for less suppression and induces a systemic decrease of immune tolerance.....	51
3.4.10 IRE+Combo promotes tumor-infiltrating CD4 <sup>+</sup> and CD8 <sup>+</sup> T cells.....	54
3.4.11 IRE+Combo promoted tumor-infiltrating CD8 <sup>+</sup> T cells are functionally effective.....	56
3.4.12 IRE+Combo promotes cDC1 and effector CD8 <sup>+</sup> T cells in tumor-drainage lymph nodes and a long term CD8 <sup>+</sup> T cell memory.....	57
3.4.13 IRE+Combo ablation eradicates distant tumors <i>via</i> modulating its immunotolerant TME and promoting tumor-infiltrating CD4 <sup>+</sup> and CD8 <sup>+</sup> T cells.....	59
3.4.14 IRE+Combo in primary tumors eradicates tumor lung metastases.....	64
3.4.15 IRE+Combo's potent therapeutic effect in two mouse breast cancer models.....	66
3.5 Discussion.....	71
References.....	76
Conflict of interest.....	81
Acknowledgements.....	81
CHAPTER 4 CONCLUSIONS AND FUTURE DIRECTIONS.....	82
References.....	85



## LIST OF FIGURES

<b>Figure 3.1</b> Enhanced immunotolerant TME is associated with tumor progression.....	37
<b>Figure 3.2</b> IRE ablation induces tumor-cell apoptosis but weak OVA-specific CD8 <sup>+</sup> T cell responses and is ineffective in inhibition of tumor growth.....	40
<b>Figure 3.3</b> IRE combined with PD-L1 blockade and TLR3/9 agonists results in potent OVA-specific CD8 <sup>+</sup> T cell responses and antitumor immunity.....	42
<b>Figure 3.4</b> CD8 <sup>+</sup> T cell depletion assay.....	45
<b>Figure 3.5</b> IRE combined with PD-L1 blockade and TLR3/9 agonists modulates immune cell profiling in TME.....	47
<b>Figure 3.6</b> IRE combined with PD-L1 blockade and TLR3/9 agonists downregulates PDL-1 expression in TME.....	50
<b>Figure 3.7</b> IRE+Combo modulates immune cells and cytokines in blood and promotes CD8 <sup>+</sup> T cells in IRE+Combo-treated tumor tissues and in tumor-drainage lymph nodes.....	52
<b>Figure 3.8</b> IRE+Combo promotes tumor-infiltrating CD4 <sup>+</sup> and CD8 <sup>+</sup> T cells in TME.....	55
<b>Figure 3.9</b> IRE+Combo promoted functionally effective tumor-infiltrating CD8 <sup>+</sup> T cells.....	56
<b>Figure 3.10</b> IRE+Combo promotes cDC1 and effector CD8 <sup>+</sup> T cells in tumor-drainage lymph nodes.....	58
<b>Figure 3.11</b> IRE+Combo induces “abscopal” effect on eradication of distant tumors by converting immunotolerant TME in distant tumors.....	60
<b>Figure 3.12</b> IRE+Combo treatment of primary tumors inhibits lung tumor metastasis.....	65
<b>Figure 3.13</b> IRE+Combo effectively eradicates tumors or significantly inhibits tumor growth in two mouse breast cancer models.....	66

**Supplementary Figure 3.14** A systemical analysis of immune cell profiling in TME by flow cytometry.....67

**Supplementary Figure 3.15** Analysis of peripheral blood OVA-specific CD8<sup>+</sup> T cell responses by flow cytometry.....69

**Supplementary Figure 3.16** A systemical analysis of tumor-drainage lymph nodes by flow cytometry.....70

## LIST OF ABBREVIATIONS

Ab	Antibody
APCs	Antigen presenting cells
cDC1	Conventional dendritic cell type 1
CTLs	Cytotoxic T lymphocytes
CTLA-4	Cytotoxic T-lymphocyte-associated protein 4
DCs	Dendritic cells
ds RNA	Double-stranded RNA
ECM	Extracellular matrix
FDA	Food and Drug Administration
Foxp3	Forkhead box 3
FLT3L	FMS-like tyrosine kinase 3 ligand
GM-CSF	Granulocyte macrophage colony-stimulating factor
HIFU	High intensity focused ultrasound
ICP	Immune cell profiling
ICOS	Inducible T-cell costimulator
IDO	Indole 2,3-dioxygenase
IFN	Interferon
Ig	Immunoglobulin
IL	Interleukin
iNOS	Inducible nitric oxide synthase
IRE	Irreversible electroporation
LAPC	Locally advanced pancreatic carcinoma
LN	Lymph node
LPS	Lipopolysaccharides
mAb	Monoclonal antibody
MAC	Membrane attack complex
M-CSF1R	Macrophage colony-stimulating factor 1 receptor

MHC	Major Histocompatibility
MDSCs	Myeloid-derived suppressive cells
M1	Macrophage type 1
M2	Macrophage type-2
MMP	Matrix metalloproteinase
MWA	Microwave ablation
NK	Natural killer
ODNs	Oligonucleotides
OVA	Ovalbumin
PAMPs	Pathogen associated molecular patterns
pDCs	Plasmacytoid Dendritic cells
PD-1	Programmed death 1
PDL-1	Programmed death 1 Ligand
Poly-IC	Polyinosinic-polycytidic acid
RFA	Radiofrequency ablation
PRRs	Pattern recognition receptors
ROS	Reactive oxygen species
STING	Stimulator of interferon genes
TAMs	Tumor-associated macrophages
TCR	T cell receptor
TGF	Transforming growth factor
Th	T helper
TILs	Tumor-infiltrating lymphocytes
TIM-3	T-cell immunoglobulin and mucin domain 3
TLR	Toll-like receptor
TME	Tumor microenvironment
TNF	Tumor necrosis factor
Treg	Regulatory T cell
VEGF	Vascular endothelial growth factor

# **CHAPTER 1 LITERATURE REVIEW**

## **1.1 Overview of the immune system**

The immune system is a group of tissues, cells and molecules responsible for host defence against invading microbes. A fundamental part of the immune system is distinguishing between self and non-self, which is critical to avoid injury of host cells. Two types of immune responses are used by the host: innate and adaptive immune responses [1]. The innate immune response is generated within minutes to hours from exposure to a pathogen. It is a non-specific response that effectively eliminates most invading microbes. On the other hand, the induction of adaptive immune response requires more time because immune cells such as T and B cells need to undergo clonal expansion to perform their effector functions. Innate and adaptive immune systems are linked together, and both are required for an efficient immune response [2].

### **1.1.1 Innate immunity**

#### **1.1.1.1 Innate defence components**

The innate immune system consists of various cellular and molecular components.

##### **(i) Cellular components**

###### **➤ Phagocytes**

- Phagocytes, including neutrophils and macrophages, are leukocytes that recognize pathogen-associated molecular patterns (PAMPs) by their non-specific pathogen recognition receptors (PRRs). Upon recognition, they ingest and destroy pathogens by phagocytosis. Pathogens are eliminated inside lysosomes by reactive oxygen species (ROS) and other hydrolytic enzymes such as lysozymes, cathepsins and proteases [2, 3]. Neutrophils are short lived cells that constantly circulate in the bloodstream and immediately respond to any breach of the epithelial barrier. They also induce the inflammation process to recruit other immune cells to the site of

infection. Macrophages are long-lived cells that reside in many tissues; in addition to their microbicidal activity, they also repair any tissue damage [2, 3].

- Dendritic cells (DCs) are a special class of phagocytes that also function as professional antigen presenting cells (APCs), which prime naïve T lymphocytes to become effector cells. Dendritic cells are essential cells that link innate and adaptive immunity [4, 5].
- Mast cells/basophils are both granulocytes that contain cytoplasmic granules filled with histamine and other mediators. Mast cells reside in tissues while basophils circulate in the blood; both express high affinity receptors for Immunoglobulin (Ig) E antibody (Ab). When an allergen binds IgE on its surface, these cells release histamine and induce inflammation [5].
- Eosinophils are granulocytes that circulate in the blood to protect the host from parasites [5].
- Natural killer (NK) cells are lymphocytes that function to combat intracellular infection. They recognize and directly kill infected cells by inducing cell apoptosis using perforin and granzyme B. They also secrete interferon (IFN)  $\gamma$  to induce an anti-viral state and increase the phagocytic ability of macrophages to kill an ingested pathogen [5].

(ii) Soluble factors

These include complement, cytokines and other plasma proteins [5].

### **1.1.1.2 Mechanism of innate immune responses**

Cells involved in innate immunity have non-specific receptors called PRRs. These receptors can recognize PAMPs such as lipopolysaccharides (LPS), viral DNA, or viral RNA. The binding of these PAMPs to PRRs triggers a signalling cascade that drives the expression of genes coding inflammatory cytokines such as interleukin (IL)-6, IL-12, IFN  $\gamma$ , and tumor necrosis factor (TNF)- $\alpha$ . These cytokines induce inflammation, which is essential to recruit other immune cells to the site of infection [6-8]. The first group of cells to respond are neutrophils, which eliminate pathogens by phagocytosis. Neutrophils also secrete chemokines that attract other immune cells to the infection site. Macrophages and DCs are the cells eliminating pathogens in tissues. NK cells kill viral infected cells and induce an antiviral effect. Phagocytes also ingest microbes that are tagged

with Abs, a process called opsonization. The complement is activated through a cascade involving proteolytic cleavage of different plasma proteins. Activated complement functions to destroy pathogens tagged with IgM via the membrane-attack complex (MAC) [6-8].

## **1.1.2 Adaptive immunity**

### **1.1.2.1 Adaptive immunity components**

(i) Humoral immunity: A type of adaptive immune response in which Abs are responsible for eliminating microbes or toxins. B lymphocytes differentiate into plasma cells, which produce specific Abs that bind to specific antigens on microbes and tag them for elimination by phagocytes [9].

(ii) Cellular immunity: This type of adaptive immunity is mediated mainly by clusters of CD4<sup>+</sup>, CD8<sup>+</sup>, CD4<sup>+</sup>Foxp3<sup>+</sup> regulatory T (Treg) and B cells. Activation of naïve CD4<sup>+</sup> T cells to become T helper (Th) cells can help DC's activation of CD8<sup>+</sup> T cells. Activated CD8<sup>+</sup> T become effector cytotoxic T lymphocytes (CTLs). These CTLs effectively kill infected cells and thus eliminate the reservoir of infection. The activation of B cells also requires the involvement of CD4<sup>+</sup> Th cells for differentiation into plasma cells capable of antibody secretion [10].

#### **1.1.2.2 CD4<sup>+</sup> T cells**

CD4<sup>+</sup> T cells are a type of T lymphocytes matured in the thymus. They have T cell receptor (TCRs) that recognize specific antigens associated with major histocompatibility complex (MHC)-II presented by APCs, mainly DCs. This antigen presentation occurs in the lymph node (LN) where DCs activate naïve CD4<sup>+</sup> T cells by presenting specific antigens associated with MHC-II to CD4<sup>+</sup> TCRs, leading to becoming effector Th cells [10, 11]. CD4<sup>+</sup> Th cells can be divided into two types of Th immune responses, Th1 and Th2. Th1 cells produce cytokines such as IFN  $\gamma$  and IL-2 to promote CD8<sup>+</sup> CTL responses against tumor and infectious diseases while Th2 cells produce cytokines such as IL-4 and IL-10 and promote allergy diseases [10, 11].

### **1.1.2.3 CD8<sup>+</sup> T cells**

Similar to CD4<sup>+</sup> T cells, CD8<sup>+</sup> T lymphocytes are also matured in the thymus. In the LN, DCs present specific antigens associated with MHC I to TCRs of CD8<sup>+</sup> T cells, leading to proliferation and differentiation of CD8<sup>+</sup> T cells into effector CTLs [3, 10]. CD8<sup>+</sup> CTLs can recognize specific antigens on target cells such as infected or transformed cells and directly kill them by perforin- and granzyme B-mediated apoptosis. CD8<sup>+</sup> T cells play an important role in defence immunity against tumors and infectious diseases [3, 10].

### **1.1.2.4 CD4<sup>+</sup>Foxp3<sup>+</sup> Treg cells**

CD4<sup>+</sup>Foxp3<sup>+</sup> Treg cells are a type of natural polyclonal CD4<sup>+</sup> T cell necessary for maintaining immune homeostasis and peripheral tolerance. They complete their differentiation in the thymus, and then migrate to peripheral tissues. They express transcription factor forkhead box 3 (Foxp3) and secrete inhibitory cytokines such as transforming growth factor (TGF)- $\beta$  and IL-10 [10]. CD4<sup>+</sup>Foxp3<sup>+</sup> Treg cells suppress over-reactive immune responses and protect the host from autoimmune diseases through their modulation of T cells and DCs in a cell-to-cell contact-dependent fashion [12].

### **1.1.2.5 Mechanism of immune responses mediated by CD4<sup>+</sup> and CD8<sup>+</sup> T cells**

CD4<sup>+</sup> and CD8<sup>+</sup> T cell activation requires two signals: one through TCR, which recognizes specific antigens presented by DCs, and the other through CD28 for co-stimulatory molecule CD80. Both signals are essential for an effective immune response, and the lack of co-stimulatory signals leads to T cell anergy [13, 14]. Upon activation, T cells undergo clonal expansion and become effector cells that secrete effector cytokines. CD4<sup>+</sup> T cells recognize antigens in the context of MHC II molecules and become effector Th cells involved and required in both humoral and cell-mediated immunity [8]. CD8<sup>+</sup> T cells, on the other hand, recognize antigens in the context of MHC I molecules and become effector CTLs that are mainly required in cell-mediated immunity [13, 14].



### **1.1.3 Link between innate and adaptive immunity**

The immune cells of the innate and adaptive systems work cooperatively manner to defend the host against pathogens. Activation of innate immune cells by PAMPs leads to stimulation of adaptive immune responses. A critical example of this cooperation is DCs, the most potent APCs for activating naïve T cells [15, 16]. APCs capture microbial antigens and display them to CD4<sup>+</sup> and CD8<sup>+</sup> T cells, leading to their cell proliferation and differentiation. Mature and activated DCs in LNs can present specific antigens associated with MHC II or I to CD4<sup>+</sup> and CD8<sup>+</sup> T cells, respectively. Based upon different cytokines secreted by DCs, active DCs drive the proliferation process and dictate the type of developing CD4<sup>+</sup> and CD8<sup>+</sup> T cell immune responses [15, 16].

### **1.1.4 Anti-tumor immunity**

CD8<sup>+</sup> CTLs are considered the main subset of immune cells for fighting tumor cells. When primed with their specific antigen by DCs, naïve CD8<sup>+</sup> T cells become effector CTLs. These CTLs migrate into the tumor site under the influence of chemokines CXCL9 and CXCL10 secreted by DCs [17]. Activated CTLs can directly kill tumor cells through perforin- and granzyme-mediated apoptosis. Tumor cells can inhibit activated CTLs by expressing programmed death ligand 1 (PDL-1) on their surface, which binds to the inhibitory PD1 on CTLs, leading to CTL dysfunction. This is an important mechanism used by the tumor cells to effectively evade the immune response [18].

## **1.2 Toll-like receptors**

### **1.2.1 Role of TLRs in our immune defence**

A conserved group of proteins called Toll-like receptors (TLRs) is a type of PRR located on the plasma or endosomal membrane of host cells. They can recognize a wide range of PAMPs such as LPS, flagellin, viral RNA or viral DNA. Interaction between these receptors and their ligands triggers a signaling pathway that produces different cytokines to activate various innate immune cells. As a result, these activated cells, such as DCs, can efficiently prime T cells to stimulate adaptive immune responses [19, 20].

### **1.2.2 CpG as TLR9 agonist**

CpG oligodeoxynucleotides (ODNs) are short synthetic oligonucleotides with unmethylated CpG motifs that function as TLR9 agonists. CpG binds to TLR9 on the endosomes of dendritic cells and macrophages, leading to DC activation and strong DC-induced Th1 immune responses [21]. Intratumoral administration of CpG ODNs represents an effective way to stimulate anti-tumor immune responses because it induces intratumoral DC activation, leading to activation of tumor-specific CD8<sup>+</sup> CTLs and NK cell responses [22]. In addition, intratumoral administration of CpG also effectively reverses the suppressive activity of myeloid-derived suppressor cells (MDSCs) by stimulating their conversion into the more immunogenic subtype tumoricidal type-1 macrophages (M1) [23].

Two studies using intratumoral CpG are in phase I clinical trials, in which CpG is being used to treat skin cancer. One study has shown improvement in the generation of tumor-specific CD8<sup>+</sup> T cells, which led to systemic tumor regression when CpG was administered alone or combined with radiotherapy; the other has shown the induction of partial tumor regression [24-26]. Combining CpG with cytotoxic T-lymphocyte antigen 4 (CTLA-4) blockade was found to have a synergistic anti-tumor effect, promoting rejection of bi-laterally implanted B16-Ovalbumin (B16-Ova) melanoma [27]. Intratumoral injection of CpG-ODNs combined with low doses of radiotherapy applied to treat patients with lymphoma has entered phase I/II clinical trials and has shown regression of untreated tumors (abscopal effect); this study indicates the administration of CpG

may offer an efficient way to amplify an active systemic anti-tumor immunity [25]. CpG was one of the first adjuvants to be combined with tumor ablation [28]. Induction of long-term immune memory was shown in a B16-OVA melanoma model; when CpG was combined with cryoablation, 50% of mice survived upon a re-challenge study [29, 30]. This combinatorial approach was also applied with other ablative therapies such as radiotherapy and High intensity focused ultrasound (HIFU) [31-33].

### **1.2.3 Poly IC as TLR3 agonist**

Double-stranded RNA (dsRNA) are components of viruses only; therefore, they naturally stimulate the PRRs on host innate immune cells. Polyinosinic-polycytidylic acid (Poly-IC) is a synthetic dsRNA that functions as a TLR3 agonist, binding to TLR3 on DC and macrophages endosomes and leading to the production of IL-12 and stimulation of strong CD4<sup>+</sup> Th1 responses [34]. Poly-IC has been used as a vaccine adjuvant for cancer immunotherapy to improve the immunogenicity of these vaccines. This results in the stimulation of innate and adaptive immune responses by Poly-IC and the modulation of immunosuppressive tumor microenvironment (TME), which promotes the vaccine-induced anti-tumor immune response [35].

The combination of Poly-IC and radiotherapy with the injection of FMS-like tyrosine kinase 3 ligand (FLT3L) in the A20 lymphoma tumor model has been shown to promote DC recruitment and enhance anti-tumor immune responses [36]. Other studies with Poly-IC combined with radiotherapy have also shown promising therapeutic effects, such as tumor regression in primary and distant tumors and an increased number of surviving mice in different tumor models [37, 38]. Poly IC has also been combined with CD40 monoclonal antibody (mAb), which results in the induction of the largest number of OVA-specific T cells compared to other TLR agonists [39]. Many studies involving the combination of Poly-IC with different TLR agonists such as TLR7 or TLR9 have yielded promising results. For example, treatment of B16-OVA melanoma lung metastasis using aerosols containing both Poly-IC and CpG reduced lung metastases and stimulated NK cell cytotoxic activity [40].

## **1.3 PD-1 blockade**

### **1.3.1 PD-1/PDL-1 interaction**

PD-1 is a surface inhibitory protein that is intrinsically expressed on activated T cells, B cells, NK cells, macrophages and DCs to regulate their induced immune responses. Its ligand PDL-1 is intrinsically expressed on APCs and endothelial, epithelial and lymphoid cells [18, 41]. Tumor cells and other immunosuppressive immune subsets in the TME express PDL-1 on their cell surfaces. The interaction of PD1/PDL-1 triggers a signalling pathway to inhibit activated CD8<sup>+</sup> T cells, which suppresses their anti-tumor immune response. This inhibition of activated CD8<sup>+</sup> T cell-mediated immune responses is a significant obstacle to cancer immunotherapy [18].

### **1.3.2 PD-1 blockade using anti-PDL-1 Ab**

The new approach of targeting PD1/PDL-1 interaction has gained a lot of interest in the scientific community as many studies have shown the anti-PDL-1 Ab can enhance T cell activity and inhibit tumor growth [42]. Antibodies targeting the immune checkpoint PD1, its ligand PDL-1 or both have been applied in many cancer treatments. Phase III clinical trial studies involving nivolumab, an antibody against PD1, demonstrate a higher survival rate among patients with advanced melanoma using this anti-PD1 Ab protocol after one year. Therefore, nivolumab has been approved by the Food and Drug Administration (FDA) to treat advanced melanoma patients [43, 44]. Other PD1 and PDL-1 drugs have also subsequently been approved by the FDA for cancer treatment, such as pembrolizumab and cemiplimab as anti-PD1 drugs and durvalumab, atezolizumab and avelumab as anti-PDL-1 drugs [45].

Although successful, these PD1/PDL-1 Abs showed limited therapeutic efficacy as not all cancer patients respond to them. Therefore, different approaches to combining this PD1 blockade protocol with other agents are being developed to improve their effectiveness as a cancer therapy. For example, PD1 blockade has been combined with other immune checkpoint inhibitors, chemotherapy, and immunostimulatory cytokines [46]. A study by Takeda et al. to develop a vaccine adjuvant for cancer showed that combining ARNAX, a TLR3 agonist, with anti-PDL-1 Ab

reduces the resistance to PD-1 blockade and stimulates tumor-specific CTL responses [47]. Combining the blockade of both PD-1 and CTLA-4, another immune checkpoint, showed amplified anti-tumor immune responses compared to monotherapy with either one [48]. Pre-clinical studies that used different mouse tumor models have demonstrated improved therapeutic outcomes when radiotherapy is combined with PD-1 blockade. The use of radiotherapy or chemotherapy has proven successful in relieving tumor burden and providing tumor-associated antigens for T cell activation [48].

Similarly, tumor ablative techniques such as radiofrequency ablation (RFA), when combined with PD-1 blockade, have shown an increase in tumor-specific T cell responses and growth inhibition of distant tumors. Another combinatorial study demonstrated that incomplete RFA tumor ablation lowers the therapeutic efficacy of cancer immunotherapy by anti-PD-1 Ab [49]. A recent study using a pancreatic mouse tumor model showed combining irreversible electroporation (IRE) with anti-PD-1 Ab prolongs mouse survival, as well as enhanced tumor infiltration by CD8<sup>+</sup> T cells and induction of a long-term memory immune response [50]. Many other studies applying different combinatorial approaches that aim to overcome the resistance of PD-1 blockade by cancer patients are currently underway [46].

## **1.4 Tumor microenvironment**

### **1.4.1 Overview of an immunotolerant TME**

The TME is a complex heterogeneous environment that consists of extracellular matrix (ECM), stromal cells (such as fibroblasts, mesenchymal stromal cells, pericytes, occasionally adipocytes, and blood and lymphatic vascular networks) and immune cells (including T and B lymphocytes, NK cells and tumor-associated macrophages (TAMs), and different subsets of tolerant immune cells) [51, 52]. Tumor cells are actively interacting with all these cells within the TME as well as the ECM. The interaction between a variety of immune and non-immune cells within the TME and the effect of their secreted molecules results in an immunosuppressive and pro-angiogenic environment [51, 52]. As a result of this suppressive TME, tumor cells can successfully evade any immune surveillance. The infiltration of inflammatory immune cells such as macrophages, DCs, lymphocytes, and NK cells at an early stage of tumor development is crucial to inhibit tumor growth. However, this anti-tumor immune response is inhibited by immunosuppressive immune cells such as MDSCs, type 2-polarized macrophages (M2), and CD4<sup>+</sup>Foxp3<sup>+</sup> T reg cells in well-developed tumors [51, 52].

### **1.4.2 Immunotolerant cells in the TME**

Tumor cells can recruit bone marrow-derived cells and induce their differentiation into cell subsets that support and facilitate tumor survival [51]. TAMs promote tumor growth by stimulating angiogenesis, invasion, and metastasis. In the TME, these TAMs can differentiate into two subsets of macrophages: M1 and M2. The anti-inflammatory M2 cells contribute to an immunosuppressive TME by secreting anti-inflammatory cytokines such as TGF $\beta$  and IL-10. They promote tumor progression and metastasis through their ability to induce angiogenesis and tissue remodelling. M2 cells also produce chemokine CCL2 for recruitment of suppressor CD4<sup>+</sup>Foxp3<sup>+</sup> Treg cells [53]. MDSCs are one of the significant immunosuppressive populations in the TME. They inhibit the anti-tumor immune response mounted by CD8<sup>+</sup> T cells through the secretion of arginase, nitric oxide synthase (iNOS), and inhibitory cytokines such as TGF $\beta$  and IL-10 [54, 55]. MDSCs also stimulate the expansion of CD4<sup>+</sup>Foxp3<sup>+</sup> Treg cells in the TME through the secretion of indole 2,3-

dioxygenase (IDO). They also promote angiogenesis and metastases via matrix metalloproteinase-9 (MMP9), prokineticin-2, and vascular endothelial growth factor (VEGF) production [54, 55]. Other important suppressor cells in the TME are CD4<sup>+</sup>Foxp3<sup>+</sup> Treg cells, which suppress activated CTLs by secreting inhibitory cytokines such as TGFβ and IL-10; they also stimulate the expression of inhibitory molecules such as PD-1 on the surface of activated CD8<sup>+</sup> T cells. The interaction between PD-1-expressing activated T cells and PDL-1 widely expressed on tumor cells, MDSCs, and M2 cells leads to T cell inhibition and suppression of antitumor immunity [12]. Plasmacytoid dendritic cells (pDC) contribute to the immunosuppressive TME by inducing suppressor CD4<sup>+</sup>Foxp3<sup>+</sup> Treg cells via the inducible T-cell costimulator (ICOS)/ICOSL pathway or the production of IDO [56].

### **1.4.3 Immunogenic cells in the TME**

Pro-inflammatory M1 cells are considered one of the essential immunogenic cell subsets within the TME. They secrete pro-inflammatory cytokines such as TNFα and IL-2 to induce inflammation and recruit other effector immune cells to the TME. They also produce reactive oxygen/nitrogen species to kill tumor cells [53, 55]. Tumor infiltrating lymphocytes (TILs), especially CD8<sup>+</sup> T cells, are critical for the antitumor response. Antigen-specific CTLs can effectively recognize tumor cells and directly kill them. Naïve CD8<sup>+</sup> T cells are first primed with their specific tumor antigens in the LN by DCs to become effector CTLs. They undergo clonal expansion, migrate to the TME, and recognize and kill tumor cells [55, 57, 58]. A superior stimulator of CD8<sup>+</sup> T cells is the conventional dendritic cell type-1 (cDC1). These cells migrate to tumor-draining LNs and prime naïve CD8<sup>+</sup> T cells with their specific tumor antigens, leading to CTL activation. These cells produce CXCL9 and CXCL10 chemokines that can attract activated T cells to the TME. They also make IL-12 to stimulate CD8<sup>+</sup> T cell proliferation and enhance their effector function. Intratumoral cDC1 can thus effectively cross-present specific tumor antigens to and activate CD8<sup>+</sup> T cells within the TME [59-61].

#### **1.4.4 Contribution of tumor cells to an immunotolerant TME**

Tumor cells use various mechanisms to evade immune surveillance and promote their survival. They affect the structure of the ECM through modification of its protein components. This modulation of the ECM provides tumor cells with access to cell proliferation signals and helps them to avoid any growth suppressors, inducing tumor angiogenesis, invasion and metastasis [52, 62]. Tumor cells shift to anaerobic glycolysis over oxidative glycolysis to overcome the lack of oxygen and nutrients. Acidosis is the result of this shift; however, tumor cells use a proton extrusion mechanism to alter the PH. Tumor cells can survive these harsh conditions, but the hypoxia and acidosis in TME create a toxic environment in which other immune cells cannot survive [52, 62]. In the TME, tumor cells are able to stimulate immunosuppressive cells by secreting different cytokines, lipid mediators, and growth factors that target these cell populations. To support their growth and survival, tumor cells promote angiogenesis to provide a continuous supply of oxygen and nutrients. They produce VEGF, which acts on the nearby endothelial cells to facilitate the formation of new blood vessels [52, 63]. Moreover, tumor cells use the new vasculature to monitor any cells and molecules entering the TME. Tumor cells also secrete IDO, which works to catabolize tryptophan to form kynurenine. This promotes the differentiation of naïve T cells into CD4<sup>+</sup>Foxp3<sup>+</sup> Treg cells and increases suppressor functions of MDSCs via upregulation of IL-6 expression [51, 64]. The chronic inflammation within the TME induces T cell exhaustion, leading to their dysfunction [51, 58]. PDL-1<sup>+</sup> tumor cells also stimulate the expression of PDL-1 on MDSCs and M2 cells. The interaction between PD1-expressing activated T cells and PDL-1 on these cells leads to T cell inhibition and exhaustion [51, 58]. All of these factors create an immunosuppressive TME that enables tumor cells to successfully evade immune clearance.



## **1.5 Tumor ablation**

### **1.5.1 Types of tumor ablation**

Tumor ablation techniques have evolved due to the growing demand for alternative and less invasive methods for cancer treatment. Different types of tumor ablation include RFA, cryoablation, microwave ablation (MWA), HIFU, and, more recently, IRE. Except for IRE, these techniques depend on heat (RFA) or cold (cryoablation) to cause cell death. Although beneficial, these ablative methods cause some adverse effects due to their dependence on thermal energy to induce cell death in surrounding tissues, which can include important ducts, nerves, and vessels [65].

#### **1.5.1.1 IRE ablation**

IRE is a new technology for tumor ablation therapy in which an electric current punches irreversible nano-holes in tumor cell membranes, leading to tumor cell death. These IRE-created nano-holes permeabilize the cell membrane and disrupt the intracellular homeostasis, which triggers cell death by apoptosis [66-69]. Compared to other tumor ablation methods, IRE is safer for nearby blood vessels, bile ducts, nerves, and the urethra. This is because no heat generated; thus, the non-cellular protein “scaffolding extracellular matrix” and nearby blood vessels remain intact. IRE-induced cell apoptosis, which is programmed cell death, will induce phagocytosis to clear up dead cell debris and lead to fast recovery and regeneration of tissue in the ablated area [67-71]. IRE technology was approved by the FDA in 2011 and, since then, has gained a lot of attention from scientists and has been used in a clinical setting to treat many cancers, including kidney, pancreas, liver, lung, and prostate tumors [72-78]. However, despite IRE being successful as an ablation therapy in terms of prolonging patient survival, many patients still die due to the recurrence of residual tumors and distant tumor metastasis [72-78]. Therefore, working on improving the therapeutic effects of IRE treatment is an important goal to achieve better results for cancer patients.

### **1.3.2 Current IRE combinational therapy for cancer**

IRE ablation treatment alone has proven beneficial as it prolongs the survival of cancer patients. However, patients often die from local tumor recurrence [72-78]. IRE ablation alone provides specific-tumor antigens for the stimulation of DCs in TME [79]. However, the immunosuppressive TME efficiently suppresses the anti-tumor immune responses by activated CD8<sup>+</sup> T cells. Therefore, other immunostimulatory agents are required in addition to IRE ablation to help overcome the immunosuppressive TME and promoting effective anti-tumor immunity that can eradicate local tumors and metastases [51, 58].

Subsequent combinatorial studies have been done with the aim to improve the outcome of IRE treatment. In one study, IRE was combined with allogenic NK cell immunotherapy to treat pancreatic and primary liver cancer, with the results showing prolonged patient survival compared using IRE alone [80, 81]. Another study using a lung tumor model combined IRE with the intratumoral administration of the stimulator of interferon genes (STING), with results showing the significant inhibition of tumor growth [82]. IRE has well known safety and efficacy for the treatment of locally advanced pancreatic carcinoma (LAPC); however, this therapy has room for improvement. Studies combining IRE treatment with radiotherapy, chemotherapy, or both to treat LAPC have demonstrated that treatment with combined therapy results in a significantly higher patient survival rate compared to IRE-only treatment [83, 84].

Most IRE previous studies have only reported inhibition of tumor growth and boosting of non-specific CD8<sup>+</sup> T cell responses, but no immune cell profiling (ICP) analysis in the TME. Two recent reports in animal pancreatic cancer models showed both tumor inhibition and analysis of ICP in the TME, but no analysis of tumor-specific CD8<sup>+</sup> T cell responses, which is the critical measure of anti-tumor immunity. The first study tested IRE combined with PD-1 blockade in a KRAS<sup>+</sup> pancreatic tumor model, with results demonstrating tumor growth inhibition in 33% of treated mice and the induction of memory T cell responses [85]. The second study applied IRE treatment combined with TLR7 and PD-1 blockade in a KPC pancreatic tumor model, with results showing the treatment with IRE alone inhibited 20-35 % of KPC tumors but adding TLR7 and PD-1

blockade improved the IRE treatment outcome and inhibited distant tumors in ~60 % of mice [50]. More studies are needed to enhance the therapeutic effects of IRE ablation to achieve better results for cancer patients.

## References

1. Abbas, A.K., Lichtman, Andrew H. H., Pillai, Shiv, *Basic Immunology: Functions and Disorders of the Immune System*. 2012: Elsevier Health Sciences.
2. Chaplin, D.D, *Overview of the immune response*. J Allergy Clin Immunol, 2010. **125**(2 Suppl 2): S3-23.
3. Marshall et al., *An introduction to immunology and immunopathology*. Allergy Asthma Clin Immunol, 2018. **14**(Suppl 2): 49.
4. Diebold, S.S., *Activation of dendritic cells by toll-like receptors and C-type lectins*. Handb Exp Pharmacol, 2009 (188): p. 3-30.
5. Delves, P.J. and I.M. Roitt, *The immune system. Second of two parts*. N Engl J Med, 2000. **343**(2): p. 108-17.
6. Medzhitov, R. and C.A. Janeway, Jr., *Innate immunity: impact on the adaptive immune response*. Curr Opin Immunol, 1997. **9**(1): p. 4-9.
7. Beutler B., *Innate immunity: an overview*. Mol immunol, 2004. 40: p. 845-859.
8. Turvey S. E., *Innate immunity*. J Allergy Clin Immunol, 2010. 125(2): S24-S32.
9. Parkin, J. and B. Cohen, *An overview of the immune system*. Lancet, 2001. **357**(9270): p. 1777-89.
10. Bonilla FA, Oettgen HC., *Adaptive immunity*. J Allergy Clin Immunol, 2010. **125**(2 Suppl 2): S33-40.
11. Mosmann, T.R. and S. Sad, *The expanding universe of T-cell subsets: Th1, Th2 and more*. Immunol Today, 1996. **17**(3): p. 138-46.
12. Ohue, Y. & Nishikawa, H. *Regulatory T (Treg) cells in cancer: Can Treg cells be a new therapeutic target?* Cancer Sci, 2019. **110**: p. 2080-2089.
13. Schoenberger, S.P., et al., *T-cell help for cytotoxic T lymphocytes is mediated by CD40-CD40L interactions*. Nature, 1998. **393**(6684): p. 480-3.
14. Schwartz, R.H., *A cell culture model for T lymphocyte clonal anergy*. Science, 1990. **248**(4961): p. 1349-56.
15. Netea, M.G., et al., *Toll-like receptors and the host defence against microbial pathogens: bringing specificity to the innate-immune system*. J Leuk boil, 2004. **75**(5): p. 749-755.

16. Hoebe, K., E. Janssen, and B. Beutler, *The interface between innate and adaptive immunity*. Nat Immunol, 2004. **5**(10): p. 971-4.
17. Nolz JC., *Molecular mechanisms of CD8(+) T cell trafficking and localization*. Cell Mol Life Sci, 2015. **72**(13): p. 2461-2473.
18. Sharpe A. H., et al., *The function of programmed cell death 1 and its ligands in regulating autoimmunity*. Nat Immunol, 2007. **8**(3): p. 239-45.
19. Fitzgerald KA, Kagan JC, *Toll-like Receptors and the control of Immunity*. Cell, 2020. **180**(6): p. 1044-1066.
20. Urban-Wojciuk Z, et al., *The Role of TLRs in Anti-cancer Immunity and Tumor Rejection*. Front. Immunol, 2019. **10**:2388.
21. Hemmi H, et al., *A Toll-like receptor recognizes bacterial DNA*. Nature, 2000. **408**(6813): p. 740-5.
22. Vollmer J, Krieg AM, *Immunotherapeutic applications of CpG oligodeoxynucleotide TLR9 agonists*. Adv Drug Deliv Rev, 2009. **61**: p. 195-204.
23. Hidekazu Shirota & Dennis M. Klinman, *Effect of CpG ODN on monocytic myeloid derived suppressor cells*. OncoImmunology, 2012. **1**(5): p. 780-782.
24. Hofmann MA, Kors C, Audring H, Walden P, Sterry W, Trefzer U, *Phase I evaluation of intralesionally injected TLR9-agonist PF-3512676 in patients with basal cell carcinoma or metastatic melanoma*. J Immunother, 2008. **31**(5): p. 520-7.
25. Brody JD, Ai WZ, Czerwinski DK, Torchia JA, Levy M, Advani RH, et al., *In situ vaccination with a TLR9 agonist induces systemic lymphoma regression: a phase I/II study*. J Clin Oncol, 2010. **28**: p. 4324-32.
26. Molenkamp BG, Sluijter BJ, van Leeuwen PA, Santegoets SJ, Meijer S, Wijnands PG, et al., *Local administration of PF-3512676 CpG-B instigates tumor-specific CD8+ T-cell reactivity in melanoma patients*. Clin Cancer Res, 2008. **14**: p. 4532-42.
27. Reilley M.J, Morrow, B., Ager, C.R. et al., *TLR9 activation cooperates with T cell checkpoint blockade to regress poorly immunogenic melanoma*. J Immunotherapy Cancer, 2019. **7**: 323.
28. Van den Bijgaart R.J.E, et al., *Immune Modulation Plus Tumor Ablation: Adjuvants and Antibodies to Prime and Boost Anti-Tumor Immunity In Situ*. Front. Immunol, 2021. **12**: 617365.
29. Nierkens S, den Brok MH, Garcia Z, Togher S, Wagenaars J, Wassink M, et al., *Immune adjuvant efficacy of CpG oligonucleotide in cancer treatment is founded specifically upon TLR9 function in plasmacytoid dendritic cells*. Cancer Res, 2011. **71**(20): p. 6428–37.

30. Noubade R, Majri-Morrison S, Tarbell KV, *Beyond cDC1: Emerging Roles of DC Crosstalk in Cancer Immunity*. Front Immunol, 2019. **10**: 1014.
31. Xu A, Zhang L, Yuan J, Babikr F, Freywald A, Chibbar R, et al., *TLR9 agonist enhances radiofrequency ablation-induced CTL responses, leading to the potent inhibition of primary tumor growth and lung metastasis*. Cell Mol Immunol, 2019. **16**(10): p. 820–32.
32. Monjazebe AM, Kent MS, Grossenbacher SK, Mall C, Zamora AE, Mirsoian A, et al., *Blocking Indolamine-2,3-Dioxygenase Rebound Immune Suppression Boosts Antitumor Effects of Radio-Immunotherapy in Murine Models and Spontaneous Canine Malignancies*. Clin Cancer Res Off J Am Assoc Cancer Res, 2016. **22**(17): p. 4328–40.
33. Chavez M, Silvestrini MT, Ingham ES, Fite BZ, Mahakian LM, Tam SM, et al., *Distinct immune signatures in directly treated and distant tumors result from TLR adjuvants and focal ablation*. Theranostics, 2018. **8**(13): p. 3611–28.
34. Martins KA, Bavari S, Salazar AM, *Vaccine adjuvant uses of poly-IC and derivatives*. Expert Rev Vaccines, 2015. **14**(3): p. 447-59.
35. Matsumoto M., & Seya T., *TLR3: Interferon induction by double-stranded RNA including poly (I:C)*. Adv Drug Deliv Rev, 2008. **60**(7): p. 805-812.
36. Hammerich L, Marron TU, Upadhyay R, Svensson-Arvelund J, Dhainaut M, Hussein S, et al., *Systemic clinical tumor regressions and potentiation of PD1 blockade with in situ vaccination*. Nat Med, 2019. **25**(5): p. 814–24.
37. Blair TC, Bambina S, Alice AF, Kramer GF, Medler TR, Baird JR, et al., *Dendritic Cell Maturation Defines Immunological Responsiveness of Tumors to Radiation Therapy*. J Immunol, 2020. **204**(12): p. 3416–24.
38. Yoshida S, Shime H, Takeda Y, Nam JM, Takashima K, Matsumoto M, et al., *Toll-like receptor 3 signal augments radiation-induced tumor growth retardation in a murine model*. Cancer Sci, 2018. **109**(4): p. 956–65.
39. Ahonen CL, Doxsee CL, McGurran SM, Riter TR, Wade WF, Barth RJ, et al., *Combined TLR and CD40 triggering induces potent CD8+ T cell expansion with variable dependence on type I IFN*. J Exp Med, 2004. **199**(6): p. 775–84.
40. Le Noci V, et al., *Poly(I:C) and CpG-ODN combined aerosolization to treat lung metastases and counter the immunosuppressive microenvironment*. OncoImmunology, 2015. **4**(10): e1040214.
41. Han Y, Liu D, Li L, *PD-1/PDL-1 pathway: current researches in cancer*. Am j Cancer Res, 2020. **10**(3): p. 727-742.

42. Dong H, Strome SE, Salomao DR, Tamura H, Hirano F, Flies DB, et al., *Tumor-associated B7 H1 promotes T-cell apoptosis: a potential mechanism of immune evasion*. Nat Med, 2002. **8**: p. 793–800.
43. Robert C, Long GV, Brady B, Dutriaux C, Maio M, Mortier L, et al., *Nivolumab in previously untreated melanoma without BRAF mutation*. New Engl J Med, 2015. **372**: p. 320–30.
44. Schadendorf D, Hodi FS, Robert C, Weber JS, Margolin K, Hamid O, et al., *Pooled analysis of long-term survival data from phase II and Phase III trials of ipilimumab in unresectable or metastatic melanoma*. J Clin Oncol, 2015. **33**: p. 1889–94.
45. Guo L, Wei R, Lin Y, Kwok HF, *Clinical and Recent Patents Applications of PD-1/PDL-1 Targeting Immunotherapy in Cancer Treatment-Current Progress, Strategy, and Future Perspective*. Front Immunol, 2020. **11**: 1508.
46. Vanneman, M. and Dranoff, G, *Combining immunotherapy and targeted therapies in cancer treatment*. Nat. Rev. Cancer, 2012. **12**: 237.
47. Takeda et al., *A TLR3-Specific Adjuvant Relieves Innate Resistance to PDL-1 Blockade without Cytokine Toxicity in Tumor Vaccine Immunotherapy*. Cell Reports, 2017. **19**: p. 1874-1887.
48. Wu X., et al., *Application of PD-1 blockade in cancer immunotherapy*. Comput Struct Biotechnol J, 2019. **17**: p. 661-674.
49. Shi L, Chen L, Wu C, Zhu Y, Xu B, Zheng X, et al., *PD-1 Blockade Boosts Radiofrequency Ablation-Elicited Adaptive Immune Responses against Tumor*. Clin Cancer Res Off J Am Assoc Cancer Res, 2016. **22**(5): p. 1173–84.
50. Narayanan, J. S. S. et al., *Irreversible electroporation combined with checkpoint blockade and TLR7 stimulation induced antitumor immunity in a murine pancreatic cancer model*. Cancer Immunol Res, 2019. **7**(10): p. 1714-1726.
51. Pitt, J.M. et al., *Targeting the tumor microenvironment: removing obstruction to anticancer immune responses and immunotherapy*. Ann Oncol, 2016. **27**: p. 1482-1492.
52. Roma-Rodrigues C, Mendes R, Baptista PV, Fernandes AR, *Targeting tumor microenvironment for cancer therapy*. Int J Mol Sci, 2019. **20**(4): 840.
53. Chanmee, T., Ontong, P., Konno, K. & Itano, N, *Tumor-associated macrophages as major players in the tumor microenvironment*. Cancers, 2014. **6**: p. 1670-1690.
54. Fleming, V. et al., *Targeting myeloid-derived suppressor cells to bypass tumor-induced immunosuppression*. Front Immunol, 2018. **9**: 398.

55. Lei X, Lei Y, Li JK, Du WX, Li RG, Yang J, Li J, Li F, Tan HB, *Immune cells within the tumor microenvironment: Biological functions and roles in cancer immunotherapy*. *Cancer Lett*, 2020. **470**: p. 126-133.
56. Conrad, C. et al., *Plasmacytoid dendritic cells promote immunosuppression in ovarian cancer via ICOS costimulation of Foxp3(+) T-regulatory cells*. *Cancer Res*, 2012. **72**: p. 5240-5249.
57. Williams, M. A. & Bevan, M. J., *Effector and memory CTL differentiation*. *Annu Rev Immunol*, 2007. **25**: p. 171-192.
58. Xia, A., Zhang, Y., Xu, J., Yin, T. & Lu, X. J., *T cell dysfunction in cancer immunity and immunotherapy*. *Front Immunol*, 2019. **10**: 1719.
59. Li, L. et al., *Cross-dressed CD8alpha+/CD103+ dendritic cells prime CD8+ T cells following vaccination*. *Proc Natl Acad Sci USA*, 2012. **109**: p. 12716-12721.
60. Jahchan N. S., et al., *Tuning the tumor myeloid microenvironment to fight cancer*. *Front Immunol*, 2019. **10**: 1611.
61. Liu Y, Cao X., *Intratumoral dendritic cells in the anti-tumor immune response*. *Cell Mol Immunol*, 2015. **12**(4): p. 387-90.
62. Pickup, M.W., Mouw, J.K., Weaver, V.M., *The extracellular matrix modulates the hallmarks of cancer*. *EMBO Rep*. 2014. **15**: p. 1243–1253.
63. De Palma, M., Biziato, D., Petrova, T.V., *Microenvironmental regulation of tumour angiogenesis*. *Nat. Rev. Cancer*, 2017. **17**: p. 457–474.
64. Belli C, Trapani D, Viale G, D'Amico P, Duso BA, Della Vigna P, Orsi F, Curigliano G., *Targeting the microenvironment in solid tumors*. *Cancer Treat Rev*, 2018. **65**: p. 22-32.
65. Ahmed M, Brace C. L., Lee F. T. Jr, Goldberg S. N., *Principles of and advances in percutaneous ablation*. *Radiology*, 2011. **258**(2): p. 351-69.
66. Tekle E, et al., *Phagocytic clearance of electric field induced “apoptosis-mimetic” cells*. *BBRC*, 2008. **376**: p. 256-260.
67. Bulvik B, Rozonblum N, Gourevich S, et al., *Irreversible electroporation versus radiofrequency ablation*. *Radiol*, 2016. **280**: p. 414-424.
68. Ansari D, Kristoffersson S., Andersson R, et al., *The role of irreversible electroporation for locally advanced pancreatic cancer: a systematic review of safety and efficiency*. *Scand J Gastroenterol*, 2017. **52**: p. 1165-1171.
69. Paiella S, Pastena M, D’Onofrio M, et al., *Palliative therapy in pancreatic cancer: Interventional treatment with RFA/IRE*. *Translational Gastroenterol Hepatol*, 2018. **3**: e80.



70. Rubinsky B., *Irreversible electroporation in medicine*. Tech Cancer Res Treat, 2007. **6**: p. 255-260.
71. Lee E. W, Thai S, Kee S. T., *Irreversible electroporation: a novel image-guided cancer therapy*. Gut Liver, 2010. **Suppl 1**(Suppl 1): S99-S104.
72. Zhu J, Bao J, Zhu C and Fu Q., *Cancer treatments of the irreversible electroporation*. Int J Clin Res 7 Trials, 2018. **3**: p. 129.
73. Martin R., et al., *Irreversible electroporation therapy in management of locally advanced pancreatic adenocarcinoma*. J Am Coll Surg, 2012. **215**: p. 361-369.
74. Narayanan G., et al., *Percutaneous irreversible electroporation for down staging and control of unresectable pancreatic adenocarcinoma*. J Vasc Interv radiol, 2012. **23**: p. 1613-1621.
75. Martin R., et al., *Irreversible electroporation in locally advanced pancreatic cancer: potential improved overall survival*. Ann Surg Oncol, 2013. **20**: p. 443-449.
76. Cannon R., et al., *Safety and early efficiency of irreversible electroporation for hepatic tumors in proximity to vital structures*. J Surg Oncol, 2013. **107**: p. 544-549.
77. Usman M., et al., *Irreversible electroporation of lung neoplasm. A case series*. Med Sci Monit, 2012. **18**(6): CS43-47.
78. Rubinsky J., et al., *Optimal parameters for the destruction of prostate cancer using irreversible electroporation*. J Urol, 2008. **180**: p. 2668-2674.
79. Lyu, T., et al., *Irreversible electroporation in primary and metastatic hepatic malignancies*. Medicine, 2017. **96**(17): e6386.
80. Lin M, Liang S, Wang X., et al., *Short-term clinical efficacy of percutaneous irreversible electroporation combined with allogenic natural killer cell for treating metastatic pancreatic cancer*. Immunol Lett, 2017. **186**: p. 20-7.
81. Yang Y., et al., *Safety and short-term efficacy of irreversible electroporation and allogenic natural killer cell immunotherapy combination in the treatment of patients with unresectable primary liver cancer*. Cardiovasc Intervent Radiol, 2019. **42**(1): p. 48-59.
82. Go EJ., et al., *Irreversible electroporation and STING agonist for effective cancer immunotherapy*. Cancers, 2020. **12**(11): 3123.
83. Xu K., et al., *Irreversible electroporation and adjuvant chemoradiotherapy for locally advanced pancreatic carcinoma*. J Cancer Res Ther, 2020. **16**(2): 280-285.

84. Oikonomou D., et al., *Irreversible Electroporation (IRE) Combined with Chemotherapy Increases Survival in Locally Advanced Pancreatic Cancer (LAPC)*. Am J Clin Oncol, 2021. **44**(7): p. 325-330.
85. Zhao J., et al., Irreversible electroporation reverses resistance to immune checkpoint blockade in pancreatic cancer. Nat Commun, 2019. **10**: 899.

## **CHAPTER 2 HYPOTHESIS AND OBJECTIVES**

### **HYPOTHESIS**

We hypothesize that IRE ablation combined with TLR3/9 agonists and PD-1 blockade (IRE+Combo) induces efficient CTL responses, leading to complete tumor eradication via enhanced conversion of immunotolerant TME.

### **OBJECTIVES**

1. Assessing its CTL responses and immunity against primary tumor in mouse OVA-expressing EG7 lymphoma model;
2. Assessing its “abscopal” effect and immunity against distant tumor in mouse EG7 lymphoma model;
3. Assessing its conversion of immunosuppressive TME in primary and distant tumors;
4. Assessing its therapeutic effect in two breast cancer (Tg1-1 and 4T1) models.

# CHAPTER 3 DISTINCT ROLES BUT COOPERATIVE EFFECT OF TLR3/9 AGONISTS AND PD-1 BLOCKADE IN CONVERTING IMMUNOTOLERANT MICROENVIRONMENT OF IRREVERSIBLE ELECTROPORATION-ABLATED TUMORS

Fatma Babikr<sup>1,2</sup>, Jiangbo Wan<sup>3</sup>, Aizhang Xu<sup>1,2</sup>, Zhaojia Wu<sup>1,2</sup>,  
Shahid Ahmed<sup>1,2</sup>, Andrew Freywald<sup>4</sup>, Rajni Chibbar<sup>4</sup>, Yue Wu<sup>4</sup>,  
Michael Moser<sup>5</sup>, Gary Groot<sup>5</sup>, Wenjun Zhang<sup>6</sup>, Bing Zhang<sup>7</sup>, Jim Xiang<sup>1,2\*</sup>

<sup>1</sup>Saskatoon Cancer Center, Saskatchewan Cancer Agency, Saskatoon, Saskatchewan, Canada

<sup>2</sup>Department of Oncology, University of Saskatchewan, Saskatoon, Saskatchewan, Canada

<sup>3</sup>Department of Haematology, Xin-Hua Hospital, Shanghai Jiao-Tong University, Shanghai, China

<sup>4</sup>Department of Pathology, University of Saskatchewan, Saskatoon, Saskatchewan, Canada

<sup>5</sup>Department of Surgery, University of Saskatchewan, Saskatoon, Saskatchewan, Canada

<sup>6</sup>Department of Bioengineering, University of Saskatchewan, Saskatoon, Saskatchewan, Canada

<sup>7</sup>Biomedical Science and Technology Research Center, Shanghai University, Shanghai, China

**Notes:** These authors contributed equally: Fatma Babikr, Jiangbo Wan, Aizhang Xu.

**Key Words:** IRE ablation, TLR3/9-agonists, PD-1-blockade, CD8<sup>+</sup> T-cell response, antitumor immunity, primary and distant tumors, lung metastasis, conversion, tumor-microenvironment

\*Corresponding Author: Jim Xiang, Saskatchewan Cancer Agency and University of Saskatchewan, Room 4D30.1, 107 Wiggins Road, Saskatoon, Saskatchewan S7N 5E5, Canada. Phone: 306-966-7039; Fax: 306-966-7047; Email: [jim.xiang@usask.ca](mailto:jim.xiang@usask.ca)

## NOTES:

1. This manuscript was published in Cell Mol Immunol on November 15, 2021.
2. Fatma Babikr mainly worked on and contributed to Figures 2, 3, 4, 6, 7, 8 in the manuscript.

### 3.1 Abstract

Irreversible electroporation (IRE) is a new cancer-ablation technology, but methods to improve IRE-induced therapeutic immunity are only beginning to be investigated. We developed a mouse model bearing large primary (300 mm<sup>3</sup>) and medium distant (100 mm<sup>3</sup>) EG7 lymphomas engineered to express ovalbumin (OVA) as a nominal tumor-antigen. We established experimental protocols including IRE and IRE combined with Toll-like receptor (TLR)3/9-agonists (poly I:C/CpG) (IRE+pIC/CpG) or PD-1-blockade (IRE+PD-1-blockade) or both (IRE+Combo) to investigate therapeutic effects on primary and distant EG7 tumors and conversional effects on immunotolerant tumor-microenvironment (TME). We demonstrate that IRE-alone simulates very weak OVA-specific CD8<sup>+</sup> T-cell responses and does not inhibit primary tumor-growth. IRE+pIC/CpG synergistically stimulates more efficient OVA-specific CD8<sup>+</sup> T-cell responses and inhibition of primary tumor-growth than IRE+PD-1-blockade. IRE+pIC/CpG plays a major role in modulation of immune-cell profiles, but a minor role in down-regulation of PD-L1-expression in TME, and *vice versa* for IRE+PD-1-blockade. IRE+Combo cooperatively induces potent OVA-specific CD8<sup>+</sup> T-cell immunity and rescues exhausted intratumoral CD8<sup>+</sup> T-cells, leading to eradication of not only primary, but also untreated concomitant distant tumors and lung metastases. IRE+Combo efficiently modulates immune-cell profiling as evidenced by reduction of immunotolerant type-2 macrophages (M2), myeloid-derived suppressor-cells, plasmacytoid dendritic cells and regulatory T-cells and by increase of immunogenic M1, CD169<sup>+</sup> macrophages, type-1 conventional dendritic cells and CD8<sup>+</sup> T-cells, leading to conversion of immunotolerance in not only primary, but also untreated distant TMEs. IRE+Combo also shows effective therapeutic effect in two breast cancer models. Therefore, our results suggest IRE+Combo is a promising strategy to improve cancer IRE-ablation therapy.

## 3.2 Introduction

The tumor microenvironment (TME) plays an important role in regulating tumor progression, metastases, and therapies and is composed of a variety of tumor-associated, immune, stromal, and myeloid cell-subsets [1]. These tumor-associated cellular populations can be divided into two major groups with different phenotypes and distinct functional (i.e., immunogenic and immunotolerant) effects. The immunogenic group includes (i) tumoricidal CD11b<sup>+</sup>F4/80<sup>+</sup>MHCII<sup>+</sup> type-1 macrophages (M1) secreting inflammatory cytokines driving polarization of immunogenic CD4<sup>+</sup> Th1 cell responses and halting tumor growth, [2] (ii) CD11b<sup>+</sup>F4/80<sup>+</sup>CD169<sup>+</sup> macrophages (M169) dominating antitumor immunity by cross-presenting apoptotic tumor cell's antigen to CD8<sup>+</sup> T cells, [3] and (iii) type-1 conventional CD8<sup>+</sup>CD103<sup>+</sup>CD11c<sup>+</sup>CD11b<sup>-</sup> dendritic cells (cDC1), a superior stimulator of CD8<sup>+</sup> T cell responses in the TME [4]. The immunotolerant group includes (i) pro-tumorigenic CD11b<sup>+</sup>F4/80<sup>+</sup>MHCII<sup>-</sup> type-2 macrophages (M2) producing suppressive TGF- $\beta$  and IL-10 and promoting tumor angiogenesis, [5] (ii) CD11b<sup>+</sup>Gr1<sup>+</sup>Ly6G<sup>+</sup> myeloid-derived suppressor cells (MDSCs), the major player or the “Queen Bee” for an immunotolerant TME [6] activating CD4<sup>+</sup>CD25<sup>+</sup>Foxp3<sup>+</sup> regulatory T (Treg) cells and producing inhibitory TGF- $\beta$ , arginase-1, and IDO (indoleamine 2,3-dioxygenase) molecules, [7] (iii) CD317<sup>+</sup>B220<sup>+</sup> plasmacytoid DCs (pDCs) favoring suppressive Treg cell expansion, [8] and (iv) CD4<sup>+</sup>CD25<sup>+</sup>Foxp3<sup>+</sup> Treg cells with an inhibitory effect on CD8<sup>+</sup> T cell responses *via* secretion of suppressive IL-10 and TGF- $\beta$  and expression of inhibitory PD-1 (programmed cell death protein-1) and CTLA-4 (cytotoxic T lymphocyte-associated protein-4) molecules [9]. The TME is profoundly immunosuppressive when the presence of the above immunotolerant cells predominates. Although CD8<sup>+</sup> T cells play an important role in the host defense against tumors, [10] they are often blocked from entering tumors [11] or become dysfunctional in an immunotolerant TME [12]. The immunotolerant TME thus becomes a key reason why most immunotherapies based upon stimulation of tumor-specific CD8<sup>+</sup> T cell responses against tumors continuously display limited efficacy. Therefore, developing new emergent approaches by targeting the immunotolerant TME represents a critical topic in cancer immunotherapies [1].

Irreversible electroporation (IRE) is a new non-thermal form of cancer-ablation technology that delivers short bursts of current to ‘punch’ irreversible nano-holes in cell membranes, leading to massive tumor cell apoptosis [13]. Compared to radiofrequency ablation (RFA) with heat-induced

collateral damage, IRE is safe to nearby blood vessels, bile ducts, and nerves [14]. IRE-ablation therapy has been applied to cancers in many locations, including liver, pancreas, breast, lung, and prostate tumors [15]. However, IRE ablation-induced antitumor immune responses are too weak to eradicate local primary tumor growth and patients often have local or distant tumor recurrence [16, 17]. Therefore, improving the therapeutic effects of IRE ablation is an urgent need for cancer-ablation therapy. However, methods to improve IRE-induced therapeutic immunity are only beginning to be investigated.

Recently, Li's group showed IRE-ablation alone increased vascular density and permeability, and IRE-ablation combined with PD-1 blockade induced an increase of tumor-infiltrating CD8<sup>+</sup> T-cells, eradicated 33% of KRAS<sup>+</sup> pancreatic tumors, but only mildly modulated the TME by increasing the CD8<sup>+</sup> T-to-Treg ratio [18]. In a more recent study, White's group demonstrated IRE-ablation combined with Toll-like receptor-7 (TLR7) agonist and PD-1 blockade improved the therapeutic effect *via* increasing cDC1 in the TME, resulting in the inhibition of primary KPC4580P pancreatic tumor growth and regression of distant tumors in ~60% of mice [19]. However, only non-specific, but not tumor-specific, CD8<sup>+</sup> T cell responses (the critical measurement for IRE-induced antitumor immunity) were assessed in their mouse pancreatic cancer models.

TLRs are evolutionarily ancient family of pattern recognition receptors that sense and trigger DC maturation, and most TLR agonists have been shown to significantly enhance adaptive immunity [20]. For example, TLR3 agonist poly I:C (pIC) and TLR9 agonist CpG found to enhance CD4<sup>+</sup> Th1 and CD8<sup>+</sup> cytotoxic T cell responses [21, 22] are used for targeting innate sensing in TME to improve immunotherapy [23, 24]. PD-1-blockade using anti-PD-1 or anti-PD-L1 antibodies that stimulates potent antitumor immunity *via* blocking inhibitory PD-1/PD-L1 pathway in CD8<sup>+</sup>PD-1<sup>+</sup> T cells and rescuing T cell exhaustion [25] has been commonly used in clinical implications in cancer immunotherapy [26]. PD-1 blockade combined with TLR3 or TLR9 agonists was also found to enhance cancer immunotherapies [27, 28]. We recently performed an RFA study in an ovalbumin (OVA)-expressing EG7 lymphoma model, and demonstrated that administration of TLR9 agonist CpG significantly enhanced RFA-induced tumor OVA-specific CD8<sup>+</sup> T cell responses, leading to inhibition of not only primary tumor growth but lung metastases as well [29].

In the present study, we performed IRE-ablation combined with PD-1 blockade as well as TLR3 agonist pIC and TLR9 agonist CpG (i.e., IRE+PD-1 blockade+pIC/CpG or IRE+Combo) in mice

bearing well-established EG7 lymphomas, followed by investigation of OVA-specific CD8<sup>+</sup> T-cell responses and the therapeutic effect on eradication of primary and distant EG7 tumors and lung metastases. We systematically assessed immune cell profiles in the TME by quantitatively measuring both immunogenic and immunotolerant cell subsets. We demonstrated IRE+pIC/CpG synergistically stimulated potent OVA-specific CD8<sup>+</sup> T cell responses, leading to significant inhibition of primary tumor growth; the effects were stronger than those in IRE+PD-1 blockade-treated groups. We also found TLR3/9 agonists were more effective in promoting immunogenic cells (M1, M169, cDC1, CD4<sup>+</sup> and CD8<sup>+</sup> T cells) and reducing immunotolerant cells (M2, Treg cells, MDSCs, and pDCs), but less efficient in down-regulating PD-L1 (PD-ligand-1) expression in immunotolerant M2, MDSCs and EG7 tumor cells in the TME than PD-1 blockade. Combined IRE+Combo cooperatively induced potent OVA-specific CD8<sup>+</sup> T cell immunity and rescued tumor-infiltrating exhausted CD8<sup>+</sup> T cells, leading to complete eradication of both primary and distant tumors as well as lung metastases *via* dramatic conversion of the immunotolerant TME into an immunogenic TME in both primary and distant tumors. Furthermore, IRE+Combo also showed effective therapeutic effect in two mouse Tg1-1 and 4T1 breast cancer models. Taken together, our results suggest that IRE+Combo is a promising strategy to improve the cancer IRE-ablation therapy.



### 3.3 Materials and methods

#### 3.3.1 Reagents, cell lines and animals

Fluorescein isothiocyanate (FITC)-anti-CD8 antibody (Ab) was obtained from Bio-Rad (Hercules, CA). Phycoerythrin (PE)-H-2K<sup>b</sup>/OVA<sub>257-264</sub> tetramer (PE-tetramer) was obtained from Fred Hutchinson Cancer Research Center (Seattle, WA). The following Abs and reagents were obtained from Biolegend (San Diego, CA): FITC-anti-CD8, FITC-anti-CD3, PE-anti-CD45.1, Alexa Fluor-anti-CD45.1, PE-anti-CD4, PE-anti-CD25, PECy5-anti-CD11c, APC-anti-CD11b, APC/cy7-anti-I-A/I-E (MHCII), Alexa Fluor 700-anti-Ly6G, BV421-anti-CD103, PECy5-anti-F4/80, anti-Gr1, BV421-anti-CD169, PECy5-anti-CD8, anti-CD317, anti-CD220, BV421-anti-PD-L1, PECy5-PE-anti-IDO, PE-arginase, PE-anti-TGF- $\beta$ , PECy5-anti-FoxP3, PECy5-anti-TNF- $\alpha$ , PECy5-anti-IFN- $\gamma$ , and Zombie Aqua Fixable Viability Kit. CpG oligodeoxynucleotides 1826 (CpG ODN 1826) and poly:IC (pIC) were obtained from Invitrogen Inc. (San Diego, CA). Cytotfix/Cytoperm kits and lysing buffer were purchased from BD Bioscience (Franklin Lakes, NJ). Anti-mouse PD-L1 antibody for the *in vivo* experiment was obtained from Bioxcell (Lebanon, NH). Mouse lymphoma cell line EL4 and ovalbumin (OVA) transgene-transfected EL4 cell line called EG7 were obtained from American Type Culture Collection (ATCC, Rockville, MD) while OVA transgene-transfected B16 melanoma cell line BL6-10<sub>OVA</sub> was generated in our laboratory [29]. EL4 cells were maintained in RPMI medium (Life Technologies, Carlsbad, CA), 10% fetal calf serum (FCS), while OVA-expressing EG7 and BL6-10<sub>OVA</sub> cells were maintained in the above medium plus G418 (0.5 mg/mL; Life Technologies). Female 6- to 8-week-old C57BL/6 (B6, CD45.2<sup>+</sup>), B6.1 (CD45.1<sup>+</sup>), and OVA-specific TCR transgenic OT-I mice were purchased from Jackson Laboratory (Bar Harbor, ME). CD45.1<sup>+</sup> OT-I mice were obtained by cross-breeding B6.1 with OT-I mice. All animal experiments were approved by the Animal Research Ethics Board, University of Saskatchewan (Protocol# 20160056).

#### 3.3.2 IRE ablation combined with TLR3/9 agonists and PD-1 blockade

EG7 cells were subcutaneously (s.c.) injected into right flanks of B6 mice ( $3 \times 10^6$  cells/mouse). Tumor growth was measured using digital calipers. Once tumors reached  $\sim 300 \text{ mm}^3$  (8-9 mm in

diameter), calculated using the formula  $A/2 \times B^2$ , where A and B are the long and short tumor dimensions, respectively, we first assessed whether TLR3/9 agonists (pIC and CpG) and PD-1 blockade (anti-PD-L1 Ab) and a combination of the above (pIC/CpG+PD-1 blockade; Combo) stimulate OVA-specific CTL responses. For CpG and/or pIC administration, mice were intratumorally (i.t.) injected with 10  $\mu$ g of CpG and/or 10  $\mu$ g of pIC in 30  $\mu$ L of PBS for a total of three injections in three positions at peripheral areas of the tumor. Anti-PD-L1 Ab injections (200  $\mu$ g/mouse) were simultaneously given intraperitoneally (i.p.) every 2 days for a total of four injections. Seven days post PD-1 blockade or TLR agonist injection, mouse tail blood samples were collected for assessment of OVA-specific CD8<sup>+</sup> T cell responses using PE-tetramer and FITC-CD8 Ab by flow cytometry. To perform IRE ablation, mice bearing  $\sim$ 300 mm<sup>3</sup> EG7 tumors were anesthetized by inhalation of isoflurane gas (5% isoflurane for anesthesia induction; 2% for maintenance) [29]. Hair over the tumor area was removed, and two insulated custom-built pulse-delivery metal electrode needles (0.2 mm in diameter, separated by 5 mm center-to-center) of a custom-made IRE device [30] were inserted into the tumor to deliver electric pulses. The IRE parameters (voltage: 1,200 V/cm; pulse duration: 90  $\mu$ s; pulse repetition frequency: 1 Hz; number of repetition pulses: 100) were similar to a previous IRE-ablation protocol for animal tumor models [18]. The needles were subsequently reoriented by 90° and the above process repeated once. Following all procedures, mice were given s.c. injections of buprenorphine (0.05 mg/kg of body weight) for pain control. Mice recovered post treatment on a warming blanket. To assess whether pIC, CpG and PD-1 blockade potentiate IRE-induced CTL responses and antitumor immunity, we further developed seven different treatments by combining IRE-ablation with pIC, CpG, and PD-1 blockade. These include (i) IRE control, (ii) IRE+PD-1 blockade, (iii) IRE+pIC, (iv) IRE+CpG, (v) IRE+pIC/CpG, (vi) IRE+PD-1 blockade+pIC/CpG (IRE+Combo) and (vii) Combo alone. For CpG and/or pIC adjuvant administration, mice were similarly i.t. injected with 10  $\mu$ g of CpG and/or 10  $\mu$ g of pIC in 30  $\mu$ L of PBS for a total of three injections in three positions at peripheral areas of the tumor post IRE-ablation. Anti-PD-L1 Ab injections (200  $\mu$ g/mouse) were similarly i.p. given every 2 days starting 1 day prior to IRE for a total of four injections. Seven days post IRE, mouse tail blood samples were collected for assessment of OVA-specific CD8<sup>+</sup> T cell responses by flow cytometry, followed by daily monitoring of tumor growth or regression. To examine whether IRE+Combo-induced CD8<sup>+</sup> T cell responses affect distant tumor growth, B6 or B6.1 mice were s.c. injected with EG7 cells on the right and left flanks of the lower back ( $3 \times 10^6$  and  $1 \times 10^6$

cells/mouse, respectively). When right primary and left distant tumors respectively reached  $\sim 300$  and  $\sim 100 \text{ mm}^3$ , IRE+Combo or IRE or Combo alone was performed on the right primary tumors. Distant tumor growth or regression was monitored daily. To assess whether IRE+Combo-induced  $\text{CD8}^+$  T cell responses protect mice from tumor lung metastasis, B6 mice bearing primary tumors and control naïve mice were intravenously (i.v.) injected with BL6-10<sub>OVA</sub> cells ( $0.5 \times 10^6$  cells/mouse) to form lung tumor metastases 7 days prior to primary tumors reaching  $\sim 300 \text{ mm}^3$ . We then performed IRE+Combo treatment for eradication of primary tumors 7 days after BL6-10<sub>OVA</sub> cell injection. Mouse lung tissues were collected 21 days after BL6-10<sub>OVA</sub> cell injection. Black tumor colonies in lungs were counted and confirmed by histopathological examination. For ethical reasons, mice bearing tumors  $\sim 2,500 \text{ mm}^3$  ( $\sim 17 \text{ mm}$  in diameter) were sacrificed and recorded as deaths.

### **3.3.3 $\text{CD8}^+$ T cell depletion study**

Female B6 mice (5 mice/group) were i.p. injected with three doses of anti- $\text{CD8}$  Ab ( $200 \mu\text{g/injection}$ ) on consecutive days prior to IRE+Combo treatment. Successful depletion was confirmed by flow cytometry analysis of mouse peripheral blood. Mice were then treated with IRE or IRE+Combo therapy 1 day after the last Ab injection, followed by monitoring tumor growth or regression. The anti- $\text{CD8}$  Ab was further i.p. injected once every 3 days for a total of five injections to maintain the depletion during the study.

### **3.3.4 Analysis of OVA-specific $\text{CD8}^+$ T cell responses**

To measure OVA-specific  $\text{CD8}^+$  T cell responses, peripheral blood samples were collected by tail nicking into a collection tube containing anti-coagulant heparin from tumor-bearing mice subjected to different IRE-ablation treatments 7 days post IRE. To assess the IRE+Combo-induced long-term T cell memory, IRE+Combo-treated mice with complete primary tumor regression for 30 days were i.v. boosted with recombinant *Listeria monocytogenes* expressing OVA (rLmOVA) ( $1,000$  colony-forming units/mouse) [31]. Mouse tail blood samples were collected 4 days post rLmOVA injection. PE-tetramer ( $10 \mu\text{L}$ ) was added to each tube followed by incubation for 30 min at room

temperature protected from light. FITC-CD8 Ab was then added to each tube and incubated for 30 min at room temperature. Red blood cells were lysed using BD lysing buffer (BD Bioscience). Samples were analyzed for measurement of OVA-specific CD8<sup>+</sup> T cell responses by flow cytometry.

### **3.3.5 Flow cytometric analysis of tumor-infiltrating immune cell profiling**

To assess tumor-infiltrating immune cells, B6.1 (CD45.1<sup>+</sup>) mice were challenged with EG7 cells. This approach enabled us to distinguish recipient CD45.1<sup>+</sup> mouse immune cells from CD45.2<sup>+</sup> EG7 tumor cells when analyzing tumor single cell suspensions by flow cytometry. Two sources (untreated and IRE-treated) of tumor tissues were used for preparation of single cell suspensions. To compare the tolerance extent of the TME in different sized tumors, tumor tissues were collected when tumors grew to 4, 6, and 8-9 mm in diameter, respectively. Tumor tissue single cell suspensions were prepared using a Tumor Dissociation Kit (Miltenyi Inc, San Diego, CA) according to manufacturer's instruction. Briefly, tumor tissues were also collected from the peripheral area of tumors treated with different IRE protocols 3 days post IRE. The collected tumor tissues were first cut into 1 mm<sup>3</sup> fragments and then incubated in 5 mL of RPMI medium containing 1 mg/mL of collagenase IV and 0.2 mg/mL of DNase-I at 37° C for 30 min, followed by brief homogenization with a syringe plunger. Cell suspensions were further filtered through a 40-µm filter. Erythrocytes were finally lysed by incubation of cells with red cell lysis buffer (0.84% Tris-ammonium chloride) for 5 min. To exclude dead cells from analysis, live-dead cell staining with Zombie Aqua Fixable Viability dye was performed according to the manufacturer's instructions prior to any antibody staining. Cell suspensions were then stained with a cocktail of antibodies against a combination of molecular markers used to distinguish different immune cell populations such as immunogenic cDC1, M1, M19, CD4<sup>+</sup> and CD8<sup>+</sup> T cells as well as immunotolerant M2, MDSCs, pDCs, and Treg-cells, as we and others previously described [18, 19, 29, 32]. Briefly, live tumor-infiltrating leukocyte populations were gated for initial analysis of CD45.1<sup>+</sup> immune cell populations distinctive from CD45.2<sup>+</sup> EG7 tumor cells. Neutrophils and monocytes were later removed from the host mouse CD45.1<sup>+</sup> cell population based on the expression of Ly6G [32]. Various immune cell populations were then progressively gated by antibodies against their cell markers for analysis, respectively. For example, the macrophage population was gated as

CD11b<sup>+</sup>F4/80<sup>+</sup> cells to further measure MHCII expression for quantification of the % CD11b<sup>+</sup>F4/80<sup>+</sup>MHCII<sup>-</sup> M2 and % CD11b<sup>+</sup>F4/80<sup>+</sup>MHCII<sup>+</sup> M1 in CD11b<sup>+</sup>F4/80<sup>+</sup> macrophages (Supplementary Figure 3.14A) or to further measure MHCII and CD169 expression for quantification of the % CD11b<sup>+</sup>F4/80<sup>+</sup>MHCII<sup>+</sup>CD169<sup>+</sup> M169 macrophage [3, 33] in CD11b<sup>+</sup>F4/80<sup>+</sup> macrophages (Supplementary Figure 3.14B). DC populations were gated as CD11c<sup>+</sup> cells to further analyze the expression of CD8, CD103, and MHCII for quantification of the % CD8<sup>+</sup>CD103<sup>+</sup>MHCII<sup>+</sup> cDC1 in CD11c<sup>+</sup> DC population (Supplementary Figure 3.14C). The monocyte population was gated as CD45.1<sup>+</sup> cells to further sequentially assess the expression of CD11b and Gr1/Ly6G for quantification of the % CD11b<sup>+</sup>Gr1<sup>+</sup>Ly6G<sup>+</sup> MDSCs in the CD45.1<sup>+</sup> cell population with a calculation formula of % (CD11b<sup>+</sup>CD45.1<sup>+</sup> cells × Gr1<sup>+</sup>Ly6G<sup>+</sup> cells) (Supplementary Figure 3.14D). The monocyte population was gated as CD45.1<sup>+</sup> cells to further sequentially assess expression of CD11b/Gr1 and CD317/B220 for quantification of the % CD11b<sup>-</sup>CD317<sup>+</sup>Gr1<sup>-</sup>B220<sup>+</sup> pDCs in CD45.1<sup>+</sup> cell population with a calculation formula of % (CD11b<sup>-</sup>Gr1<sup>-</sup> cells × CD317<sup>+</sup>B220<sup>+</sup> cells) (Supplementary Figure 3.14E). The monocyte population was gated as CD45.1<sup>+</sup> cells to further measure CD3 and CD4 or CD8 expression for quantification of the % CD4<sup>+</sup> or CD8<sup>+</sup> T cells in CD3<sup>+</sup> T cell population (Supplementary Figure 3.14F). The monocyte population was gated as CD45.1<sup>+</sup> cells to further sequentially measure CD3/CD4 for quantification of CD4<sup>+</sup> T cells and CD4/Foxp3 expression for quantification of % immunotolerant CD4<sup>+</sup>Foxp3<sup>+</sup> Treg cells in CD4<sup>+</sup> T cell population (Supplementary Figure 3.14G). In addition, EG7 tumor cell population was gated as live CD45.1<sup>-</sup> or CD45.2<sup>+</sup> cells (Supplementary Figure 3.14H). Gated cell populations such as M2, MDSCs and tumor cells were also analyzed for expression of cell surface PD-L1 by flow cytometry. For intracellular staining, cells were first stained for surface markers, then fixed and permeabilized using the Cytotfix/Cytoperm kit (BD Bioscience) and stained with Abs against intracellular markers such as Foxp3, IDO and arginase-1. Stained cells were analyzed by flow cytometry. All flow cytometry data were acquired with a CytoFLEX cytometer (Beckman Coulter Inc) and analyzed using FlowJo (10.4.0) software (FlowJo, LLC, Ashland, OR).

### **3.3.6 CD8<sup>+</sup> T cell proliferation and cytotoxicity assays**

To assess CD8<sup>+</sup> T cell proliferation and cytotoxic effects, we first enzymatically prepared tumor single cell suspensions as described above, followed by purification of live cells with ficoll-density

gradient centrifugation using Ficoll-Paque PREMIUM 1.084 Solution (GE Healthcare Biosciences Inc, Uppsala, Sweden) according to manufacturer's instruction. We then further purified tumor-infiltrating CD8<sup>+</sup> T cells from tumor single cell suspensions using CD8<sup>+</sup> T Cell Isolation Kit (StemCell Tech Inc, Vancouver, BC, Canada) according to manufacturer's instruction. To measure T cell proliferation, CD8<sup>+</sup> T cells purified from IRE-, IRE+Combo-, and Combo-treated tumor tissues ( $0.5 \times 10^6$  cells/well in U-bottomed 96-well plate) were incubated at 37°C in RPMI medium containing 10% FCS, IL-2 (40 U/ml) and OVAI (SIINFEKL) peptide or control (un-related) Mut1 (FEQNTAQP) peptide (0.1 nM) for 48 hrs, [34] followed by cell counting. To assess T cell cytotoxicity, the purified CD8<sup>+</sup> T cells derived from IRE-, IRE+Combo, and Combo-treated tumor tissues were first incubated in RPMI medium containing 10% FCS, phosphomolybdic acid (PMA, 0.081  $\mu$ M) and ionomycin (1.34  $\mu$ M) (Sigma-Aldrich, St. Louis, MO) at 37°C for 1 hr, [35, 36] and then used as effector cells in a T cell cytotoxicity assay [31]. Briefly, EG7 and EL4 tumor cells labeled with GranToxiLux (a cell-permeable fluorogenic granzyme-B substrate) using GranToxiLux®-PLUS Kit (OncoImmunit Inc, Gaithersburg, MD) according to manufacturer's instruction were used as target cells and control target cells, respectively. Mixtures of effector CD8<sup>+</sup> T cells with GranToxiLux-labeled target cells (10:1 and 2:1) in culture medium were incubated at 37°C for 1 hr, followed by flow cytometry analysis that detects the fluorescent light emitted due to the fluorogenic granzyme-B substrate cleavage (GBSC) in the target cells undergoing cell apoptosis [31].

### **3.3.7 Tumor-draining lymph node cell analysis**

Tumor-draining lymph nodes (TDLN) of IRE+Combo- or control IRE-treated mice were collected 7 days post IRE and homogenized by forcing tissues through a 40- $\mu$ m nylon mesh with a syringe plunger. Single cell suspensions were stained with Abs against CD8, CD11c, and CD103 for detection of cDC1 by flow cytometry. For endogenous cytokine analysis of CD8<sup>+</sup> T cells, single cell suspensions were first stimulated with PMA (0.081  $\mu$ M) and ionomycin (1.34  $\mu$ M), 3  $\mu$ g/mL of brefeldin A (BD Biosciences), and 2  $\mu$ M monensin (BD Biosciences) for 5 h in complete RPMI, then fixed and permeabilized using Cytofix/Cytoperm kits (BD Bioscience) followed by staining with Abs against intracellular IFN- $\gamma$  and TNF- $\alpha$  molecules. Cells were analyzed by flow cytometry. Data were acquired with a CytoFLEX cytometer and analyzed using FlowJo software.

### **3.3.8 Cytokine ELISA analyses**

Sera were collected from tumor-bearing mice 3 days post IRE+Combo- or IRE-ablation or Combo alone. Cytokines (IL-2, IFN- $\gamma$  and TGF- $\beta$ ) in mouse sera were measured using Mouse IL-2, IFN- $\gamma$  and TGF- $\beta$  ELISA Kits (Abcam Inc) according to manufacturer's instructions.

### **3.3.9 Immunohistochemistry**

Frozen tumors were completely embedded in optimal cutting temperature (OCT) compound, then 6- $\mu$ m cryostat sections cut and used for immunohistochemical detection. Briefly, slides were fixed with cold acetone for 20 min, then rinsed with PBS two times for 5 min each. Slides were incubated in 3% hydrogen peroxide for 10 min to block the endogenous peroxidase, then rinsed with PBS two times for 5 min each. Tissue sections were blocked with 1% BSA at room temperature for 30 min and incubated with polyclonal rabbit anti-CD8 and anti-Ly6G Abs, respectively, in PBS with 1% BSA at 4 °C overnight in a humidified chamber for detection of tumor-infiltrating CD8<sup>+</sup> T cells, and MDSCs, respectively [37]. After washing with PBS three times, the sections were incubated with HRP-labelled anti-rabbit IgG Ab for 30 min at room temperature, followed by DAB (3, 3-diaminobenzidine) developing solution. Hematoxylin was used for counterstaining. The sections were dehydrated using an increasing gradient ethanol (75, 90, 100%) and xylene, then mounted with a coverslip using permanent mounting media. The slides were imaged using a microscope at 50 $\times$  and 200 $\times$  magnification.

### **3.3.10 Statistical analysis**

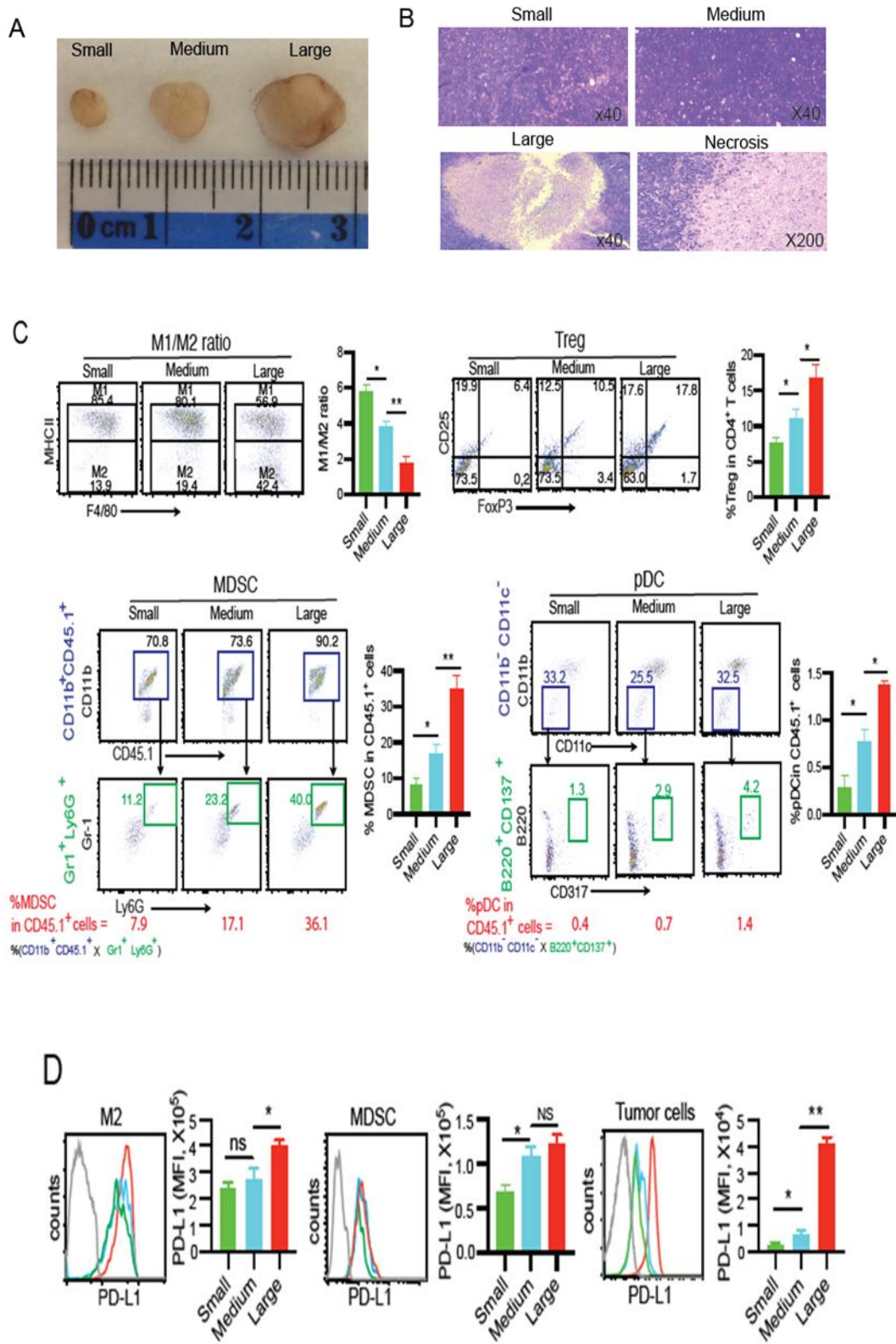
Data were analyzed using GraphPad Prism, version 8 (GraphPad Software Inc.). Tumor growth curves were first analyzed with two-way ANOVA, and groups were compared with Tukey test. Kaplan-Meier survival curves were analyzed with a log-rank test. Student's two-tailed t-test was applied to compare two experimental groups. Multiple comparisons were conducted using one-way ANOVA followed by Tukey test. A value of  $p < 0.05$  was considered statistically significant. Results are presented as mean  $\pm$  standard error of the mean (SEM).

## 3.4 Results

### 3.4.1 TME immunotolerance increases with tumor stage

To check whether tumor stage affects TME development, different sizes (4, 6, and 8-9 mm diameter or ~30, ~100, and ~300 mm<sup>3</sup> in volume) of subcutaneous (s.c.) EG7 lymphomas (**Figure 3.1A**) grown in B6.1 mice were sectioned for histopathological examination. We found some focal tumor necrosis areas in the center part of the large tumors (**Figure 3.1B**), possibly due to lack of blood supply, but not in small or medium-sized tumors. To assess TME immunotolerance, we performed flow cytometry using single cell suspensions prepared from tumor tissues (**Supplementary Figure 3.14**). We observed a trend toward an increase of immunotolerant CD11b<sup>+</sup>F4/80<sup>+</sup>MHCII<sup>-</sup> M2 (ranging from 13.9 to 19.4 to 42.4% of total CD11b<sup>+</sup>F4/80<sup>+</sup> macrophages), CD4<sup>+</sup>CD25<sup>+</sup>Foxp3<sup>+</sup> Treg cells (ranging from 6.4 to 10.5 to 17.8% of total CD4<sup>+</sup> T cells), CD11b<sup>+</sup>Gr1<sup>+</sup>Ly6C<sup>+</sup> MDSCs (ranging from 7.9 to 17.1 to 36.1% of total CD45.1<sup>+</sup> cells), and CD317<sup>+</sup>B220<sup>+</sup> pDCs (ranging from 0.4 to 0.7 to 1.4% of total CD45.1<sup>+</sup> cells) (**Figure 3.1C**) and toward an upregulation of immunosuppressive PD-L1 expression in MDSCs, M2, and EG7 tumor cells in tumors from small to medium to large sizes (**Figure 3.1D**). Together, our data indicate TME immunotolerance increases with tumor-progression (i.e., the later the stage, the more immunotolerant the TME). Therefore, we chose to work on a well-established EG7 tumor (~300 mm<sup>3</sup> in volume) model with a more immunotolerant TME, mimicking clinic patients with late stages of cancer. In addition, we also found that tumor cells and tumor-infiltrating immune cells comprised ~55% and ~45% in live tumor single cell suspensions, respectively (**Figure 3.1E**), and MDSCs comprising ~35% in total CD45.1<sup>+</sup> tumor-infiltrating immune cells in TME of large tumors, compared to M2 (~4%), pDCs (~1.4%) and Treg cells (~1.1%) (**Figure 3.1F**), indicating that MDSCs are the major component in tolerant immune cells in TME of large tumors.





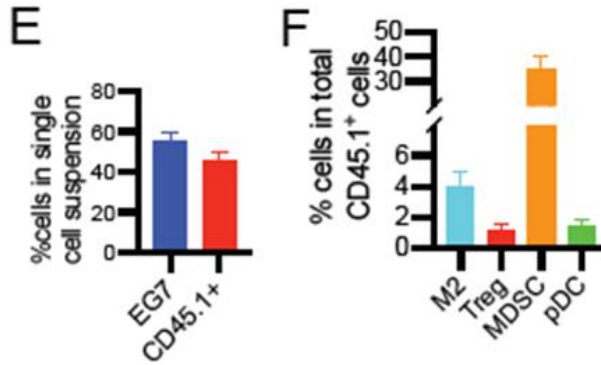


**Figure 3.1 Enhanced immunotolerant TME is associated with tumor progression.** (A) Representative image of EG7 tumors with different sizes. (B) Representative hematoxylin and eosin (H&E) staining of tissue sections of small, medium, large EG7 tumors. Black arrows, focal necrosis areas in the center of large tumor; red arrow, amplified tumor necrosis. (C) Tumor single cell suspensions (TSCSs) were enzymatically prepared from tissues of EG7 tumor with different sizes. Cell samples were stained with a cocktail of antibodies against a combination of molecular markers, and then analyzed by flow cytometry with progressive gating strategies. Last sets of representative flow cytometric plots show quantitative measurement of various immune-cell subsets. The relative abundance of (i) M1/M2 ratio calculated by % MHCII<sup>+</sup> M1/% MHCII<sup>-</sup> M2 in total CD11b<sup>+</sup>F4/80<sup>+</sup> macrophages; (ii) % Treg cells calculated by CD4<sup>+</sup>Foxp3<sup>+</sup> Treg/total CD4<sup>+</sup> T cells; (iii) % MDSCs and (iv) % pDCs in tumor-infiltrating host CD45.1<sup>+</sup> cells calculated by % (CD11b<sup>+</sup>CD45.1<sup>+</sup> cells in upper square × Gr1<sup>+</sup>Ly6G<sup>+</sup> cells in lower square) and % (CD11b<sup>-</sup>CD11c<sup>-</sup> cells in upper square × B220<sup>+</sup>CD137<sup>+</sup> cells in lower square), respectively, is described in the Methods and Supplementary Figure 3.14. (D) Flow cytometry analysis of PD-L1 expression in M2, MDSCs and tumor cells. Gray line represents control isotype antibody staining. MFI, mean fluorescence intensity. Flow cytometry plots representing one of two independent experiments (4-5 replicates each) are presented as means ± SEM. (E) The average % of CD45.2<sup>+</sup> EG7 tumor cells and CD45.1<sup>+</sup> tumor-infiltrating immune cells in TME of large tumors and (F) the average % of CD11b<sup>+</sup>F4/80<sup>+</sup>MHCII<sup>-</sup> M2, CD4<sup>+</sup>Foxp<sup>+</sup> Treg cells, Gr1<sup>+</sup>Ly6G<sup>+</sup> MDSCs and B220<sup>+</sup>CD317<sup>+</sup> pDCs in CD45.1<sup>+</sup> tumor-infiltrating immune cells were measured based upon Figure 3.1C and Supplementary Figure 3.14 (n = 5/group). \**P* < 0.05, \*\**P* < 0.01 by one-way ANOVA with Tukey test. ns, not significant.

### **3.4.2 IRE-ablation induces massive tumor cell apoptosis and weak OVA-specific CD8<sup>+</sup> T cell responses, but does not induce any significant inhibition of tumor growth in large tumors**

To assess IRE-induced tumor cell death, B6 mice were s.c. injected into right thighs with EG7 cells followed by IRE-ablation and histopathologic and flow cytometry analyses (**Figure 3.2A**). When tumors reached large sizes (8-9 mm in diameter or ~300 mm<sup>3</sup> in volume) (**Figure 3.2B**), we performed IRE-ablation (voltage: 1,200 V/cm; pulse duration: 90 μs; pulse repetition frequency: 1 Hz; number of repetition pulses: 100) using our newly constructed custom-made IRE device with two needle array electrodes (5 mm apart) (**Figure 3.2C**) [30]. To assess IRE-induced tumor cell death, we collected tumors 3 days post IRE for histological examination. IRE caused a large area of tumor cell apoptosis in the central part of tumors in association with large surrounding inflammatory areas (**Figure 3.2D**). To assess IRE-induced CD8<sup>+</sup> T cell responses and tumor growth inhibition, we conducted flow cytometry to measure CD8<sup>+</sup> T cell responses using mouse peripheral blood samples 7 days post IRE and also closely monitored tumor growth. IRE stimulated weak OVA-specific CD8<sup>+</sup> T cell responses (0.33%) (**Figure 3.2E**) but did not induce any significant inhibition of treated tumor growth, compared to untreated tumors (**Figure 3.2F**).

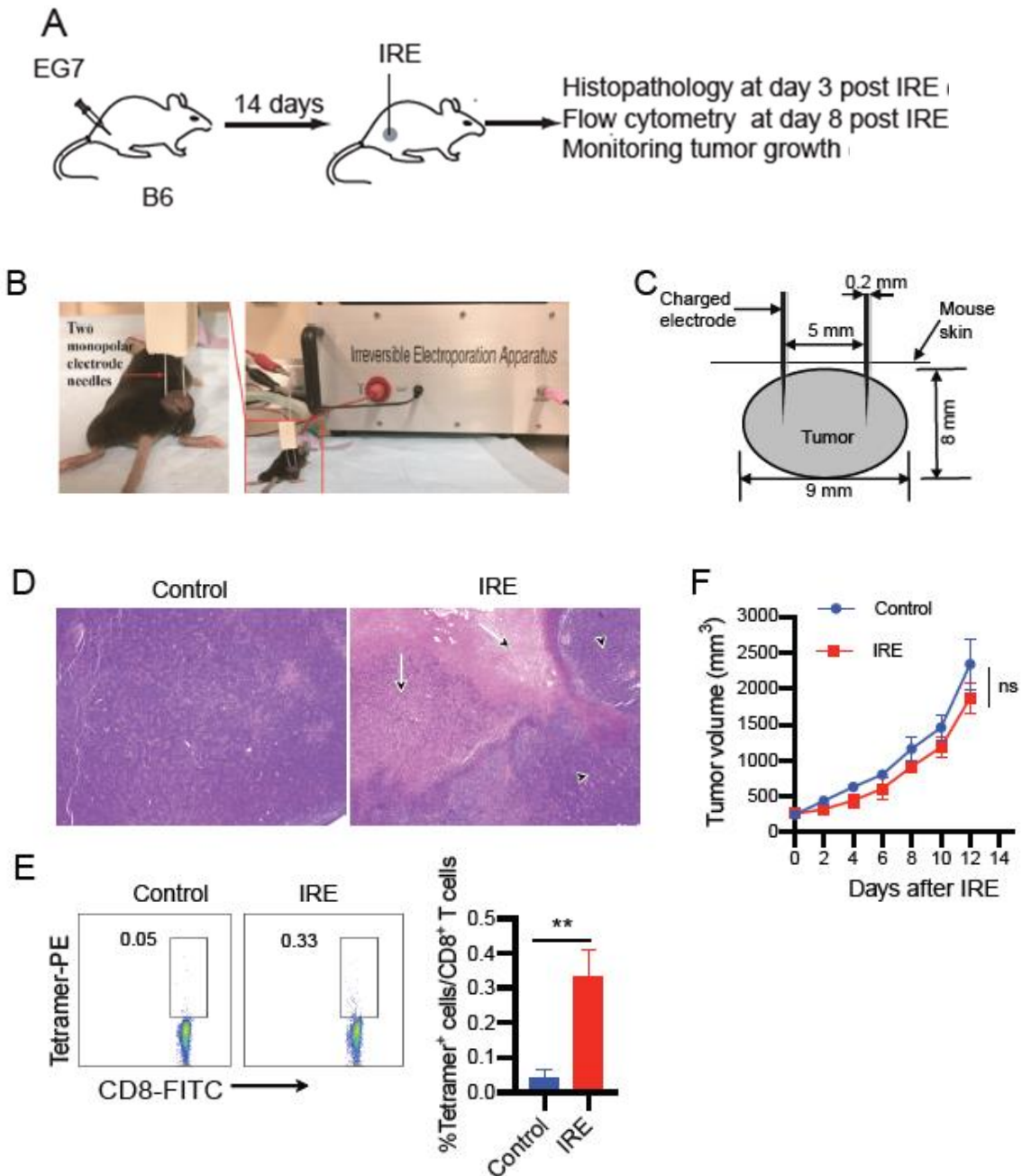


**Figure 3.2 IRE ablation induces tumor-cell apoptosis but weak OVA-specific CD8<sup>+</sup> T cell responses and is ineffective in inhibition of tumor growth.** (A) Diagram illustrating design of IRE-ablation experiment. (B) Experimental setup for IRE treatment. (C) Schematic diagram showing placement of IRE device's electrode in tumor (8-9 mm in diameter) during IRE ablation. (D) Representative H&E staining of tumor tissue sections 3 days post IRE ablation. Arrows

indicate massive apoptosis areas in IRE-treated tumor. Arrow heads indicate the surrounding tumor tissues. **(E)** Tail vein blood cells from IRE-treated or naïve control mice were stained with OVA-specific PE-Tetramer and FITC-anti-CD8 antibody, and analysed by flow cytometry. OVA-specific CD8<sup>+</sup> T cells are defined as CD8 and Tetramer double positive cells. The value in each panel represents the percentage of OVA-specific CD8<sup>+</sup> T cells among the total CD8<sup>+</sup> T cell population. \*\* $P < 0.01$  by two-tailed Student  $t$  test. **(F)** Tumor-bearing mice were monitored for tumor growth post IRE ablation. ns, not significant by two-way ANOVA with Tukey test. Flow cytometry or tumor growth plots representing one of two independent experiments are presented as means  $\pm$  SEM ( $n = 5$ /group).

### **3.4.3 Combo treatment alone only induces very weak OVA-specific CD8<sup>+</sup> T cell responses**

In this study, we selected to use anti-PD-L1 antibody for PD-1 blockade since PD-L1 expression in both the host and tumor compartment contributes to immune suppression in a non-redundant fashion [38] and anti-PD-L1 antibodies have been shown to be more effective than anti-PD-1 antibodies in blocking the PD-1/PD-L1 signaling [39, 40]. In addition, we selected to intraperitoneally (i.p.) inject anti-PD-L1 antibody into mice for PD-1 blockade such that our data become more comparable to other cancer ablation reports since the i.p. administration of PD-1 blockade is the most common route used in animal tumor models of RFA- and IRE-ablation therapy [18, 19, 41, 42, 43]. To assess whether pIC, CpG and PD-1 blockade and Combo stimulate OVA-specific CTL responses, we performed various treatments in large EG7 tumors, and measure OVA-specific CD8<sup>+</sup> T cell responses by flow cytometry (**Supplementary Figure 3.15**). We found that Combo treatment alone induced weak OVA-specific CD8<sup>+</sup> T cell responses (0.69%) in large EG7 tumors (**Figure 3.3C**), while CD8<sup>+</sup> T cell responses in other groups with treatment of PD-1 blockade, TLR3 or TLR9 agonist or TLR3/9 agonists were negligible (**Supplementary Figure 3.15**), which is consistent to previous reports using TLR agonist and PD-1 blockade [18, 41, 44]. Therefore, we selected Combo group as another control group for IRE+Combo in the following studies. In addition, Combo treatment did not show any inhibition of tumor growth (**Figure 3.3D**).

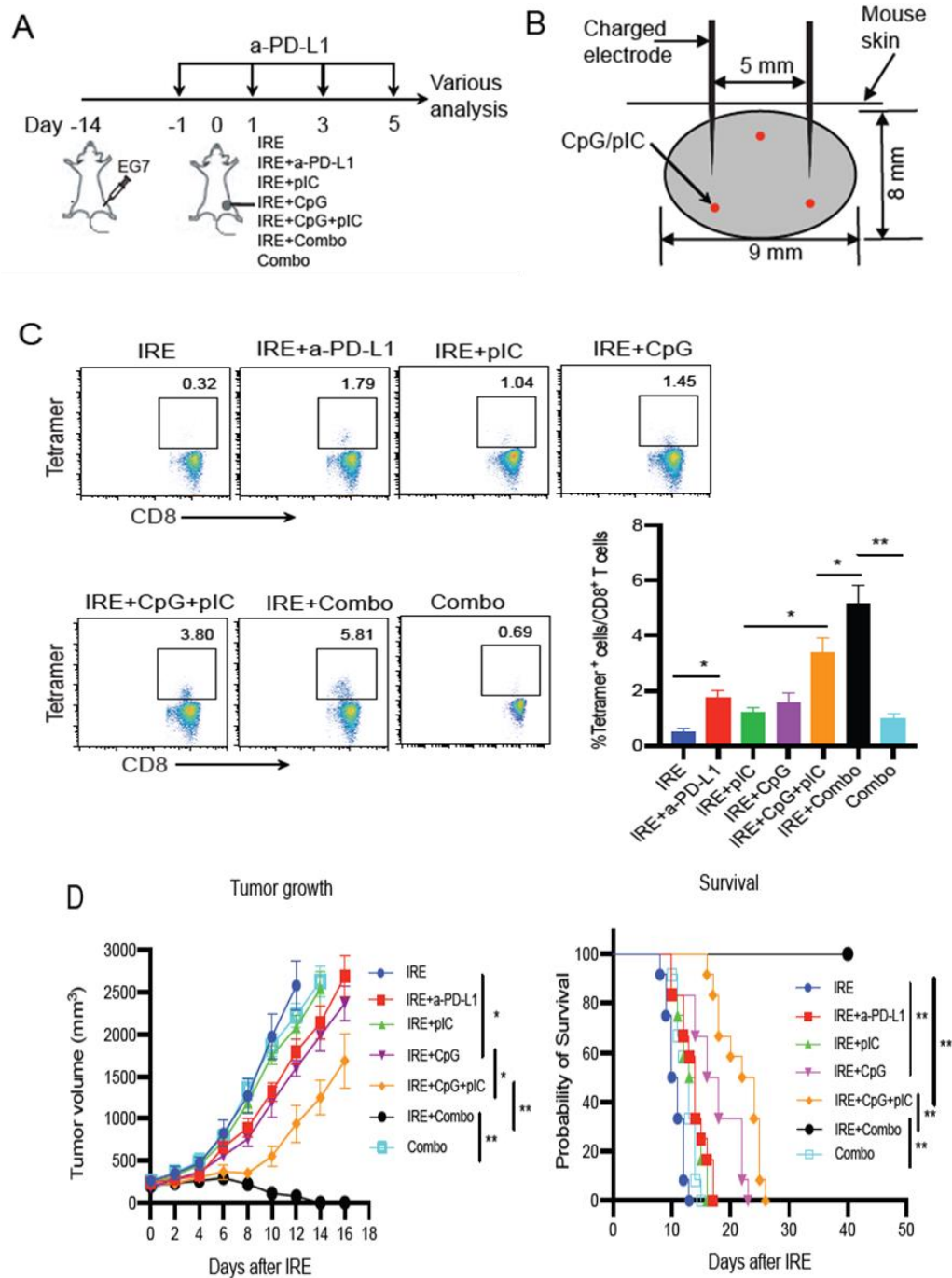


**Figure 3.3 IRE combined with PD-L1 blockade and TLR3/9 agonists results in potent OVA-specific CD8<sup>+</sup> T cell responses and antitumor immunity.** (A) Schematic diagram of IRE ablation combined with PD-1 blockade (anti-PD-L1 Ab) and/or TLR3/9 agonists (pIC/CpG) forming seven protocols including (i) IRE, (ii) IRE+anti-PD-L1, (iii) IRE+pIC, (iv) IRE+CpG, (v) IRE+pIC/CpG,

(vi) IRE+Combo and (vii) Combo alone in treatment schedules as described in the Methods. **(B)** Schematic illustrating placement of IRE device's electrode and pIC/CpG injection points (red colour) in tumor (8-9 cm in diameter) during IRE ablation. **(C)** Tail vein blood cells from mice treated with the above seven different protocols ( $n = 4/\text{group}$ ) were stained with OVA-specific PE-Tetramer and FITC-anti-CD8 antibody, and analysed by flow cytometry. The value in each panel represents the percentage of OVA-specific CD8<sup>+</sup> T cells among the total CD8<sup>+</sup> T cell population.  $**P < 0.01$  by one-way ANOVA with Tukey test. **(D)** Tumor-bearing mice were monitored for tumor growth or regression.  $*P < 0.05$ ,  $**P < 0.01$  by two-way ANOVA with *post hoc* Tukey test. Tumor-bearing mice were also monitored for mouse survival post IRE ablation. Kaplan-Meier survival analysis for the same experiments ( $n = 12/\text{group}$ ) with Log-rank test.  $**P < 0.01$ .

#### **3.4.4 PD-1 blockade enhances OVA-specific CD8<sup>+</sup> T cell responses and antitumor immunity in IRE-treated tumors**

To improve IRE-induced CD8<sup>+</sup> T cell responses, we incorporated immune checkpoint PD-1 blockade (anti-PD-L1 antibody) into our IRE-ablation protocol. When tumors reached  $\sim 300 \text{ mm}^3$  in volume, mice were first intraperitoneally (i.p.) injected with anti-PD-L1 antibody (Ab) 1 day prior to IRE and then every 2 days for a total of four times (**Figure 3.3A**). One day after the first anti-PD-L1 Ab administration, mice were subjected to IRE-ablation (**Figure 3.3A, 3.3B**). Seven days post IRE+PD-1 blockade, we performed flow cytometry to measure CD8<sup>+</sup> T cell responses and monitored tumor growth. We demonstrated PD-1 blockade significantly enhanced OVA-specific CD8<sup>+</sup> T cell responses (1.79%) compared to T cell responses (0.32%) in the IRE-ablated control group (**Figure 3.3C**). We also showed PD-1 blockade significantly inhibited tumor growth and prolonged mouse survival compared to the control IRE-ablated group (**Figure 3.3D**).

### **3.4.5 TLR3/9 agonists synergistically stimulate potent OVA-specific CD8<sup>+</sup> T cell responses and strong antitumor immunity in IRE-treated tumors**

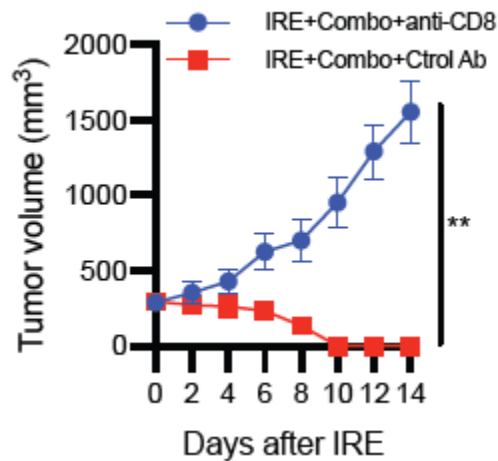
To improve IRE-induced CD8<sup>+</sup> T cell immunity, we also incorporated pIC and CpG administrations into the IRE-ablation protocol. Tumor-bearing mice were subjected to IRE immediately followed by intratumoral (i.t.) injection of either pIC (IRE+pIC) or CpG (IRE+CpG) or both (IRE+pIC/CpG) at peripheral tumor areas (**Figure 3.3B**). Seven days post IRE, we performed flow cytometry to measure CD8<sup>+</sup> T cell responses and monitored tumor growth. Although IRE+pIC and IRE+CpG promoted OVA-specific CD8<sup>+</sup> T cell responses (1.04% and 1.45%) and inhibited primary tumor growth compared to the control IRE-treated group, the latter was more efficient than the former (**Figure 3.3C, 3.3D**). Interestingly, IRE combined with TLR3/9 agonists (IRE+pIC/CpG) synergistically stimulated potent OVA-specific CD8<sup>+</sup> T cell (3.80%) responses, and significantly inhibited tumor growth and prolonged mouse survival post IRE compared to IRE+pIC or IRE+CpG alone (**Figure 3.3C, 3.3D**), indicating that TLR3/9 agonists synergistically stimulate potent OVA-specific CD8<sup>+</sup> T cell responses and strong antitumor immunity in IRE-treated tumors. In addition, IRE+pIC/CpG-induced CD8<sup>+</sup> T cell immunity was more efficient than that induced by IRE+PD-1 blockade (**Figure 3.3C, 3.3D**).

### **3.4.6 IRE+Combo cooperatively stimulates potent OVA-specific CD8<sup>+</sup> T cell responses leading to complete eradication of primary tumors**

Although an incremental improvement in OVA-specific CD8<sup>+</sup> T cell responses was observed with both IRE+PD-1 blockade or IRE+pIC/CpG compared to control IRE, each alone was still insufficient to overcome the aggressive nature of EG7 tumors (**Figure 3.3D**), suggesting a combined IRE treatment protocol incorporating both PD-1 blockade and CpG/pIC is worth assessing for potentially improved therapeutic effect. Therefore, we performed a therapeutic strategy by combining IRE-ablation with co-administered PD-1 blockade and CpG/pIC (IRE+Combo) in our EG7 tumor model (**Figure 3.3A**). Seven days post IRE, we performed flow cytometry to measure OVA-specific CD8<sup>+</sup> T cell responses and monitored tumor-growth. Our experiments revealed enhanced OVA-specific CD8<sup>+</sup> T cell responses (5.81%) (**Figure 3.3C**),



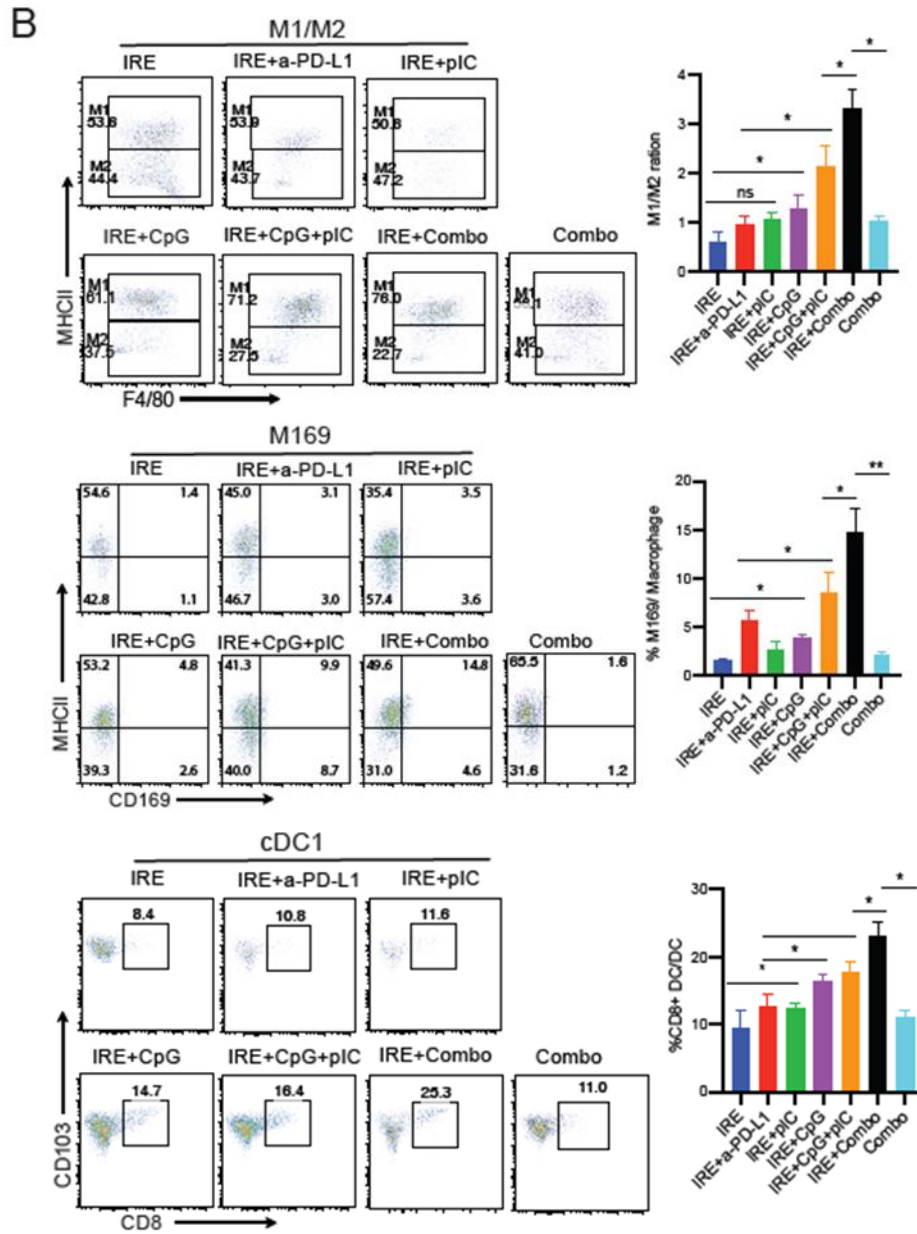
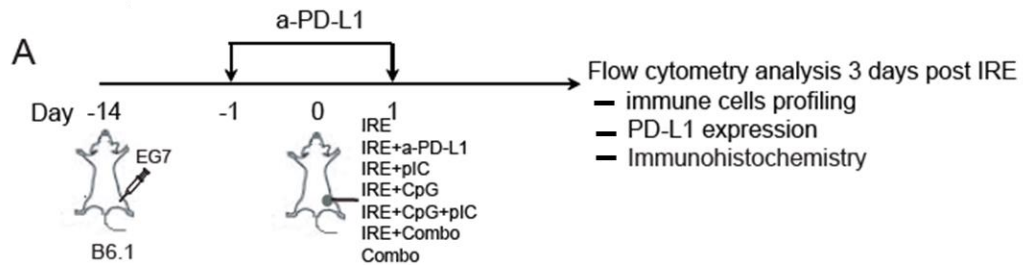
which are more efficient than CD8<sup>+</sup> T cell responses in other groups, leading to complete eradication of primary tumors with no tumor recurrence for one month (**Figure 3.3D**). To confirm IRE+Combo-induced CD8<sup>+</sup> T cell responses contribute to eradication of primary tumors, we performed a CD8<sup>+</sup> T-cell depletion assay using anti-CD8 Ab to deplete CD8<sup>+</sup> T cells 1-day prior to and once every 3 days during IRE+Combo treatment for a total of four times. This resulted in IRE+Combo completely losing its therapeutic effect in terms of eradication of primary tumors (**Figure 3.4**), which is consistent with previous studies for tumor-ablation therapy [18, 19, 29] and indicates CD8<sup>+</sup> T cells are the major effectors in IRE+Combo-induced tumor eradication.



**Figure 3.4 CD8<sup>+</sup> T cell depletion assay.** Tumor growth curves of IRE+Combo-treated tumors with and without depletion of CD8<sup>+</sup> cells using anti-CD8 and control antibody. Tumor growth or regression was monitored. Tumor-bearing mice were monitored for tumor growth post IRE-Combo ablation. \*\* $P < 0.01$  by two-way ANOVA with Tukey test. Tumor growth plots representing one of two independent experiments are presented as means  $\pm$  SEM ( $n = 4/\text{group}$ ).

### **3.4.7 TLR3/9 agonists play a major role in modulating immune cell profiles and a minor role in reducing PD-L1 expression in TME and *vice versa* for PD-1 blockade in IRE-treated tumors**

To assess the modulatory effect of TLR3/9 agonists on an immunotolerant TME, single cell suspensions prepared from peripheral areas of tumor tissues 3 days post treatments were analyzed by flow cytometry (**Figure 3.5A**) and (**Supplementary Figure 3.14**). We found that CpG more efficiently modulated immune cell profiling by increasing M1/M2 ratio and M169 and cDC1 and reducing Treg cells, MDSCs and pDCs than pIC (**Figure 3.5B**). Interestingly, we demonstrated IRE+pIC/CpG significantly increased the M1 (71.2%)/M2 (27.5%) ratio (2.6) and frequencies of immunogenic M169 (9.9% of total macrophages) and cDC1 (16.4% of total DCs) and reduced immunotolerant Treg cells (7.6% of CD4<sup>+</sup> T-cells), MDSCs (16.9% of CD45.1<sup>+</sup> cells), and pDCs (0.3% of CD45.1<sup>+</sup> cells) in IRE+pIC/CpG-treated mice compared to those in either the IRE+pIC- or IRE+CpG-treated groups. Interestingly, the modulation of immune cell profiling by IRE+pIC/CpG is also more efficient than IRE+PD-1 blockade, illustrated in the M1 (53.9%)/M2 (43.7%) ratio (1.2), M169 (3.1% of total macrophages), cDC1 (10.8% of total DCs), Treg cells (10.3% of CD4<sup>+</sup> T cells), MDSCs (29.8% of CD45.1<sup>+</sup> cells), and pDCs (0.5% of CD45.1<sup>+</sup> cells) (**Figure 3.5B**). In contrast, we found IRE+PD-1 blockade more efficiently downregulated cell-surface PD-L1 expression in M2, MDSCs, and tumor cells than IRE+pIC/CpG (**Figure 3.6A**). Taken together, our data indicate TLR3/9 agonists play a major role in modulating immune cell profiles but a minor role in down-regulating PD-L1 expression in the TME, and *vice versa* for PD-1 blockade.



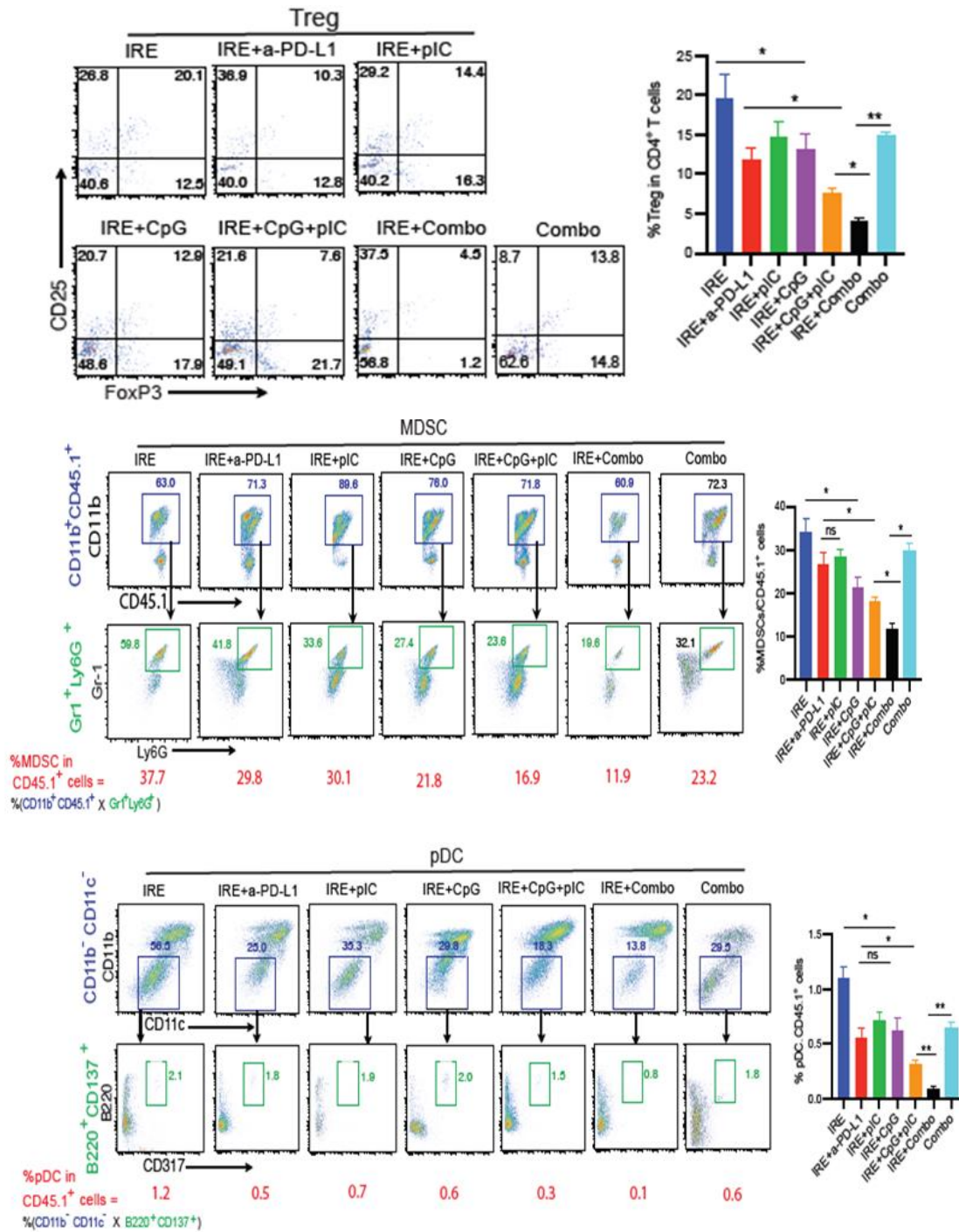
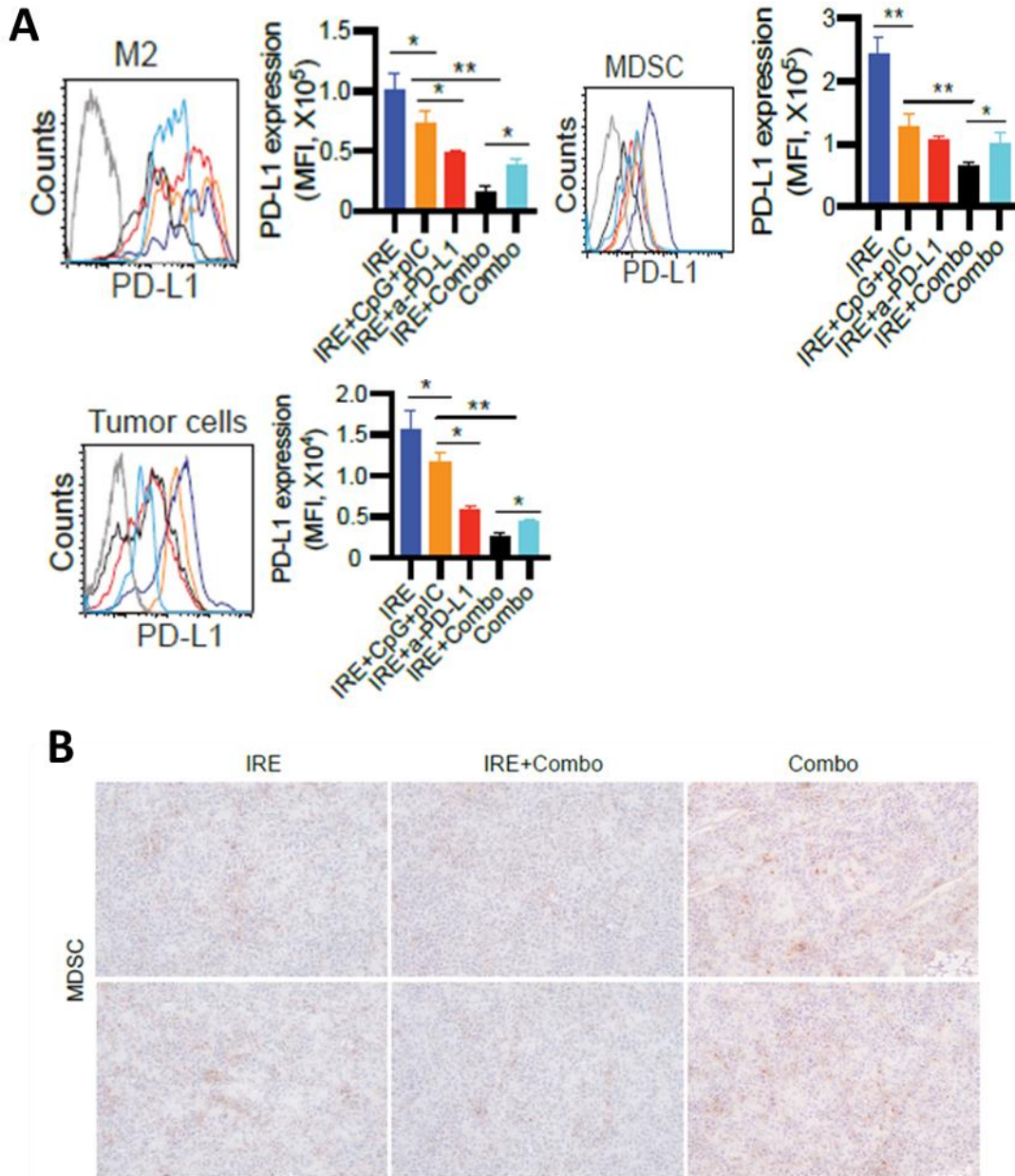


**Figure 3.5 IRE combined with PD-L1 blockade and TLR3/9 agonists modulates immune cell profiling in TME.** (A) Diagram illustrating experimental setup for analysing intratumoral immune cell subsets of B6.1 mice bearing primary tumor (8-9 mm in diameter) 3 days post IRE ablation. Single cell suspensions were enzymatically prepared from primary tumor tissues 3 days post IRE ablation. Cell samples were stained with a cocktail of antibodies, and then analyzed by flow

cytometry with progressive gating strategies. **(B)** Last sets of representative flow cytometric plots show quantitative measurement of various immune cell subsets. The relative quantitation of (i) M1/M2 ratio calculated by % MHCII<sup>+</sup> M1/% MHCII<sup>-</sup> M2 in total CD11b<sup>+</sup>F4/80<sup>+</sup> macrophages (ii) % M169 calculated by CD169<sup>+</sup>CD11b<sup>+</sup>F4/80<sup>+</sup> M169/total CD11b<sup>+</sup>F4/80<sup>+</sup> macrophages; (iii) % cDC1 calculated by CD8<sup>+</sup>CD103<sup>+</sup>CD11c<sup>+</sup> cDC1/total CD11c<sup>+</sup> DCs; (iv) % Treg cells calculated by CD4<sup>+</sup>Foxp3<sup>+</sup> Treg/total CD4<sup>+</sup> T cells; (v) % MDSCs and (vi) % pDCs in tumor-infiltrating host CD45.1<sup>+</sup> cells calculated by % (CD11b<sup>+</sup>CD45.1<sup>+</sup> cells in upper square × Gr1<sup>+</sup>Ly6G<sup>+</sup> cells in lower square) and % (CD11b<sup>-</sup>CD11c<sup>-</sup> cells in upper square × B220<sup>+</sup>CD137<sup>+</sup> cells in lower square), respectively, is described in the Methods and Supplementary Figure 3.14. \*  $p < 0.05$ , \*\*\* $P < 0.01$  by one-way ANOVA with Tukey test.

### **3.4.8 IRE+Combo potently modulates immune-cell profiling and significantly downregulates PD-L1 expression in the TME in IRE-treated tumors**

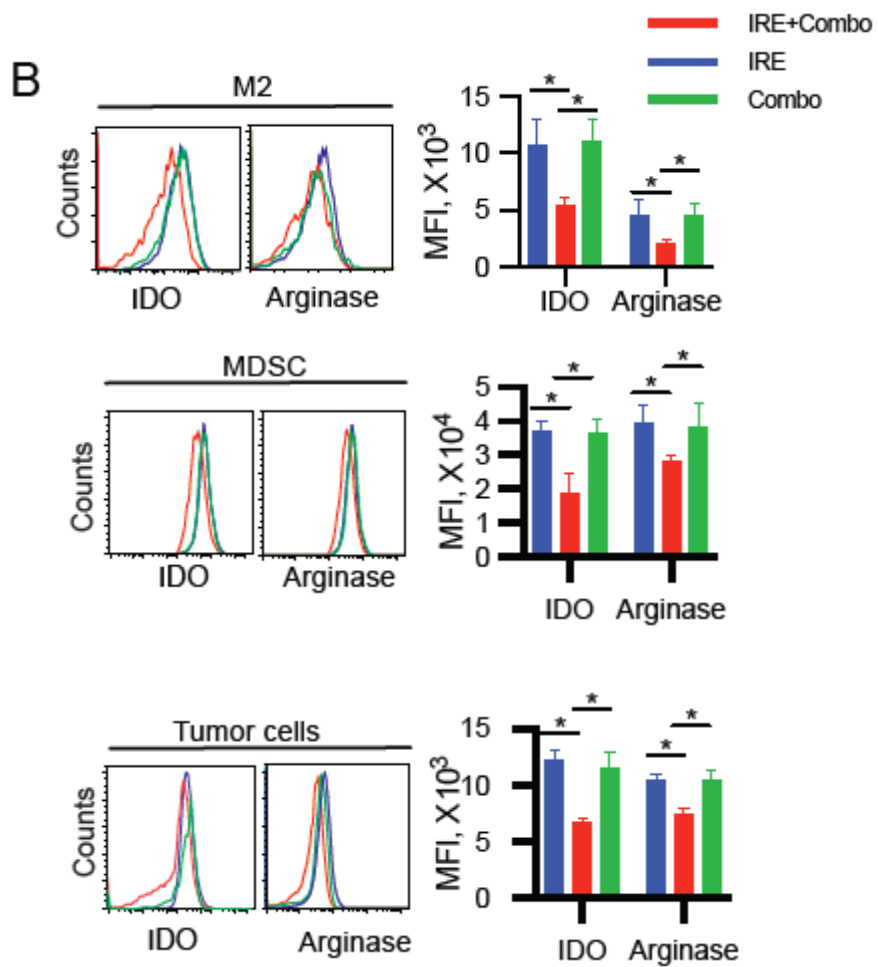
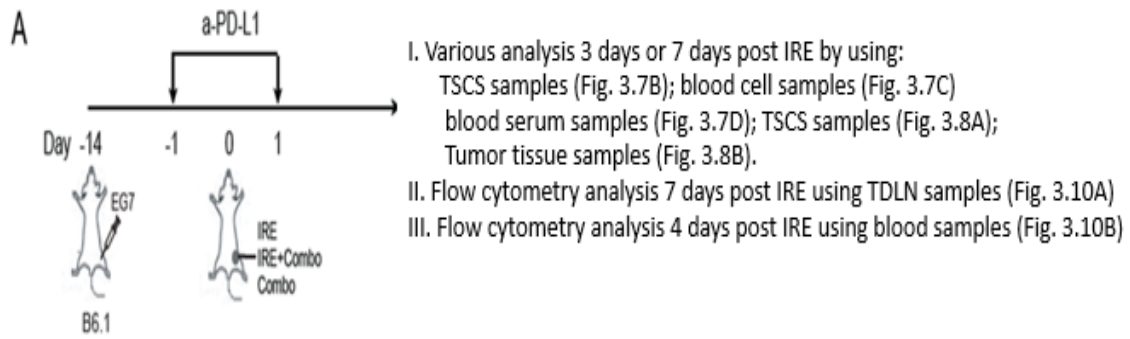
Having shown the effective therapeutic efficacy of IRE+Combo with respect to the eradication of primary tumors, we then focused on investigating its modulating effect on immune-cell profiling in the TME. We performed flow cytometry with progressive gating strategies to analyze immune-cell profiles and PD-L1 expression in single-cell suspensions enzymatically prepared from IRE+Combo-ablated tumors 3 days post IRE (**Figure 3.5A**). We demonstrated IRE+Combo cooperatively promoted the M1 (76.0%)/M2 (22.7%) ratio (3.3), increased the frequencies of immunogenic M169 (14.8% of the M population) and cDC1 (25.3% of the DC population), and reduced the frequencies of immunotolerant Treg cells (4.5% of CD4<sup>+</sup> T cells), MDSCs (11.9% of CD45.1<sup>+</sup> cells), and pDCs (0.1% of CD45.1<sup>+</sup> cells) compared to either IRE+PD-1 blockade or IRE+pIC/CpG or Combo alone (**Figure 3.5B**). The declined frequency of MDSCs in IRE+Combo-treated tumors compared to controlled IRE-treated one or Combo alone was confirmed by immunohistochemical analysis (**Figure 3.6B**). In addition, IRE+Combo more significantly downregulated PD-L1 expression in M2, MDSCs, and tumor cells in the TME than IRE+pIC/CpG or IRE+PD-1 blockade or Combo alone (**Figure 3.6A**).



**Figure 3.6 IRE combined with PD-L1 blockade and TLR3/9 agonists downregulates PDL-1 expression in TME.** (A) Cell samples were also stained with a cocktail of antibodies and then analyzed by flow cytometry. PD-L1 expression in gated M2, MDSCs and tumor cells was analyzed by flow cytometry. \*  $p < 0.05$ , \*\* $P < 0.01$  by one-way ANOVA with Tukey test. (B) Immunohistochemistry (IHC) analysis of primary tumor tissue frozen sections. Representative micrographs of IHC staining for MDSCs. Above data representing one of two independent experiments are presented as means  $\pm$  SEM ( $n = 5$ /group).

### **3.4.9 IRE+Combo edits tolerant immune and tumor cells for less suppression and induces a systemic decrease of immune tolerance**

Because we observed IRE+Combo's effect on reducing immunotolerant cell populations such as M2 and MDSCs in the TME, we next wanted to assess whether IRE+Combo edits immunotolerant M2 and MDSCs in IRE+Combo-treated tumors and affects the systemic immune tolerance. To this end, we performed various analyses 3 or 7 days post IRE for (i) expression of immunosuppressive IDO and arginase-1 in immunotolerant M2, MDSCs and tumor cells, (ii) frequencies of MDSCs and M1/M2 in blood cell samples, (iii) cytokine concentration in blood sera, (iv) frequencies of CD4<sup>+</sup> and CD8<sup>+</sup> T cells in TME and (v) frequencies of cDC1 and CD8<sup>+</sup> T cells in tumor-draining lymph nodes (TDLNs) (**Figure 3.7A**). We demonstrated that IRE+Combo significantly down-regulated suppressive IDO and arginase-1 in immunotolerant M2, MDSCs, and EG7 tumor cells 3 days post IRE, compared to IRE or Combo alone (**Figure 3.7B**), indicating that IRE+Combo edits tolerant immune and tumor cells for less suppression. In addition, the abundance of immunotolerant MDSCs and the ratio of M1 versus M2 were significantly reduced and increased, respectively, in blood of IRE+Combo-treated mice 3 days post IRE, compared to the control IRE-ablated or Combo-treated mice (**Figure 3.7C**). Finally, we tested cytokine expression in sera collected from IRE+Combo- or IRE- or Combo-treated mice 3 days post IRE using colorimetric cytokine ELISA. We showed increased concentrations of IL-2 and IFN- $\gamma$  (~700 pg/ml and ~1,100 pg/ml) and reduced concentration of TGF- $\beta$  (~8 ng/ml) in IRE+Combo-treated mouse sera, compared to those in control IRE- and Combo-treated mouse sera (**Fig 3.7D**). Taken together, our data indicate that IRE+Combo induces a systemic decrease of immune tolerance.





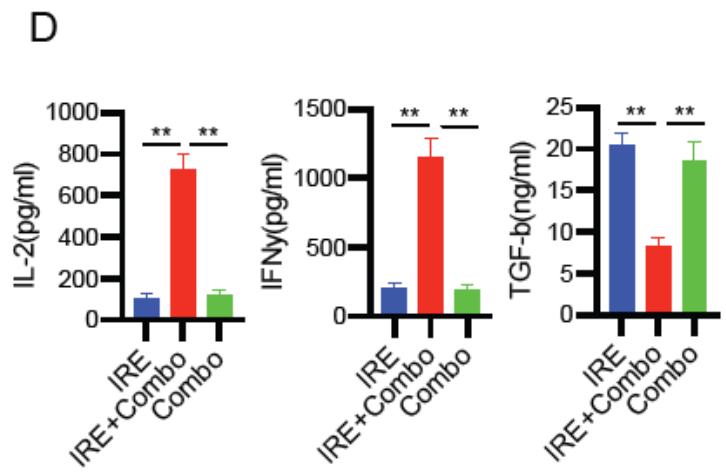
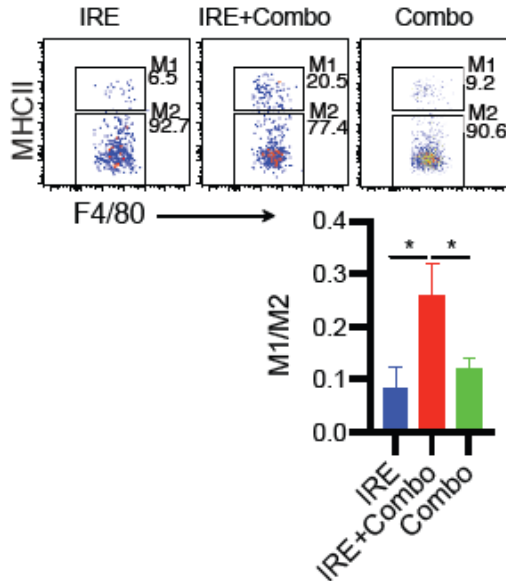
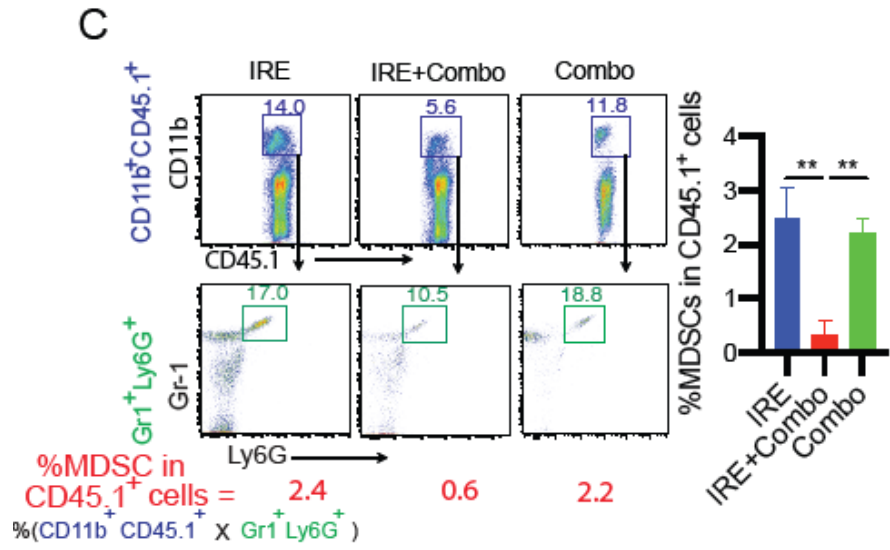


**Figure 3.7 IRE+Combo modulates immune cells and cytokines in blood and promotes CD8<sup>+</sup> T cells in IRE+Combo-treated tumor tissues and in tumor-drainage lymph nodes.** (A) Diagram illustrating experimental setup for different analyses. (B) TSCSs were enzymatically prepared from primary tumor tissues of mice treated with IRE, Combo and IRE+Combo 3 days post IRE, respectively. Cell samples were stained with a cocktail of antibodies and analyzed by flow cytometry. Expression of IDO and arginase-1 in gated M2, MDSCs and tumor cells was analyzed by flow cytometry, as described in the Methods and Supplementary Figure 3.14. Gray line represents control isotype antibody staining. MFI, mean fluorescence intensity. (C) Mouse blood was collected 3 days post IRE ablation, and blood monocytes purified by Ficoll-Hypaque density gradient centrifugation were stained with a cocktail of antibodies. The relative quantitation MDSCs calculated by % CD11b<sup>+</sup>Gr1<sup>+</sup>Ly6G<sup>+</sup> MDSCs in total monocytes and the ratio of M1 versus M2 calculated by the amount of MHCII<sup>+</sup>CD11b<sup>+</sup>F4/80<sup>+</sup> M1/the amount of MHCII<sup>-</sup>CD11b<sup>+</sup>F4/80<sup>+</sup> M2 were analyzed by flow cytometry. (D) Quantification of TGF- $\beta$ , IL-2 and IFN- $\gamma$  in mouse sera of mice 3 days post IRE ablation. Each bar is an average of 4 mice/group. Error bars indicate mean  $\pm$  SEM. \* $P < 0.05$ , \*\* $P < 0.01$  by two-tailed Student  $t$  test. One representative experiment out of two independent experiments is shown.

#### **3.4.10 IRE+Combo promotes tumor-infiltrating CD4<sup>+</sup> and CD8<sup>+</sup> T cells in TME in IRE-treated tumors**

Tumor-infiltrating T cells play an important role in tumor eradication [10, 45]. To test whether an IRE+Combo-treated TME favors T cell tumor infiltration, we first assessed the amount of tumor-infiltrating T cells in IRE+Combo-treated tumors 3 days after IRE-ablation by flow cytometry and immunohistochemical analyses (**Figure 3.7A**). We demonstrated both CD4<sup>+</sup> and CD8<sup>+</sup> T cells assessed as percentages of CD4<sup>+</sup> and CD8<sup>+</sup> T cells in the total live CD45.1 cell population were significantly elevated by 2- and 3-fold, respectively, in IRE+Combo-treated tumors, compared to control IRE-ablated or Combo-treated tumors (**Figure 3.8A**). The increased frequency of CD8<sup>+</sup> T cells in IRE+Combo-treated tumors was also confirmed by immunohistochemical analysis (**Figure 3.8B**).

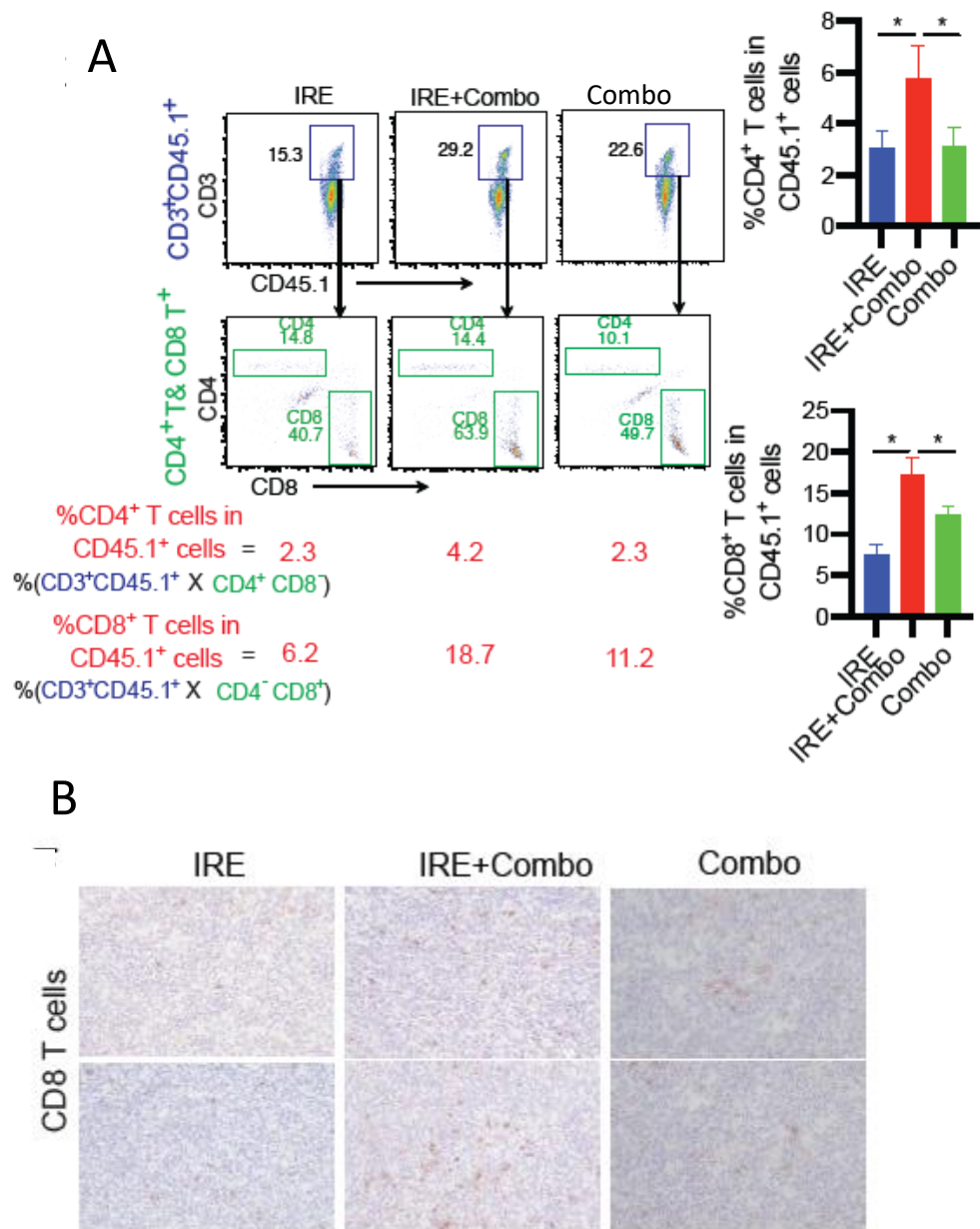


**Figure 3.8 IRE+Combo promotes tumor-infiltrating CD4<sup>+</sup> and CD8<sup>+</sup> T cells in TME (A)** TSCSs were enzymatically prepared from primary tumor tissues 3 days post IRE+Combo or IRE ablation. Cell samples were stained with a cocktail of antibodies and analyzed by flow cytometry with progressive gating strategies as described in the Methods and Supplementary Figure 3.14. Last sets of representative flow cytometric plots show quantitative measurement of CD4<sup>+</sup> and CD8<sup>+</sup> T cells in total tumor-infiltrating host CD45.1<sup>+</sup> cells by gating CD3<sup>+</sup>CD45.1<sup>+</sup> T cells for

measurement of CD4<sup>+</sup> and CD8<sup>+</sup> T cells, respectively. **(B)** IHC analysis of primary tumor tissue frozen sections. Representative micrographs of IHC staining for CD8<sup>+</sup> T cells. Each bar is an average of 4 mice/group. Error bars indicate mean  $\pm$  SEM. \**P* < 0.05, \*\**P* < 0.01 by two-tailed Student *t* test. One representative experiment out of two independent experiments is shown.

### 3.4.11 IRE+Combo promoted tumor-infiltrating CD8<sup>+</sup> T cells are functionally effective

CD8<sup>+</sup> T cell dysfunction in TME is functionally characterized by reduced proliferative capacity and diminished cytotoxicity effect, in part because of up-regulation of immune checkpoint molecules [46]. To assess whether IRE+Combo promoted tumor-infiltrating CD8<sup>+</sup> T cells are functionally effective, we purified CD8<sup>+</sup> T cells from tumor single cell suspensions derived from IRE+Combo-, IRE- and Combo-treated tumors using CD8<sup>+</sup> T Cell Isolation Kit and assessed their *in vitro* proliferative and cytotoxicity effects in T cell proliferation and cytotoxicity assays, respectively. We found that CD8<sup>+</sup> T cells derived from IRE+Combo-treated tumors were of much more efficient OVA-specific proliferative potential and cytolytic effect against EG7, but not EL4 target cells than CD8<sup>+</sup> T cells derived from control IRE- or Combo-treated tumors (**Figure 3.9A, 3.9B**).

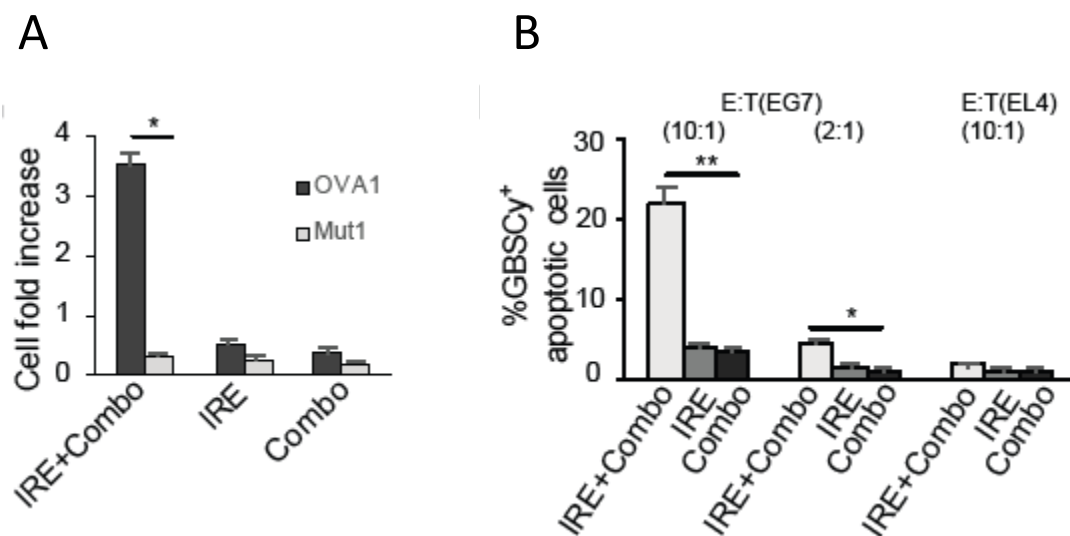


**Figure 3.9 IRE+Combo promoted functionally effective tumor-infiltrating CD8<sup>+</sup> T cells (A)** Purified CD8<sup>+</sup> T cells from TSCSs were be cultivated in medium containing IL-2 and OVAI or unrelated Mut1 peptide for three days followed by cell counting in T cell proliferation assay. **(B)** Purified CD8<sup>+</sup> T cells from TSCSs were be measured for their cytotoxicity effect in cell cytotoxicity assay, in which activated CD8<sup>+</sup> T cells and GranToxiLux-labelled EG7 or EL4 tumor cells were used as effector (E) and target (T) cells, respectively. % of positive fluorogenic granzyme-B substrate cleavage (GBSC<sup>+</sup>) were measured at E:T (10:1 and 2:1) ratio. Each bar is an average of 4 mice/group. Error bars indicate mean  $\pm$  SEM. \**P* < 0.05, \*\**P* < 0.01 by two-tailed Student *t* test. One representative experiment out of two independent experiments is shown.

#### **3.4.12 IRE+Combo promotes cDC1 and effector CD8<sup>+</sup> T cells in tumor-drainage lymph nodes and a long-term CD8<sup>+</sup> T cell memory**

To confirm IRE+Combo's effect on promoting immunogenic cells, single cell suspensions prepared from TDLNs 7 days post IRE+Combo of primary tumors were analyzed by flow cytometry (**Supplementary Figure 3.16**). We demonstrated IRE+Combo significantly promotes CD8<sup>+</sup>CD103<sup>+</sup> cDC1 (10.6% in total CD11c<sup>+</sup> DCs) and IFN- $\gamma$ /TNF- $\alpha$  double positive effector CD8<sup>+</sup> T cells (26.5% in total CD3<sup>+</sup> T-cells) in TDLNs, compared to 3.0% and 3.5% cDC1 and 6.7% and 8.9% effector CD8<sup>+</sup> T cells in the IRE-ablated control group and control Combo group, respectively (**Figure 3.10 A**). To assess whether IRE+Combo ablation induces a long-term CD8<sup>+</sup> T cell memory, we i.v. immunized IRE+Combo-treated mice with recombinant *Listeria* expressing OVA (rLmOVA) one month after complete regression of treated primary tumors. We then measured recall responses 4 days post rLmOVA boost. We demonstrated significant recall CD8<sup>+</sup> T cell responses (11.6%) in IRE+Combo-treated mice, but not in the untreated control mice (**Figure 3.10 B**), indicating IRE+Combo induces long-term CD8<sup>+</sup> T cell memory in IRE+Combo-treated mice.

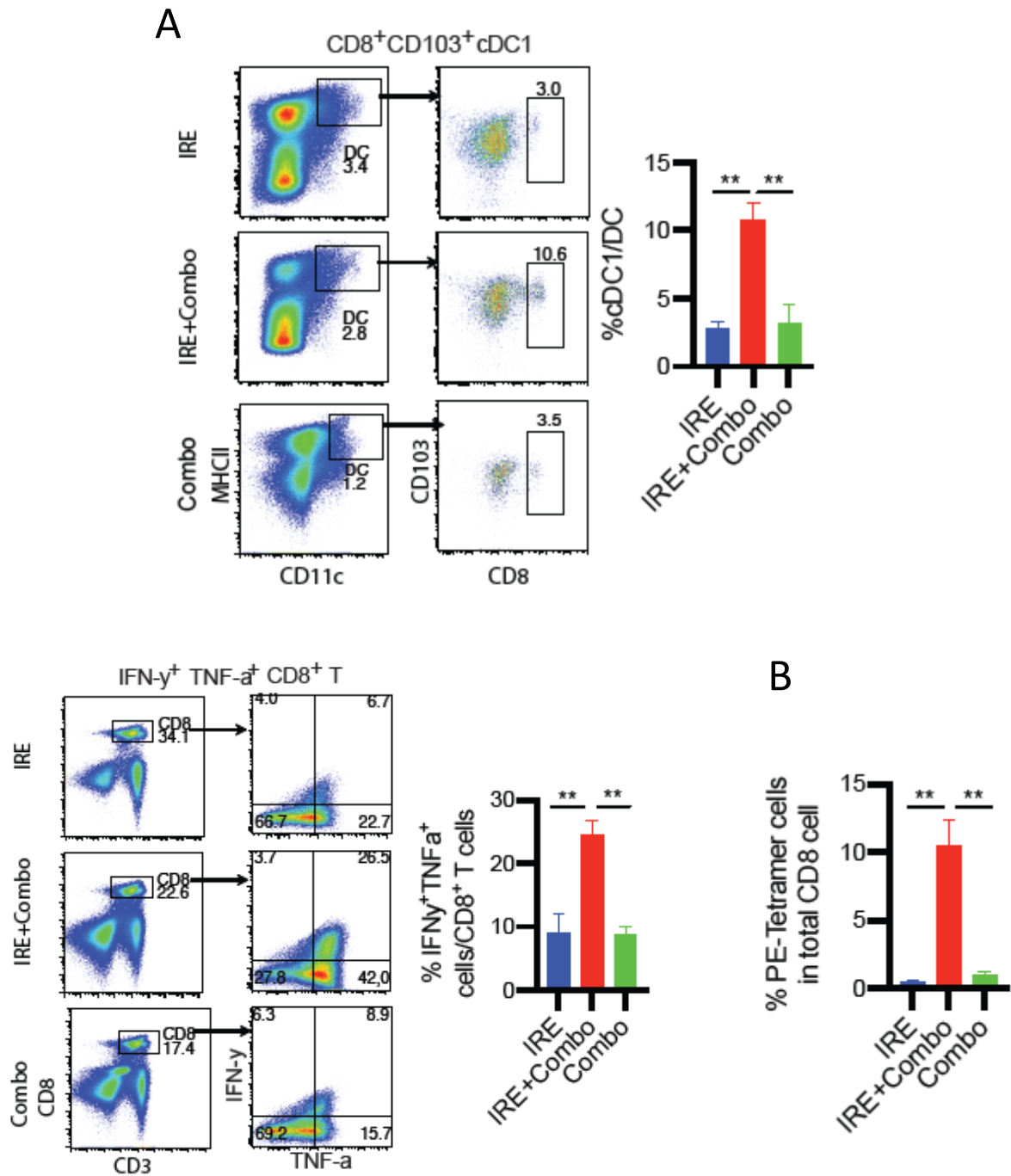


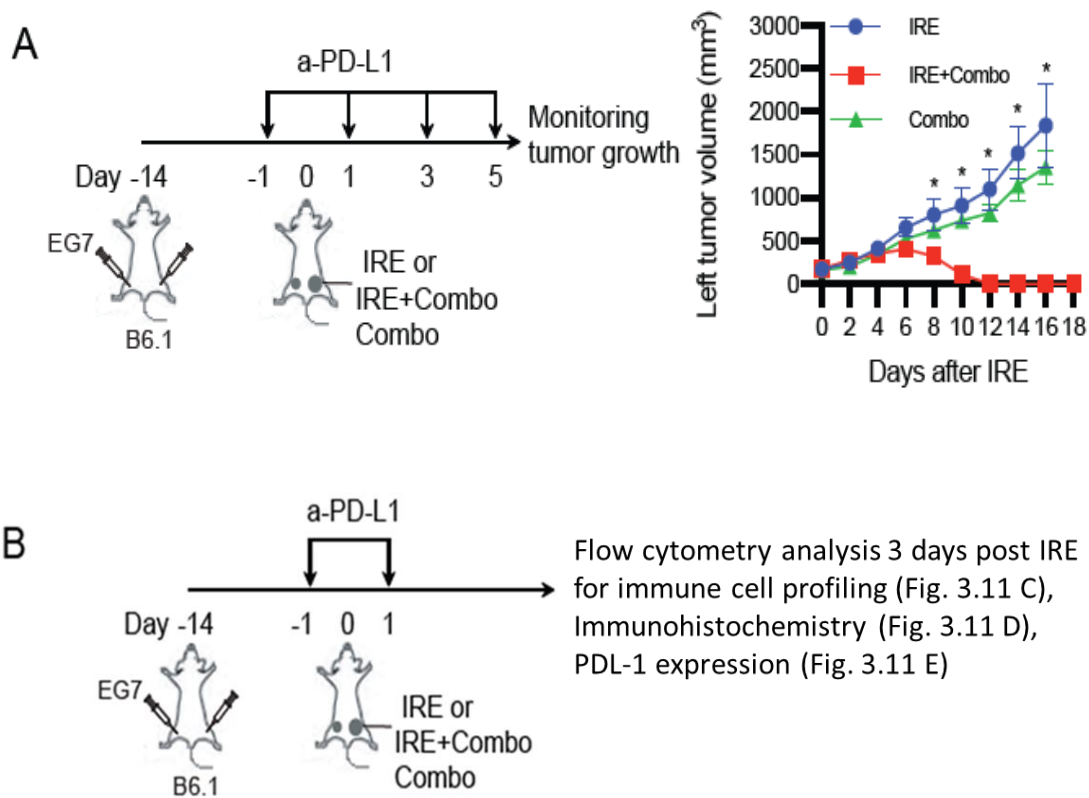
**Figure 3.10 IRE+Combo promotes cDC1 and effector CD8<sup>+</sup> T cells in tumor-drainage lymph nodes** (A) Single cell suspensions prepared from tumor-drainage lymph nodes (TDLNs) 7 days post primary tumors treated with IRE+Combo- and IRE-ablation. Cell samples were stained with a cocktail of antibodies and analyzed by flow cytometry with progressive gating strategies as described in the Methods and Supplementary Figure 3.16. Last sets of representative flow

cytometric plots show quantitative measurement of % CD8<sup>+</sup>CD103<sup>+</sup> cDC1 in total DCs by analysis of gated CD11c<sup>+</sup>MHCII<sup>+</sup> DCs and quantitative measurement of % IFN- $\gamma$ <sup>+</sup>TNF- $\alpha$ <sup>+</sup> (double positive) CD8<sup>+</sup> effector T cells in total CD3<sup>+</sup> T cells by analysis of gated CD3<sup>+</sup>CD8<sup>+</sup> T cells. **(B)** T cell memory recall responses. Mice with complete eradication of IRE+Combo-treated primary tumors for 30 days or naïve mice as a control were i.v. boosted with recombinant rLmOVA bacteria. Tail vein blood cell samples were stained with OVA-specific PE-Tetramer and FITC-anti-CD8 antibody, and OVA-specific CD8<sup>+</sup> T cell responses were then analysed by flow cytometry 4 days after the boost. Each bar is an average of 4 mice/group. Error bars indicate mean  $\pm$  SEM. \* $P$  < 0.05, \*\* $P$  < 0.01 by two-tailed Student  $t$  test. One representative experiment out of two independent experiments is shown.

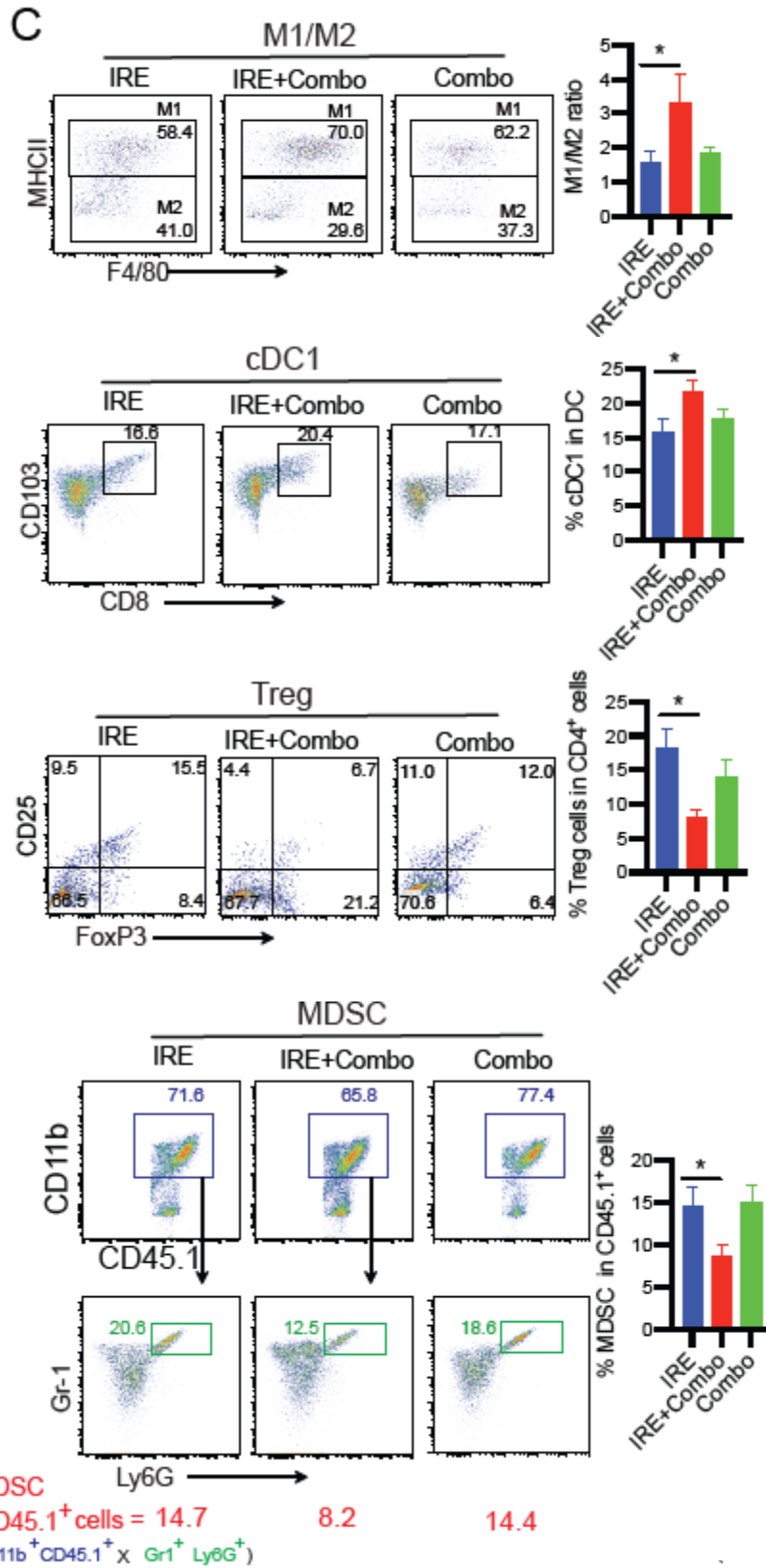
### **3.4.13 IRE+Combo ablation eradicates distant tumors *via* modulating its immunotolerant TME and promoting tumor-infiltrating CD4<sup>+</sup> and CD8<sup>+</sup> T cells**

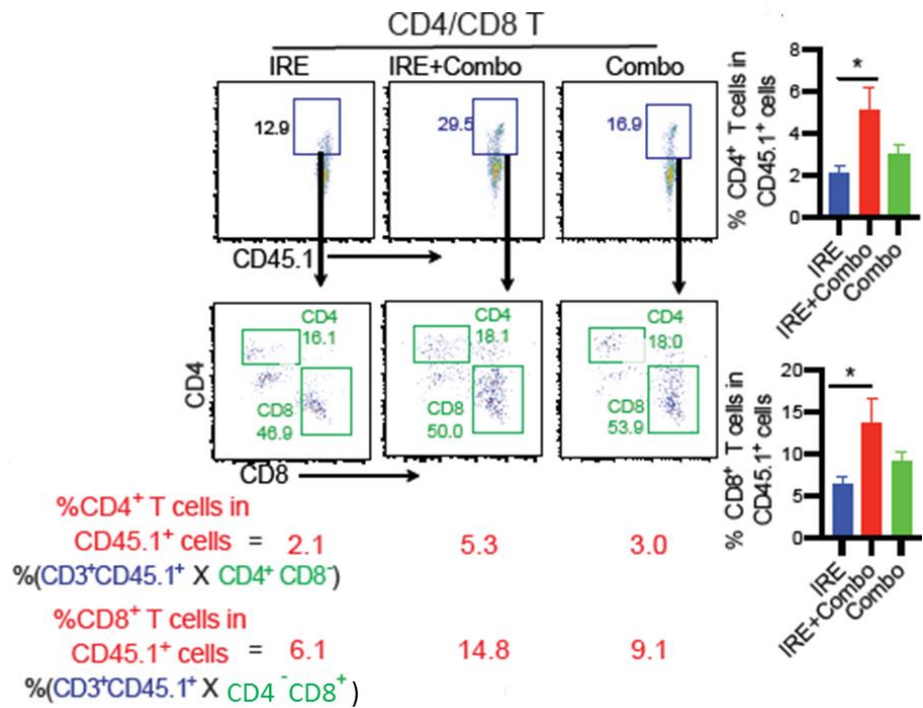
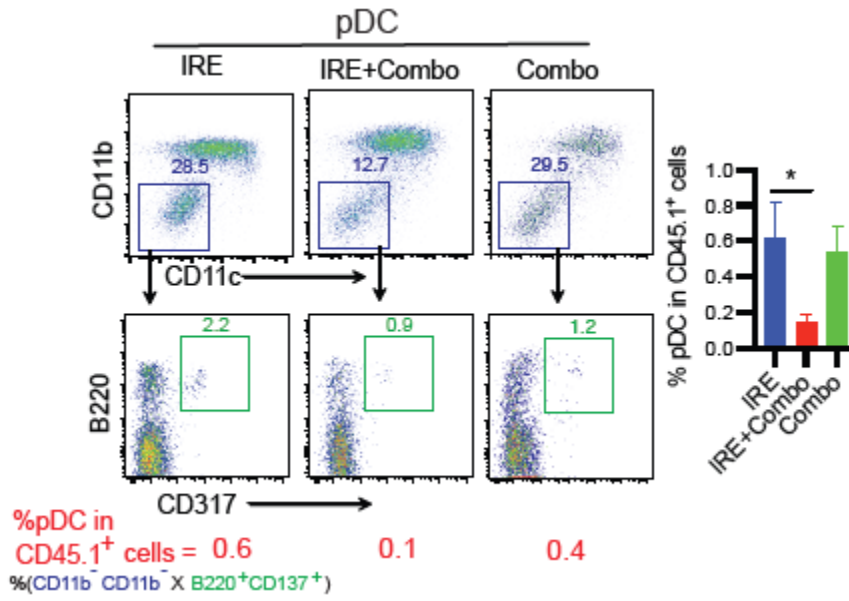
The term “abscopal” effect originally indicated a local therapy such as radiation therapy that not only shrank the targeted tumor but also led to shrinkage of untreated distant tumors [47]. To assess a potential abscopal effect of IRE+Combo ablation, we monitored growth or regression of distant (left-flank) untreated tumors following IRE+Combo therapy of primary (right-flank) tumors (**Figure 3.11 A**). Remarkably, we found distant tumors were also completely eradicated in IRE+Combo-treated mice compared to aggressively growing distant tumors in IRE- or Combo-treated control mice (**Figure 3.11 A**). To check whether IRE+Combo ablation modulates the TME in distant tumors, we analyzed immune cell profiles and PD-L1 expression by flow cytometry in single-cell suspensions prepared from distant tumors 3 days post IRE ablation of primary tumors (**Figure 3.11 B**). We demonstrated a significant increase in the M1/M2 ratio and immunogenic cDC1, a significant reduction of immunotolerant Treg cells, MDSCs, and pDCs (**Figure 3.11 C**), compared to those in distant tumors of control IRE- or Combo-treated mice. In addition, we assessed tumor-infiltrating CD4<sup>+</sup> and CD8<sup>+</sup> T cells in distant tumors by flow cytometry and immunohistochemical analyses. We demonstrated more CD4<sup>+</sup> and CD8<sup>+</sup> T cells were detected in distant tumors in mice with IRE+Combo-treated primary tumors than CD4<sup>+</sup> and CD8<sup>+</sup> T-cells in IRE- or Combo-treated control mice (**Figure 3.11 C**). The increased frequencies of CD8<sup>+</sup> T cells

in distant tumors of IRE+Combo-treated mice were confirmed in comparison to IRE- and Combo-treated mice by our immunohistochemistry data (**Figure 3.11 D**). Next, we assessed the modulatory effect on PD-L1 expression by flow cytometry and found a down-regulation of inhibitory PD-L1 in M2, MDSCs, and EG7 tumor cells in distant tumors of IRE+Combo-treated mice (**Figure 3.11 E**). Collectively, our data indicate that IRE+Combo ablation in primary tumors also eradicates distant tumors *via* conversion of an immunotolerant TME into an immunogenic TME, leading to increased CD4<sup>+</sup> and CD8<sup>+</sup> T cells in distant tumors.









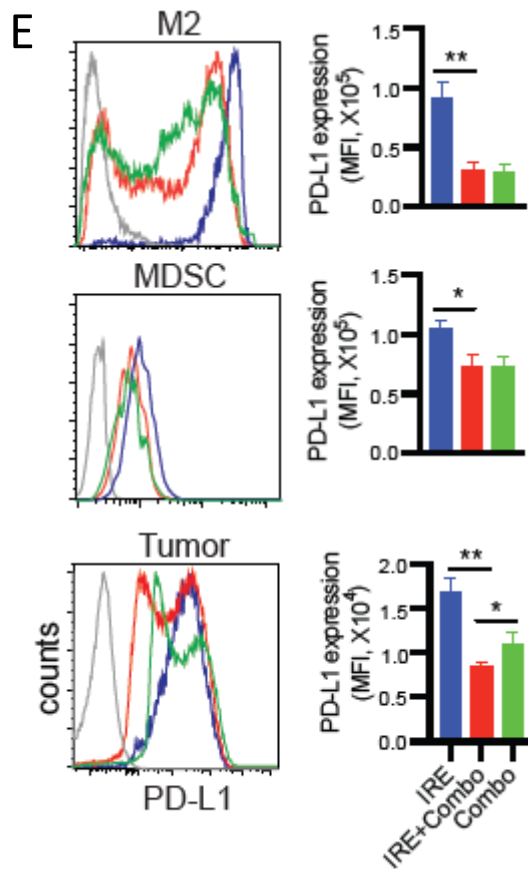
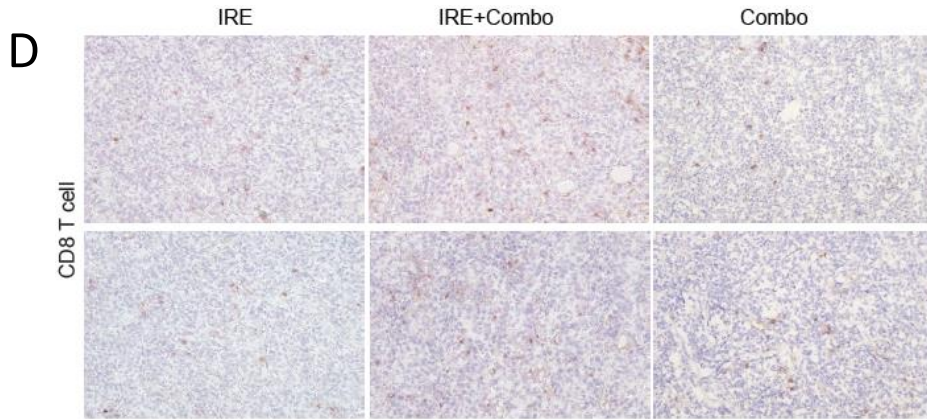


**Figure 3.11 IRE+Combo induces “abscopal” effect on eradication of distant tumors by converting immunotolerant TME in distant tumors.** (A) Schematic diagram illustrating experimental design for measurement of “abscopal” effect. B6.1 mice bearing both primary (8-9 mm in diameter) and distant (6 mm in diameter) tumors were monitored for distant tumor regression post IRE+Combo or IRE-ablation or Combo alone.  $**P < 0.01$  by two-way ANOVA with Tukey test. (B) Diagram displaying experimental design for measurement of immune cell

profiling, PD-L1 expression and IHC analyses. (C) TSCSs were enzymatically prepared from distant tumor tissues 3 days post IRE-ablation of primary tumors. Cell samples were stained with a cocktail of antibodies and analyzed by flow cytometry. Last sets of representative flow cytometric plots show quantitative measurement of various immune-cell subsets. The relative quantitation of (i) M1/M2 ratio calculated by % MHCII<sup>+</sup> M1/% MHCII<sup>+</sup> M2 in total CD11b<sup>+</sup>F4/80<sup>+</sup> macrophages (ii) % cDC1 calculated by CD8<sup>+</sup>CD103<sup>+</sup>CD11c<sup>+</sup> cDC1/total CD11c<sup>+</sup> DCs; (iii) % Treg calculated by CD4<sup>+</sup>Foxp3<sup>+</sup> Treg/total CD4<sup>+</sup> T cells; (iv) % MDSCs, (v) % pDCs and (vi) % CD4<sup>+</sup> or CD8<sup>+</sup> T cells in total tumor-infiltrating host CD45.1<sup>+</sup> cells calculated by % (CD11b<sup>+</sup>CD45.1<sup>+</sup> cells in upper square × Gr1<sup>+</sup>Ly6G<sup>+</sup> cells in lower square), % (CD11b<sup>-</sup>CD11c<sup>-</sup> cells in upper square × B220<sup>+</sup>CD137<sup>+</sup> cells in lower square) and % (CD3<sup>+</sup>CD45.1<sup>+</sup> cells in upper square × CD4<sup>+</sup> or CD8<sup>+</sup> cells in lower square), respectively, is described in the Methods and Supplementary Figure 3.14. \**P* < 0.05, \*\**P* < 0.01 by two-tailed Student *t* test. (D) IHC analysis of distant tumor tissue frozen sections post IRE- Combo- or IRE+Combo-treatment of primary tumors. Representative micrographs of IHC staining for CD8<sup>+</sup> T cells. (E) Flow-cytometry analysis of PD-L1 expression in M2, MDSCs and tumor cells. Gray line represents control isotype-antibody staining. MFI, mean fluorescence intensity. Tumor-growth and flow-cytometry plots representing one of two independent experiments are presented as means ± SEM (n = 5/group). \**P* < 0.05, \*\**P* < 0.01 by two-tailed Student *t* test.

### 3.4.14 IRE+Combo in primary tumors eradicates tumor lung metastases

To assess whether IRE+Combo ablation in primary tumors affects existing lung metastases, we i.v. injected a highly lung metastatic B16 melanoma BL6-10<sub>OVA</sub> engineered to express OVA to the mice bearing small s.c. EG7 tumors and control naïve mice, respectively (**Figure 3.12 A**). One week after melanoma cell injection, when s.c. EG7 tumors reached ~300 mm<sup>3</sup> in volume, we performed IRE+Combo treatment to mice bearing s.c. EG7 tumors. Two weeks after IRE+Combo treatment, we collected mouse lungs to visibly measure metastatic black melanoma colonies, followed by histopathological examination (**Figure 3.12 A**). We demonstrated numerous black BL6-10<sub>OVA</sub> melanoma lung colonies present in control un-treated mice, but none in IRE+Combo-treated mice (**Figure 3.12 B, 3.12 C**), indicating IRE+Combo treatment of primary tumors is able to eradicate lung tumor metastases.

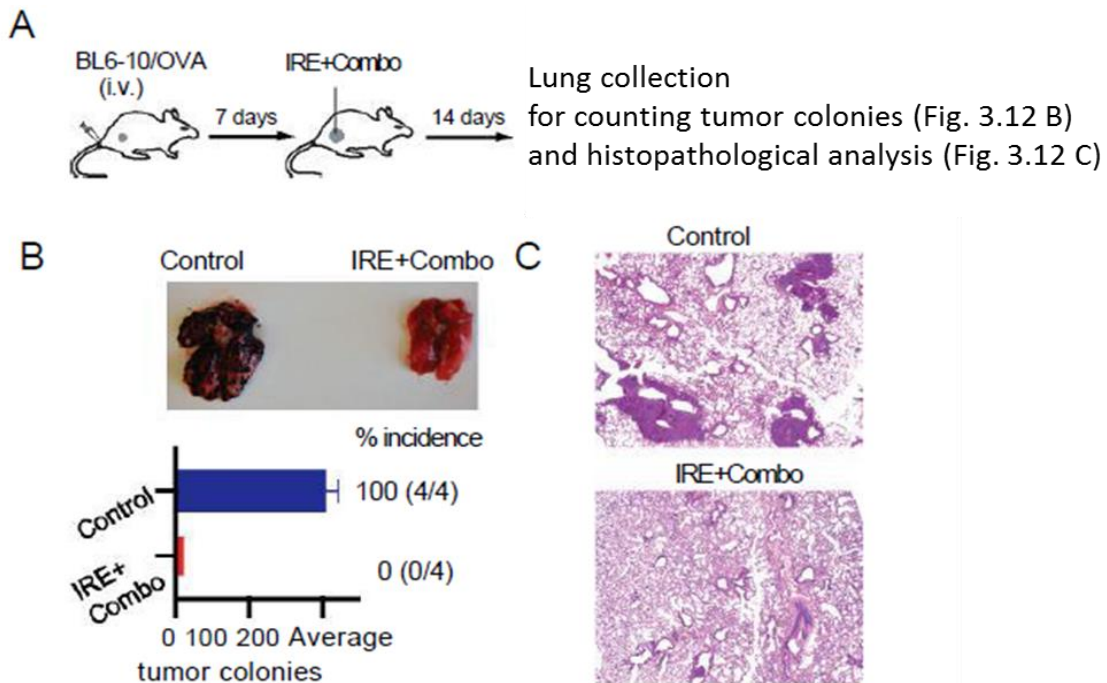


**Figure 3.12 IRE+Combo treatment of primary tumors inhibits lung tumor metastasis.** (A) Schematic diagram of experimental design for assessing the anti-metastatic activity derived from IRE+Combo treatment of primary tumors. Mice bearing small 7-day EG7 tumors or the untreated control mice (n = 4 mice/group) were i.v. injected with BL6-10<sub>OVA</sub> cells. Seven days later, IRE+Combo treatment was performed on mice bearing primary EG7 tumors (8-9 mm in diameter). Mice were sacrificed 14 days after treatment, and lung tissues were collected. (B) Black metastatic BL6-10<sub>OVA</sub> melanoma colonies in lungs were counted. (C) Representative micrographs of H&E stained tissue sections from lungs collected from control (untreated) or IRE+Combo-treated mice. One representative experiment out of two independent experiments is shown.

### 3.4.15 IRE+Combo's potent therapeutic effect in two mouse breast cancer models

Based on the effectiveness of IRE+Combo in the mouse lymphoma EG7 model, we also sought to determine its therapeutic effect in another two mouse-tumor models. We s.c. injected Tg1-1 and 4T1 breast cancer cells to FVB/NJ and BALB/c mice, respectively. When tumors reached ~300 mm<sup>3</sup> in volume, we then performed IRE+Combo in tumor-bearing mice, followed by monitoring tumor growth or regression, while tumor-bearing mice with IRE or Combo treatment were used as control groups. We found IRE+Combo completely eradicated Tg1-1 breast cancer and significantly inhibited 4T1 breast tumor growth (**Figure 3.13**), thus indicating an effective therapeutic effect of IRE+Combo in another two mouse breast cancer models.

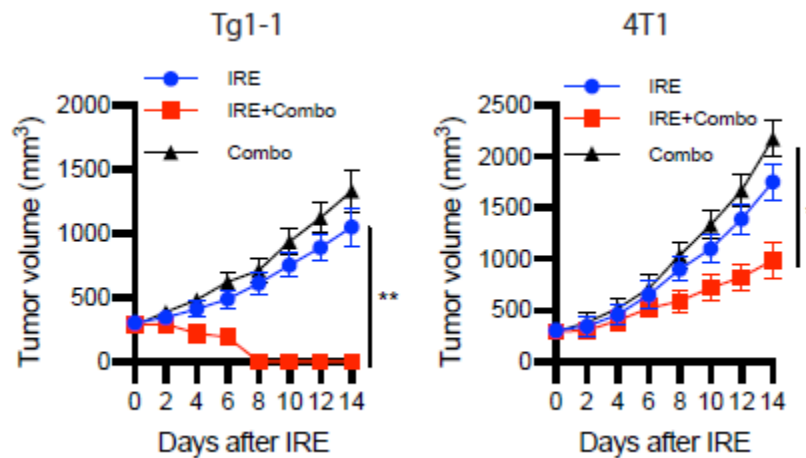
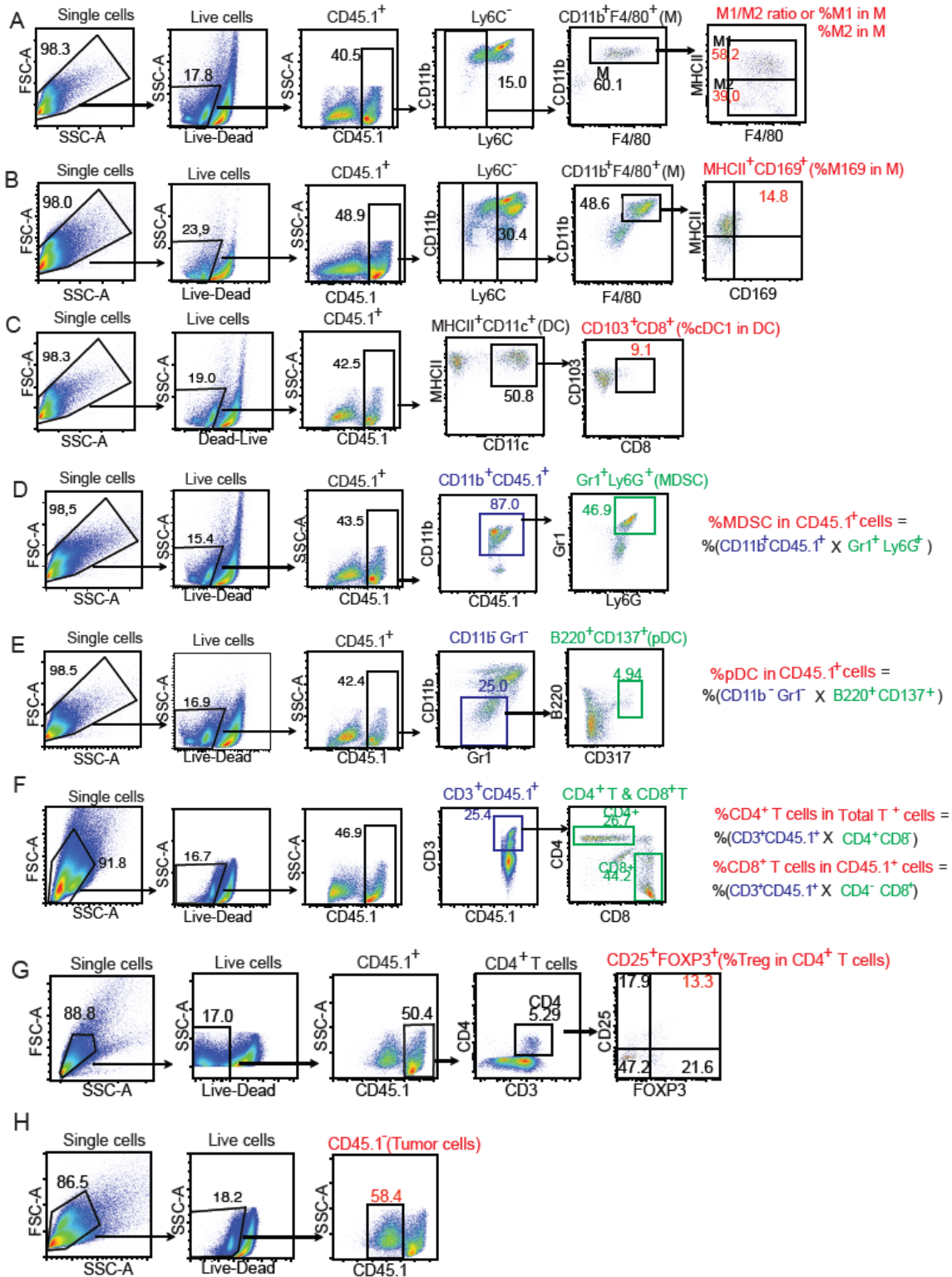


**Figure 3.13 IRE+Combo effectively eradicates tumors or significantly inhibits tumor growth in two mouse breast cancer models.** Mice bearing Tg1-1 and 4T1 breast cancer (8-9 mm in diameter) were treated with IRE, Combo and IRE+Combo, respectively. Tumor-bearing mice with IRE or Combo treatment were used as controls. Tumor-bearing mice were monitored for tumor growth or regression post IRE-Combo ablation. Tumor growth plots representing one of two independent experiments are presented as means  $\pm$  SEM ( $n = 4/\text{group}$ ).  $*P < 0.05$ ,  $**P < 0.01$  by two-way ANOVA with Tukey test.

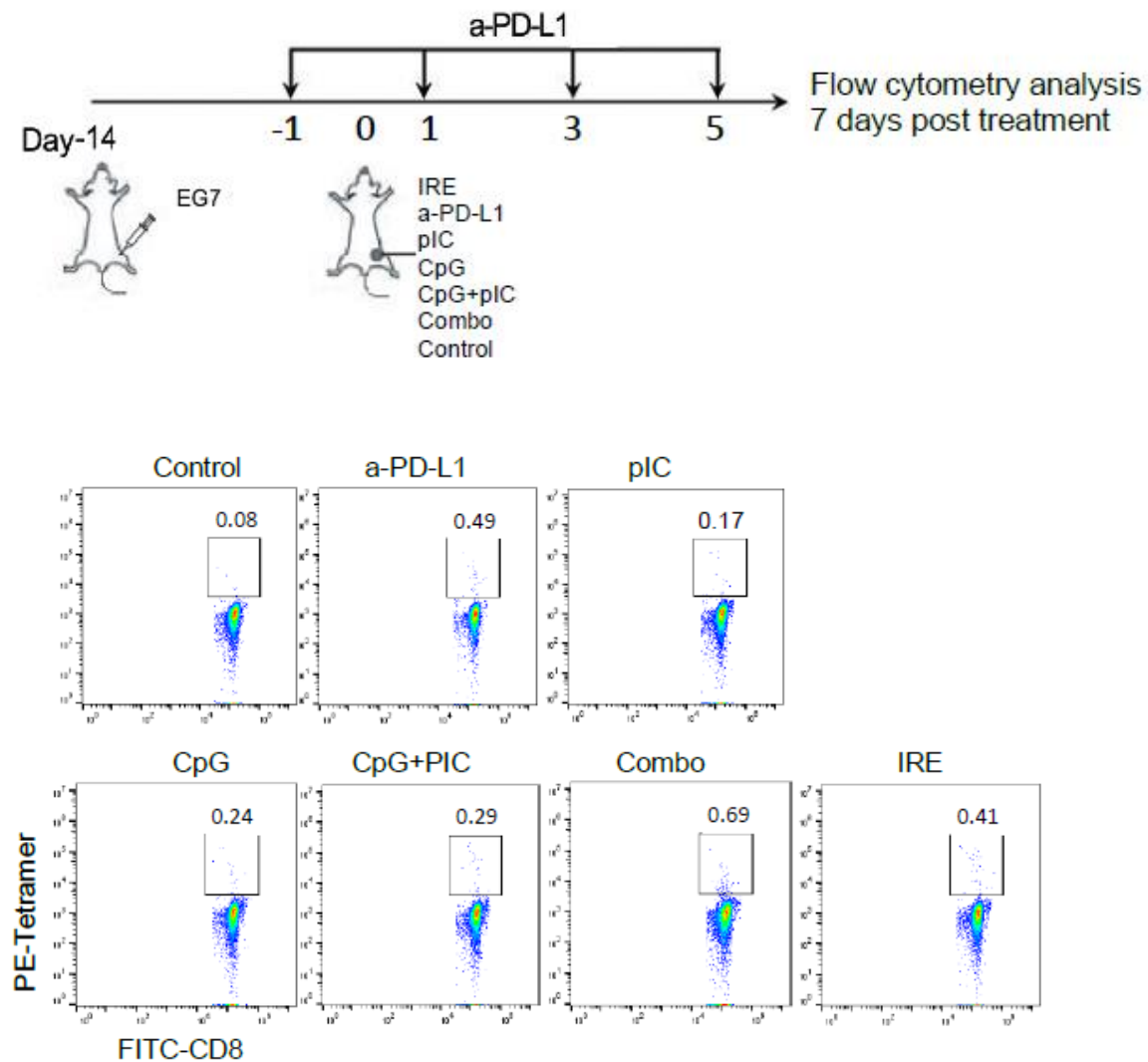


**Supplementary Figure 3.14. A systematical analysis of immune cell profiling in TME by flow cytometry.**

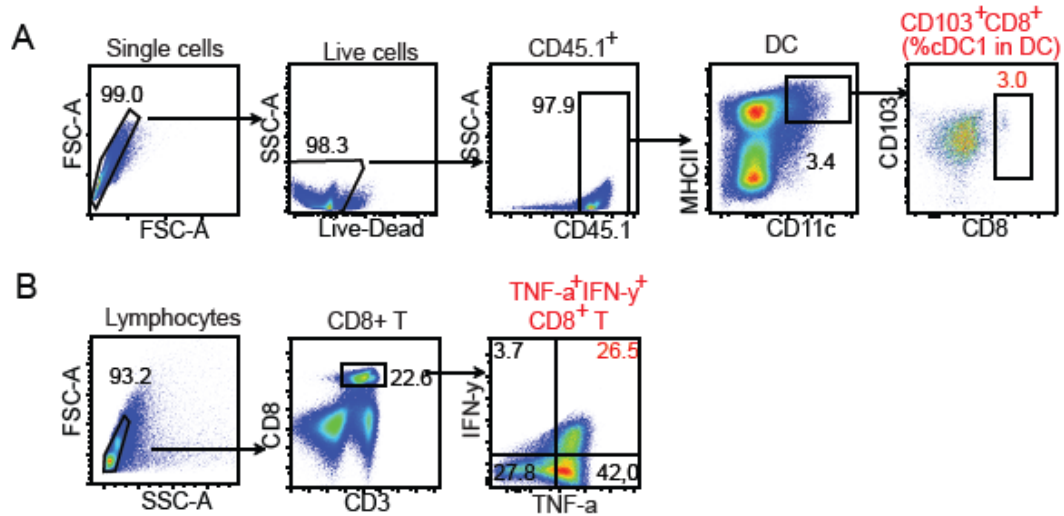
Single cell suspensions were enzymatically prepared from primary or distant tumor tissues 3 days post IRE-ablation in CD45.1<sup>+</sup> B6.1 mice bearing CD45.2<sup>+</sup> EG7 tumors. Cell samples were stained with the Zombie Aqua Fixable Viability (ZAFV) dye to exclude dead cells and a cocktail of antibodies against a combination of molecular markers used to distinguish different immune cell populations such as immunogenic cDC1, M1, M19, CD4<sup>+</sup>, and CD8<sup>+</sup> T cells as well as immunotolerant M2, MDSCs, pDCs, Treg and tumor cells. Briefly, cell populations were first gated by SCC and FSC to exclude small sizes of cellular debris. Live tumor-infiltrating leukocyte populations were then gated by ZAFV dye staining for initial analysis of CD45.1<sup>+</sup> immune cell populations distinctive from CD45.2<sup>+</sup> EG7 tumor cells. Neutrophils and monocytes were later removed from the host mouse CD45.1<sup>+</sup> cell population based on the expression of Ly6C. Various immune cell populations were then gated by antibodies against their cell markers for analysis, respectively. For example, the macrophage population was gated as CD11b<sup>+</sup>F4/80<sup>+</sup> cells to further measure MHCII expression for quantification of the % CD11b<sup>+</sup>F4/80<sup>+</sup>MHCII<sup>-</sup> M2 and % CD11b<sup>+</sup>F4/80<sup>+</sup>MHCII<sup>+</sup> M1 in the CD11b<sup>+</sup>F4/80<sup>+</sup> M population (Figure 3.14A) or to further measure MHCII and CD169 expression for quantification of the % CD11b<sup>+</sup>F4/80<sup>+</sup>MHCII<sup>+</sup>CD169<sup>+</sup> M169 in CD11b<sup>+</sup>F4/80<sup>+</sup> M population (Figure 3.14B). DC populations were gated as CD11c<sup>+</sup> cells to further analyze the expression of CD8, CD103, and MHCII for quantification of the % CD8<sup>+</sup>CD103<sup>+</sup>MHCII<sup>+</sup> cDC1 in the CD11c<sup>+</sup> DC population (Figure 3.14C). The monocyte population was gated as CD45.1<sup>+</sup> cells to further sequentially assess the expression of CD11b and Gr1/Ly6G for quantification of the % CD11b<sup>+</sup>Gr1<sup>+</sup>Ly6C<sup>+</sup> MDSCs in the CD45.1<sup>+</sup> cell population with a calculation formula of % (CD11b<sup>+</sup>CD45.1<sup>+</sup> cells × Gr1<sup>+</sup>Ly6G<sup>+</sup> cells) (Figure 3.14D). The monocyte population was also gated as CD45.1<sup>+</sup> cells to further sequentially assess expression of CD11b/Gr1 and CD317/B220 for quantification of the % CD11b<sup>-</sup>CD317<sup>+</sup>Gr1<sup>-</sup>B220<sup>+</sup> pDCs in the CD45.1<sup>+</sup> cell population with a calculation formula of % (CD11b<sup>-</sup>Gr1<sup>-</sup> cells × CD317<sup>+</sup>B220<sup>+</sup> cells) (Figure 3.14E). The monocyte population was gated as CD45.1<sup>+</sup> cells to further measure CD3 and CD4 or CD8 expression for quantification of the % CD4<sup>+</sup> or CD8<sup>+</sup> T cells in the CD3<sup>+</sup> T cell population (Figure 3.14F). The monocyte population was gated as CD45.1<sup>+</sup> cells to further sequentially measure CD3/CD4 for quantification of CD4<sup>+</sup> T cells and CD4/Foxp3 expression for quantification of % immunotolerant CD4<sup>+</sup>Foxp3<sup>+</sup> Treg cells in the CD4<sup>+</sup> T cell population (Figure



3.14G). In addition, EG7 tumor cell population was gated as live CD45.1<sup>-</sup> or CD45.2<sup>+</sup> cells (Figure 3.14H).



**Supplementary Figure 3.15. Analysis of peripheral blood OVA-specific CD8<sup>+</sup> T cell responses by flow cytometry.** A Schematic diagram showing EG7 tumor bearing mice were treated with various treatment protocols including (i) control, (ii) anti-PD-L1 Ab, (iii) pIC, (iv) CpG, (v) pIC/CpG, (vi) Combo and (vii) IRE, followed by measurement of peripheral blood OVA-specific CD8<sup>+</sup> T cell responses by flow cytometry 7 days post treatment.



**Supplementary Figure 3.16. A systematical analysis of tumor-drainage lymph nodes by flow cytometry.** Single cell suspensions were prepared from tumor-drainage lymph nodes of tumor-bearing CD45.1<sup>+</sup> B6.1 mice seven days post IRE. Cell samples were stained with the Zombie Aqua Fixable Viability (ZAFV) dye to exclude dead cells and a cocktail of antibodies against a combination of molecular markers used to distinguish cDC1 and CD8<sup>+</sup> T cells. Briefly, cell populations were first gated by SCC and FSC to exclude small sizes of cellular debris. Live cells were then gated by ZAFV dye staining. Quantification of the % CD8<sup>+</sup>CD103<sup>+</sup>MHCII<sup>+</sup> cDC1 in the CD11c<sup>+</sup> DC population (**A**) and the % CD8<sup>+</sup>IFN-γ<sup>+</sup>TNF-α<sup>+</sup> effector T cells in the CD3<sup>+</sup> T cell population (**B**) was analysed by flow cytometry.

### 3.5 Discussion

Tumor cells often evade immunosurveillance by downregulating immunogenic MHC-I molecules while upregulating expression of inhibitory molecules such as PD-L1, IDO, arginase-1, and TGF- $\beta$  [48]. Tumor growth is associated with remodeling of the TME, which often becomes more suppressive in tumors of large size [49]. By quantitatively measuring immune cell profiles and qualitatively editing myeloid and tumor cells, we demonstrate that CD45.2<sup>+</sup> tumor cells and CD45.1<sup>+</sup> tumor infiltrating immune cells comprise approximately 55% and 45% of the total tumor cell compositions, respectively. Among tumor infiltrating immune cells, MDSCs comprising approximately ~35% in total CD45.1<sup>+</sup> tumor-infiltrating immune cells in TME of large tumors represented the major population of immunotolerant cells, while M2 macrophages, pDCs and Treg cells comprised ~4%, ~1.4%, and ~1.1%, respectively. Importantly, our study provides the first evidence that more immunotolerant M2, Treg cells, MDSCs, and pDCs and more inhibitory PD-L1 expression of immunotolerant M2, MDSCs, and tumor cells are found in larger tumors, indicating a trend toward a more immunotolerant TME in larger tumors. This is possibly due to an alteration of tumor cell metabolism derived from the hypoxic and oxidative conditions in larger tumors [49-51]

In this study, we performed IRE with two needle array electrodes (5 mm apart) in mice bearing large-size primary tumors (8-9 mm in diameter or ~300 mm<sup>3</sup> in volume) with an immunotolerant TME, mimicking the situation in clinical cancer patients. This is in contrast to two recent reports similarly conducting IRE in mice but bearing small (5-6 mm in diameter or ~80 mm<sup>3</sup> in volume) [19] or medium-sized (7 mm in diameter or ~180 mm<sup>3</sup> in volume) primary tumors [18] with a less immunotolerant TME. Using an OVA transgene-engineered EG7 tumor cell line in our animal model, we were able to quantitatively measure OVA-specific CD8<sup>+</sup> T cell responses, in contrast to the two previous studies that only measured non-specific CD8<sup>+</sup> T cell responses [19]. To improve the IRE-induced therapeutic effect, we incorporated PD-1 blockade, a TLR3 agonist (pIC), and a TLR9 agonist (CpG) into IRE-ablation to form various combination therapies including IRE+PD-1 blockade, IRE+pIC, IRE+CpG, IRE+pIC/CpG, IRE+Combo and Combo alone. We then assessed OVA-specific CD8<sup>+</sup> T cell responses and anti-tumor immunity limiting tumor-growth. We demonstrated that the TLR3/9 agonists (pIC/CpG) synergistically stimulated stronger IRE-induced OVA-specific CD8<sup>+</sup> T cell responses, leading to more efficient inhibition of primary tumor growth

and prolonged mouse survival, than did PD-1 blockade. The synergistic promotive effect of the TLR3/9 agonists on promoting IRE-induced CD8<sup>+</sup> T cell responses might be derived from their synergistic abilities to drive gene expression and cytokine release [52, 53].

In addition, we further uncover distinct roles played by the TLR3/9 agonists and PD-1 blockade in the modulation of immune cell profiles and down-regulation of PD-L1 expression in the immunotolerant TME. The TLR3/9 agonists were more efficient in modulating immune cell profiles by promoting immunogenic M1 macrophages, M169 macrophages, and cDC1 cells and reducing immunotolerant M2 macrophages, pDCs Treg cells and MDSCs but less potent in downregulating PD-L1 expression on M2 macrophages, MDSCs and tumor cells, and *vice versa* for PD-1 blockade. This is possibly because the TLR3/9 agonists directly bind to TLR3/9 on the membrane of endosomes within macrophages and DCs, leading to activation of M1 macrophages, M169 macrophages, and cDC1 and promotion of M2 macrophages and MDSC differentiation into M1 macrophages [54] *via* TLR-mediated metabolic reprogramming [55] while the anti-PD-L1 Ab (PD-1 blockade) directly binds to and blocks inhibitory PD-L1 on M2 macrophages, MDSCs, and tumor cells *via* Ab binding-mediated cellular internalization of anti-PD-L1 Ab/PD-L1 complexes, [56, 57] leading to downregulation of PD-L1 expression in the TME. Heterogeneous TMEs containing different degrees of tolerant immune cells and PD-L1 expression have been found in different types of tumors or different tumors of the same tumor type, and these features are distinct tumor cell intrinsic factors and indicative of different genetic and/or phenotypic traits [50, 58, 59]. Understanding distinct role of TLR agonists and PD-L1 blockade in combating an immunotolerant TME helps in the design of better protocols to improve the therapeutic efficacy of IRE ablation based upon genetic and phenotypic characterization of individual TMEs for personalized medicine.

IRE+Combo therapy, which combines IRE-ablation-induced massive destruction in tumors with PD-1 blockade and TLR3/9 agonists, cooperatively stimulated potent peripheral OVA-specific CD8<sup>+</sup> T cell responses compared to either IRE+PD-1 blockade or IRE+pIC/CpG, leading to complete eradication of large (~300 mm<sup>3</sup>) primary tumors and long-term OVA-specific CD8<sup>+</sup> T cell memory, suggesting that IRE+Combo treatment is a potent therapeutic protocol for cancer therapy. Our mechanistic studies further revealed that IRE+Combo treatment cooperatively promoted immunogenic cDC1 and M169 macrophages and increased the M1/M2 macrophage ratio but reduced immunotolerant Treg cells, MDSCs, and pDCs in the TME compared to either

IRE+PD-1 blockade or IRE+pIC/CpG. In addition, IRE+Combo treatment downregulated immunosuppressive PD-L1, IDO and arginase-1 expression in M2 macrophages, MDSCs and EG7 tumor cells, as measured by flow cytometric analysis, indicating that IRE+Combo therapy significantly converts an immunotolerant TME into an immunogenic TME. Furthermore, IRE+Combo also increased the M1/M2 macrophage ratio, but reduced immunotolerant MDSCs in IRE+Combo-treated mouse blood. Various cytokines and chemokines contribute to the modulation of the immunotolerant TME [60]. We measured the concentration of three major cytokines including two representative immunogenic cytokines, IL-2 and IFN- $\gamma$ , and one representative immunosuppressive cytokine, TGF- $\beta$ , in mouse sera. Our data demonstrated that IRE+Combo increased IL-2 and IFN- $\gamma$  cytokine levels, but reduced the level of the immunotolerant cytokine TGF- $\beta$  in mouse sera, indicating a systemic reduction in immunotolerance and an elevation in immunogenic CD4<sup>+</sup> Th1 responses post IRE+Combo treatment. To gain better insight into the modulatory effects of IRE+Combo on cytokines and chemokines as well as immune cell subsets, cytokine/chemokine array analyses, including measurement of the important cytokines IL-12 and IFN- $\alpha$  will be carried out in the future, and some other important immune cell subsets that could be considered novel immune targets in the TME, such as Th17 cells [61, 62], should also be included in immune cell profiling analyses in the future.

It is worth noting that our data demonstrated that IRE ablation alone induced very weak CTL responses in large EG7 tumors, possibly due to remaining tumor tissues becoming more immunotolerant and accelerating tumor progression post ablation [63], and that Combo treatment alone also failed to induce efficient CTL responses, possibly due to the strong immunotolerance within the large tumor TME. Overall, IRE+Combo therapy was shown to synergistically induce potent CTL responses and antitumor immunity, leading to eradication of primary and distant tumors and lung tumor metastases, possibly due to its conversion of not only the local tolerant TME in primary tumor but also systemic immunotolerance. Therefore, our IRE+Combo protocol may represent another good example in support of the newly emerging concept that efficiently reducing the tumor burden (i.e., by IRE-ablation) and increasing the immunogenicity of the TME (i.e., by PD-1-blockade and TLR3/9 agonist administration) are two key factors for improving cancer immunotherapy [64], leading to a significantly synergistic therapeutic effect on cancer mediated by IRE+Combo.

Tumor-infiltrating CD8<sup>+</sup> T cells play an important role in eradicating malignant tumors [10, 45] and are a key factor predicting clinical outcome in cancer patients [65]. In addition to the above peripheral CD8<sup>+</sup> T cell responses, CD8<sup>+</sup> T cell responses in the TDLNs were also promoted by IRE+Combo. More importantly, IRE+Combo promoted tumor-infiltrating CD8<sup>+</sup> T cells, as indicated by flow cytometric and immunohistochemistry analyses, and converted exhausted T cells, as shown by T cell proliferation and cytotoxicity analyses, indicating the generation of an immunogenic TME favorable for CD8<sup>+</sup> T cell recruitment, expansion and effector function post IRE+Combo treatment. The increase in tumor-infiltrating CD8<sup>+</sup> T cells may result from a combination of factors, including IRE+Combo-induced elevations in immunogenic (i) M1 macrophages that polarize CD4<sup>+</sup> Th1 cell differentiation for enhancement of CD8<sup>+</sup> T cell survival and tumor infiltration; [2, 66] (ii) cDC1, a superior stimulator of CD8<sup>+</sup> T cell responses [4, 5] leading to tumor-infiltrating CD8<sup>+</sup> T cell clonal expansion and efficient T cell killing of tumor cells; [67] and (iii) M169 macrophages, which are capable of not only directly priming CD8<sup>+</sup> T cell responses [68] but also transferring tumor antigens derived from apoptotic tumor cells to cDC1s for further CD8<sup>+</sup> T cell cross-priming [3, 69]. Finally, enhanced recruitment of CD8<sup>+</sup> T cells into IRE+Combo-treated tumors may also be supported by the IRE-modulated tumor stroma with increased microvessel density and permeability, which is expected to favor T cell tumor infiltration and tumor destruction [18].

The “abscopal” effect observed in our IRE+Combo treatment has also been demonstrated in a recent report showing elimination of 3-day “palpable” distant tumors post treatment combining IRE-ablation with a TLR7-agonist and PD-1 blockade [19]. In comparison, our IRE+Combo approach, which combined IRE-ablation with both PD-1 blockade and TLR-3/9 agonists, completely eradicated not only primary tumors but also concomitant distant ~100 mm<sup>3</sup> EG7 tumors and BL6-10<sub>OVA</sub> lung metastases. We further conducted a systemic analysis of immune cell profiles in distant tumors post IRE+Combo treatment of primary tumors. Our data demonstrated IRE+Combo dramatically modulated the TME of distant tumors by reducing the frequencies of immunotolerant M2 macrophages, Treg cells, MDSCs and pDCs, which is consistent with previous reports using RFA+PD-1 blockade or RFA+CpG/PD-1 blockade therapeutic protocols [41, 42], and downregulating PD-L1 expression in M2 macrophages, MDSCs and tumor cells, leading to increased frequencies of tumor-infiltrating CD4<sup>+</sup> and CD8<sup>+</sup> T cells in the distant tumors. The Potential molecular mechanisms underlying the conversion of an immunotolerant TME to an

immunogenic TME, as observed in untreated distant tumors, are currently unclear. IRE+Combo-induced down-regulation of systemic immunotolerance could partially contribute to conversion of immunotolerant TME in distant tumors. PD-1 blockade has been reported to promote the frequencies of cDC1 and CD8<sup>+</sup> T cells and reduces the frequencies of Treg cells in distant tumors post IRE or RFA ablation [19, 41]. Our administration (i.p.) of the anti-PD-L1 Ab in the IRE+Combo protocol could specifically contribute to its conversion-promoting effect. Further elucidation of other factors responsible for the IRE+Combo-induced conversion-promoting effect on the distant tumor TME is now underway in our laboratory.

Finally, we extended our IRE+Combo therapeutic findings obtained from the mouse EG7 lymphoma model to another two mouse breast cancer models. We demonstrated that IRE+Combo completely eradicated Tg1-1 breast cancer tumors and significantly inhibited triple-negative 4T1 breast cancer growth, indicating that IRE+Combo is an effective protocol for cancer ablation therapy. The varied therapeutic effects of IRE+Combo observed in the two breast tumor models are possibly due to the heterogeneous TMEs of these two breast cancers [50, 58, 59].

Taken together, our data demonstrate that IRE+Combo induces potent CD8<sup>+</sup> T cell responses, leading to complete eradication of both primary and distant tumors as well as lung metastases by converting the immunotolerant TME into an immunogenic TME in both primary and distant tumors. These findings warrant further study in other mouse solid tumor models and in human trials for IRE ablation therapy in cancer.

## References

1. Pitt, J. M. et al. *Targeting the tumor microenvironment: removing obstruction to anticancer immune responses and immunotherapy*. *Ann Oncol*, 2016. **27**: p. 1482-1492.
2. Soncin, I. et al. *The tumour microenvironment creates a niche for the self-renewal of tumour-promoting macrophages in colon adenoma*. *Nat Commun*, 2018. **9**: p. 582.
3. Asano, K. et al. *CD169-positive macrophages dominate antitumor immunity by crosspresenting dead cell-associated antigens*. *Immunity*, 2011. **34**: p. 85-95.
4. Li, L. et al. *Cross-dressed CD8alpha+/CD103+ dendritic cells prime CD8+ T cells following vaccination*. *Proc Natl Acad Sci USA*, 2012. **109**: p. 12716-12721.
5. Chanmee, T., Ontong, P., Konno, K. & Itano, N. *Tumor-associated macrophages as major players in the tumor microenvironment*. *Cancers*, 2014. **6**: p. 1670-1690.
6. Fleming, V. et al. *targeting myeloid-deprived suppressor cells to bypass tumor-induced immunosuppression*. *Front Immunol*, 2018. **9**: 398.
7. Tesi, R. *MDSC; the most important cell you have never heard of*. *Trends in pharmacological sciences*, 2019. **40**: p. 4-7.
8. Conrad, C. et al. *Plasmacytoid dendritic cells promote immunosuppression in ovarian cancer via ICOS costimulation of Foxp3(+) T-regulatory cells*. *Cancer Res*, 2012. **72**: p. 5240-5249.
9. Ohue, Y. & Nishikawa, H. *Regulatory T (Treg) cells in cancer: Can Treg cells be a new therapeutic target?* *Cancer Sci*, 2019. **110**: p. 2080-2089.
10. Williams, M. A. & Bevan, M. J. *Effector and memory CTL differentiation*. *Annu Rev Immunol*, 2007. **25**: p. 171-192.
11. Gajewski, T. F., Schreiber, H. & Fu, Y. X. *Innate and adaptive immune cells in the tumor microenvironment*. *Nat Immunol*, 2013. **14**: p. 1014-1022.
12. Xia, A., Zhang, Y., Xu, J., Yin, T. & Lu, X. J. *T cell dysfunction in cancer immunity and immunotherapy*. *Front Immunol*, 2019. **10**: 1719.
13. Tekle, E., Wolfe, M. D., Oubrahim, H. & Chock, P. B. *Phagocytic clearance of electric field induced 'apoptosis-mimetic' cells*. *Biochem Biophys Res Commun*, 2008. **376**: p. 256-260.
14. Rubinsky, B. *Irreversible electroporation in medicine*. *Technol Cancer Res Treat*, 2007. **6**: p.255-260.
15. Lyu, T. et al. *Irreversible electroporation in primary and metastatic hepatic malignancies: A review*. *Medicine (Baltimore)*, 2017. **96**: e6386.



16. Martin, R.C., 2<sup>nd</sup>, McFarland, K., Ellis, S. & Velanovich, V. *Irreversible electroporation in locally advanced pancreatic cancer: potential improved overall survival*. *Ann Surg Oncol*, 2013. **(20 Suppl 3)**: S443-449.
17. Huang, K. W. et al. *The efficacy of combination of induction immunotherapy and irreversible electroporation ablation for patients with locally advanced pancreatic adenocarcinoma*. *J Surg Oncol*, 2018. **118**: p. 31-36.
18. Zhao, J. et al. *Irreversible electroporation reverses resistance to immune checkpoint blockade in pancreatic cancer*. *Nat Commun*, 2019. **10**: 899.
19. Narayanan, J. S. S. et al. *Irreversible electroporation combined with checkpoint blockade and TLR7 stimulation induces antitumor immunity in a murine pancreatic cancer model*. *Cancer Immunol Res*, 2019. **7**: p. 1714-1726.
20. Fitzgerald, K. A. and Kagan, J. C. *Toll-like receptor and the control of immunity*. *Cell*, 2020. **180**: p. 1044-1066.
21. Zhu, M., Xu, W., Su, H., Huang, Q. & Wang, B. *Addition of CpG ODN and Poly (I:C) to a standard maturation cocktail generates monocyte-derived dendritic cells and induces a potent Th1 polarization with migratory capacity*. *Hum Vaccin Immunother*, 2015. **11**: p. 1596-1605.
22. Lee, B. R. et al. *Combination of TLR1/2 and TLR3 ligands enhances CD4(+) T cell longevity and antibody responses by modulating type I IFN production*. *Sci Rep*, 2016. **6**: 32526.
23. Amos, S. M. et al. *Adoptive immunotherapy combined with intratumoral TLR agonist delivery eradicates established melanoma in mice*. *Cancer Immunol Immunother*, 2011. **60**: p. 671-683.
24. Liu, Z., Han C. and Fu, Y. *Targeting innate sensing in the tumor microenvironment to improve immunotherapy*. *Cell Mol Immunol*, 2020. **17**: p. 13-26.
25. Nelson, C. E. et al. *Reprogramming responsiveness to checkpoint blockade in dysfunctional CD8 T cells*. *Proc Natl Acad Sci USA*, 2019. **116**: p. 2640-2645.
26. Jiang, Y., Chen, M., Nie, H and Yuan, Y. *PD-1 and PD-L1 in cancer immunotherapy: clinical implications and future considerations*. *Hum Vaccin Immunother*, 2019. **15**: p. 1111-1122.
27. Takeda, Y. et al. *A TLR3-specific adjuvant relieves innate resistance to PD-L1 blockade without cytokine toxicity in tumor vaccine immunotherapy*. *Cell reports*, 2017. **19**: p. 1874-1887.
28. Reilly, M. J. et al. *TLR9 activation cooperates with T cell checkpoint blockade to regress poorly immunogenic melanoma*. *J Immunother Cancer*, 2019. **7**: 323.
29. Xu, A. et al. *TLR9 agonist enhances radiofrequency ablation-induced CTL responses, leading to the potent inhibition of primary tumor growth and lung metastasis*. *Cell Mol Immunol*, 2019. **16**: p. 820-832.

30. Zhang, B., Moser, M. A., Zhang, E. M., Xiang, J. & Zhang, W. *An in vitro experimental study of the pulse delivery method in irreversible electroporation*. Journal of Engineering and Science in Medical Diagnostics and Therapy, 2018. **1**: 014501.
31. Ahmed, K. A. & Xiang, J. *mTORC1 regulates mannose-6-phosphate receptor transport and T-cell vulnerability to regulatory T cells by controlling kinesin KIF13A*. Cell Discov, 2017. **3**: 17011.
32. Broz, M. L. et al. *Dissecting the tumor myeloid compartment reveals rare activating antigen-presenting cells critical for T cell immunity*. Cancer Cell, 2014. **26**: p. 638-652.
33. Chavez, M. et al. *Distinct immune signatures in directly treated and distant tumors result from TLR adjuvants and focal ablation*. Theranostics, 2018. **8**: p. 3611-3628.
34. Umeshappa, C., et al. *CD4+ Th-APC with acquired peptide/MHC class I and II complexes stimulate type I helper CD4+ and central memory CD8+ T cell responses*. J Immunol, 2009. **182**: p. 193-206.
35. Spear, S, McNeish, I.A. and Capasso, M. *Generation of orthotopic pancreatic tumors and ex vivo characterization of tumor-infiltrating T cell cytotoxicity*. J Visualized Exp, 2019. **154**: e60622.
36. Severson, J., et al *PD-1+Tim+CD8+ T lymphocytes display varied degrees of functional exhaustion in patients with regional metastatic differentiated thyroid cancer*. Cancer Immunol Res, 2015. **3**: p. 620-630.
37. Wu, C. et al. *Tumor Microenvironment following gemcitabine treatment favors differentiation of immunosuppressive Ly6C(high) myeloid cells*. J Immunol, 2020. **204**: p. 212-223.
38. Lau, J., et al. *Tumor and host cell PD-L1 is required to mediate suppression of anti-tumour immunity in mice*. Nat Communications, 2017. **8**: 14572.
39. Barber D. L., et al. *Restoring function in exhausted CD8 T cells during chronic viral infection*. Nature, 2006. **439**: p. 682-687.
40. Linhares, A. D. S., et al. *Therapeutic PD-L1 antibodies are more effective than PD-1 antibodies in blocking PD-1/PD-L1 signaling*. Sci Reports, 2019. **9**: 11472.
41. Shi, L. et al. *PD-1 blockade boosts radiofrequency ablation-elicited adaptive immune responses against tumor*. Clin Cancer Res, 2016. **22**: p. 1171-1184.
42. Silvestrini, M. T., et al. *Priming is key to effective incorporation of image-guided thermal ablation into immunotherapy protocols*. JCI Insight, 2017. **2**: e90521.
43. Erank, A., et al. *High-intensity focused ultrasound (HIFU) triggers immune sensitization of refractory murine neuroblastoma to checkpoint inhibitory therapy*. Clinical Cancer Res, 2020. **26**: p. 1152-1161.
44. den Brok M., et al. *Synergy between in situ cryoablation and TLR9 stimulation results in a highly effective in vivo dendritic cell vaccine*. Cancer Res, 2006. **66**: p. 7285-7292.

45. Nolz, J. C. *Molecular mechanisms of CD8(+) T cell trafficking and localization*. Cell Mol Life Sci, 2015. **72**: p. 2461-2473.
46. Thormmen, D. and Schumacher, T. *T cell dysfunction in cancer*. Cell, 2018. **33**: p. 547-562.
47. Liu, Y. et al. *Abscopal effect of radiotherapy combined with immune checkpoint inhibitors*. J Hematol Oncol, 2018. **11**: 104.
48. Zitvogel, L., Tesniere, A. & Kroemer, G. *Cancer despite immunosurveillance: immunoselection and immunosubversion*. Nat Rev Immunol, 2006. **6**: p. 715-727.
49. Roma-Rodrigues, C., Mendes, R., Baptista, P. V. & Fernandes, A. R. *Targeting tumor microenvironment for cancer therapy*. Int J Mol Sci, 2019. **20**: 840.
50. Sormendi, S. & Wielockx, B. *Hypoxia pathway proteins as central mediators of metabolism in the tumor cells and their microenvironment*. Front Immunol, 2018. **9**: 40.
51. Sooriakumaran, P and Kapa, R. *Angiogenesis and tumor hypoxia response in prostate cancer: A review*. Int J Surg, 2005. **3**: p. 61-67.
52. Naoolitani, G., Rinaldi, A., Bertoni, F., Sallusto, F., Lanzavecchia, A. *Select Toll-like receptor agonist combinations synergistically trigger a T helper type-1 polarizing program in dendritic cells*. Nat Immunol, 2005. **6**: p. 769-776.
53. Tross, D., Petrenko, L., Klaschik, S., Zhu, Q., Klinman, D.M. *Global changes in gene expression and synergistic interactions induced by TLR9 and TLR3*. Mol Immunol, 2009. **46**: p. 2557- 2564.
54. Le Noci, V. et al. *Poly(I:C) and CpG-ODN combined aerosolization to treat lung metastases and counter the immunosuppressive microenvironment*. Oncoimmunology, 2015. **4**: e1040214.
55. Prodam, F., Chiochetti, A. & Dianzani, U. *Diet as a strategy for type 1 diabetes prevention*. Cellular & Molecular Immunology, 2018. **15**: p. 1-4.
56. Contreras, A. M. et al. *Correlation between anti-PD-L1 tumor concentrations and tumor-specific and nonspecific biomarkers in a melanoma mouse model*. Oncotarget, 2016. **7**: 76891.
57. Rudkouskaya, A. & Barroso, M. *Internalization and trafficking of PD-L1 in MDAMB231 breast cancer cells*. The FASEB Journal, 2017. **31**: p. 809.7-809.7.
58. Junttila, M. R. & de Sauvage, F. J. *Influence of tumour microenvironment heterogeneity on therapeutic response*. Nature, 2013. **501**: p. 346-354.
59. Li, J. et al. *Tumor cell-intrinsic factors underlie heterogeneity of immune cell infiltration and response to immunotherapy*. Immunity, 2018. **49**: p. 178-193 e117.
60. Landskron, G., Fuente, M. D. I., Thuwajit, P., Thuwajit, C., Hermoso, M. A. *Chronic inflammation and cytokines in the tumor microenvironment*. J Immunol Res, 2014. **2014**: Article ID 149185.

61. Zou, W and Restifo, N. P. *Th17 cells in tumor immunity and immunotherapy*. Nat Rev Immunol, 2010. **10**: p. 248-256.
62. Bilska, M., et al. *Th17 and IL-17 as novel immune targets in ovarian cancer therapy*. J Oncol, 2020. **2020**: Article ID 8797683.
63. Shi, L., et al. *Inflammation induced by incomplete radiofrequency ablation accelerates tumor progression and hinders PD-1 immunotherapy*. Nat Commun, 2019. **10**: 5421.
64. Zappasodi, R., Merghoub, T. & Wolchok, J. D. *Emerging concepts for immune checkpoint blockade-based combination therapies*. Cancer Cell, 2018. **33**: p. 581-598.
65. Galon, J. et al. *Type, density, and location of immune cells within human colorectal tumors predict clinical outcome*. Science, 2006. **313**: p. 1960-1964.
66. Huang, H. et al. *CD4+ Th1 cells promote CD8+ Tc1 cell survival, memory response, tumor localization and therapy by targeted delivery of interleukin 2 via acquired pMHC I complexes*. Immunology, 2007. **120**: p. 148-159.
67. Fearon, D. T. *Immune-suppressing cellular elements of the tumor microenvironment*. Annual Review of Cancer Biology, 2017. **1**: p. 241-255.
68. Bernhard, C. A., Reid, C., Kochanek, S. & Brocker, T. *CD169+ macrophages are sufficient for priming of CTLs with specificities left out by cross-priming dendritic cells*. Proc Natl Acad Sci USA, 2015. **112**: p. 5461-5466.
69. van Dinther, D. et al. *Functional CD169 on macrophages mediates interaction with dendritic cells for CD8(+) T cell cross-priming*. Cell Rep, 2018. **22**: p. 1484-1495.

## **CONFLICT OF INTEREST**

The authors declare no competing financial interest.

## **ACKNOWLEDGEMENT**

This work was supported by J.X. grants from the Saskatchewan Cancer Agency (SCA), Saskatchewan Health Research Foundation (SHRF), College of Medicine Research Awards (CoMRAD), Royal University Hospital Foundation (RUHF) and Prostate Cancer Fight Foundation (PCFF). F.B. and A.X. were supported by Lisa Rendall Breast Cancer Graduate Student Scholarship and Postdoctoral Fellowship, respectively, from SCA.

## **CHAPTER 4 CONCLUSIONS AND FUTURE DIRECTION**

Our data demonstrate that IRE ablation alone induces very weak CTL responses in large EG7 tumors, possibly due to the remaining tumor tissues becoming more immunotolerant and accelerating tumor progression post ablation [1]. Combo treatment alone also fails to induce efficient CTL response, possibly due to strong immunotolerance within the TME of large tumors. Collectively, the IRE+Combo therapy synergistically induces potent CTL responses and antitumor immunity leading to eradication of primary and distant tumors and lung tumor metastases, possibly due to its conversion of not only the local tolerant TME in the primary tumor but also the reduction of a systemic immunotolerance. Therefore, our IRE+Combo protocol may represent a good example in support of the newly emerging concept that efficiently reducing tumor burden (i.e., by IRE ablation) and increasing the immunogenicity of the TME (i.e., by PD-1 blockade and TLR3/9 agonists) are two key factors to improve cancer immunotherapy [2], leading to a synergistic therapeutic effect on IRE+Combo-ablated cancer. In addition, our IRE+Combo therapeutic results in our animal tumor model indicate that targeting immunotolerant subsets in the TME may be a future direction towards improved immunotherapy and IRE-ablated cancer therapy.

The immunotolerant TME is a major hurdle for currently applied cancer immunotherapies. The TME is a complex heterogeneous environment that includes different stromal and immune cells. Tumor cells control the TME by secreting cytokines and mediators to stimulate the differentiation of immunosuppressive cells and thus promote tumor survival and progression [3]. Therefore, targeting the TME will help cancer patients achieve better outcomes with current conventional cancer treatments, such as chemotherapy, radiotherapy, and ablation therapy. Tumor cells enhance tissue remodelling and alter the ECM structure to facilitate angiogenesis and support their survival. Therapies with anti-angiogenic agents have shown promising results in clinical trials, such as increased patient survival [4]. The targets of these anti-angiogenic agents include vascular VEGF, VEGF receptors (VEGFR) and MMP. In addition, VEGF or VEGFR have been combined with chemotherapy to treat advanced tumors [5-8].

Specific immune cells in the TME support tumor progression and metastases, such as TAMs, MDSCs, and CD4<sup>+</sup>Foxp3<sup>+</sup> Treg cells. One strategy to lower the infiltration of TAMs and MDSC into the TME was to use anti-macrophage colony-stimulating factor 1 receptor (M-CSF1R) neutralizing antibodies [9, 10]. CD4<sup>+</sup>Foxp3<sup>+</sup> Treg cells are critical immunosuppressive cells in the TME because of their inhibitory effect on activated CTLs [11]. Depletion of CD4<sup>+</sup>Foxp3<sup>+</sup> Tregs was done in one study by using antibodies against their surface markers CTLA-4 and OX-40, combined with intratumoral administration of TLR9 agonist CpG. The results showed systemic anti-tumor immune responses that eradicate tumors in mice [12]. Immunomodulatory cytokines, such as IL-2, IL-12, TNF- $\alpha$ , type I IFNs, and granulocyte-macrophage colony-stimulating factor (GM-CSF), have been used [13]. In particular, GM-CSF, which stimulates DC maturation and thus enhances T cell responses, is used in many clinical trials to promote anti-tumor immune responses [14-18]. Combining GM-CSF with CTLA-4 blockade is associated with better outcomes and prolonged patient survival compared to CTLA-4 monotherapy [19].

One of the current and vital strategies to enhance anti-tumor immune responses is targeting immune checkpoint inhibitors, such as PD-1, CTLA-4, and T-cell immunoglobulin and mucin domain 3 (Tim-3). In the TME, CD4<sup>+</sup>Foxp3<sup>+</sup> Treg cells stimulate the expression of inhibitory PD-1 molecules on activated CTLs. The interaction between PD-1 on activated CTLs and PDL-1 expressed on tumor cells and other immunosuppressive cells leads to T cell exhaustion. The upregulation of PDL-1 expression is considered one of the essential mechanisms that tumour cells use to suppress anti-tumor T cell responses [20]. Several mAbs for PD-1 and PDL-1 blockade have been recently approved by the FDA, and more clinical trials are currently being done. However, PD-1 blockade has shown limited efficacy as a monotherapy due to developed patient resistance. Therefore, combinatorial approaches have been designed to improve PDL1 resistance by patients. Combining PD1-blockade with CTLA-4 blockade has shown a synergic effect that led to higher survival rates among patients compared to either monotherapy [20]. Studies with PD-1 blockade combined with TLR agonists, such as TLR3, have also shown enhanced T cell responses [21]. Recent studies involving IRE for cancer ablation in combination with PD-1 blockade and TLR7 have demonstrated improvement in the anti-tumor immunity by increasing immunogenic cDC1 in the TME [22, 23].

Our study demonstrates that IRE ablation, when combined with PD-1 blockade and TLR3/9, has successfully converts an immunotolerant TME into an immunogenic TME. IRE ablation induced massive cell apoptosis and provided specific-tumor antigens for the uptake by DCs for T cell activation [24, 25]. TLR3 and TLR9 have worked synergistically to stimulate DC maturation and strong CD4<sup>+</sup> Th1 and CTL responses [26, 27]. PD-1 blockade rescues the exhausted T-cells and thus enhances their anti-tumor immune response [28, 29]. This cooperative work between IRE ablation, TLR3/9, and PD-1 blockade leads to the complete eradication of primary and distant tumors and lung metastases.

Taken together, we speculate that a combinatorial therapy using IRE ablation combined with multiple immune checkpoint inhibitors as well as different immune-targeting agents may represent a future direction with respect to the development of new and effective immunotherapeutic strategies for modulating the immunotolerant TME and enhancing the anti-tumor immunity for the treatment of various solid tumors.



## References

1. Shi, L., et al., *Inflammation induced by incomplete radiofrequency ablation accelerates tumor progression and hinders PD-1 immunotherapy*. Nat Commun, 2019. **10**: 5421.
2. Zappasodi, R, Merghoub, T. & Wolchok, J. D., *Emerging concepts for immune checkpoint blockade-based combination therapies*. Cancer Cell, 2018. **33**: p. 581-598.
3. Pitt, J.M. et al., *Targeting the tumor microenvironment: removing obstruction to anticancer immune responses and immunotherapy*. Ann Oncol, 2016. **27**: p. 1482-1492.
4. Sounni, N.E., Noel, A., *Targeting the tumor microenvironment for cancer therapy*. Clin. Chem, 2013. **59**: p. 85–93.
5. Fukumura, D., Jain, R.K., *Tumor microenvironment abnormalities: Causes, consequences, and strategies to normalize*. J. Cell. Biochem, 2007. **101**: p. 937–949.
6. Roma-Rodrigues C, Mendes R, Baptista PV, Fernandes AR, *Targeting tumor microenvironment for cancer therapy*. Int J Mol Sci, 2019. **20**(4): 840.
7. Chu, Q.S., Forouzes, B., Syed, S., et al., *A phase II and pharmacological study of the matrix metalloproteinase inhibitor (MMPI) COL-3 in patients with advanced soft tissue sarcomas*. Investig. New Drugs, 2007. **25**: p. 59–367.
8. Gu, Y., Lee, H.M., Golub, L.M., et al., *Inhibition of breast cancer cell extracellular matrix degradative activity by chemically modified tetracyclines*. Ann Med, 2005. **37**: p. 450–460.
9. Szebeni, G.J., Vizler, C., Nagy, L.I., et al., *Pro-tumoral inflammatory myeloid cells as emerging therapeutic targets*. Int J Mol Sci, 2016. **17**: 1958.
10. Noy, R., Pollard, J.W., *Tumor-associated macrophages: From mechanisms to therapy*. Immunity, 2014. **41**: p. 49–61.
11. Ohue, Y. & Nishikawa, H. *Regulatory T (Treg) cells in cancer: Can Treg cells be a new therapeutic target?* Cancer Sci, 2019. **110**: p. 2080-2089.
12. Marabelle A, Kohrt H, Sagiv-Barfi I et al., *Depleting tumor-specific Tregs at a single site eradicates disseminated tumors*. J Clin Invest, 2013. **123**: p. 2447–2463.
13. Van der Jeught K, Bialkowski L, Daszkiewicz L et al., *Targeting the tumor microenvironment to enhance antitumor immune responses*. Oncotarget, 2015. **6**: p. 1359–1381.
14. Dai S, Wei D, Wu Z et al., *Phase I clinical trial of autologous ascites-derived exosomes combined with GM-CSF for colorectal cancer*. Mol Ther, 2008. **16**: p. 782–790.

15. Emens LA, Asquith JM, Leatherman JM, et al., *Timed sequential treatment with cyclophosphamide, doxorubicin, and an allogeneic granulocyte-macrophage colony-stimulating factor-secreting breast tumor vaccine: a chemotherapy dose ranging factorial study of safety and immune activation*. J Clin Oncol, 2009. **27**: p. 5911–5918.
16. Fagerberg J., *Granulocyte-macrophage colony-stimulating factor as an adjuvant in tumor immunotherapy*. Med Oncol, 1996. **13**: p. 155–160.
17. Pol, J., Bloy, N., Buque, A., et al., *Trial watch: peptide-based anticancer vaccines*. Oncoimmunology, 2015. **4**: e974411.
18. Kaufman, H. L., Ruby, C. E., Hughes, T., et al., *Current status of granulocyte macrophage colony-stimulating factor in the immunotherapy of melanoma*. J Immunother Cancer, 2014. **2**: 11.
19. Hodi, F. S., Lee S., McDermott, D. F., et al., *Ipilimumab plus sargramostim vs ipilimumab alone for treatment of metastatic melanoma: a randomized clinical trial*. JAMA, 2014. **312**: p. 1744–1753.
20. Jiang, Y., Chen, M., nie, h and Yuan, Y., *PD-1 and PDL-1 in cancer immunotherapy: clinical implications and future considerations*. Hum Vaccin Immunother, 2019. **15**: p. 1111-1122.
21. Takeda et al., *A TLR3-Specific Adjuvant Relieves Innate Resistance to PDL-1 Blockade without Cytokine Toxicity in Tumor Vaccine Immunotherapy*. Cell Reports, 2017. **19**: p. 1874-1887.
22. Zhao J., et al., *Irreversible electroporation reverses resistance to immune checkpoint blockade in pancreatic cancer*. Nat Commun, 2019. **10**: 899.
23. Narayanan, J. S. S. et al., *Irreversible electroporation combined with checkpoint blockade and TLR7 stimulation induced antitumor immunity in a murine pancreatic cancer model*. Cancer Immunol Res, 2019. **7**(10): p. 1714-1726.
24. Lee E. W, Thai S, Kee S. T., *Irreversible electroporation: a novel image-guided cancer therapy*. Gut Liver, 2010. **Suppl 1**(Suppl 1): S99-S104.
25. Lyu, T., et al., *Irreversible electroporation in primary and metastatic hepatic malignancies*. Medicine, 2017. **96**(17): e6386.
26. Naoolitani, G., Rinaldi, A., Bertoni, F., Sallusto, F., Lanzavecchia, A. *Select Toll-like receptor agonist combinations synergistically trigger a T helper type-1 polarizing program in dendritic cells*. Nat Immunol, 2005. **6**: p. 769-776.
27. Tross, D., Petrenko, L., Klaschik, S., Zhu, Q., Klinman, D.M. *Global changes in gene expression and synergistic interactions induced by TLR9 and TLR3*. Mol Immunol, 2009. **46**: p. 2557- 2564.

28. Contreras, A. M. et al. *Correlation between anti-PD-L1 tumor concentrations and tumor-specific and nonspecific biomarkers in a melanoma mouse model*. *Oncotarget*, 2016. **7**: 76891.
29. Rudkouskaya, A. & Barroso, M. *Internalization and trafficking of PD-L1 in MDAMB231 breast cancer cells*. *The FASEB Journal*, 2017. **31**: p. 809, 807-809, 807.